

UNIVERSITÀ DEGLI STUDI DI BERGAMO

Facoltà di Ingegneria
Dipartimento di Ingegneria Industriale

DOTTORATO DI RICERCA IN
TECNOLOGIE PER L'ENERGIA E L'AMBIENTE
XXVI ciclo
Anno 2013



in cooperation with



**INTEGRATED DESIGN METHODS FOR NATURAL
VENTILATION**

Doctoral thesis:
Annamaria Belleri

Supervisors:
Prof. Marco Marengo
Ing. Roberto Lollini

© 2014

Dipartimento di Ingegneria Industriale. Università degli studi di
Bergamo

ISBN XXX-XX-XXXXXX-XX-X

Open access copy available at: <http://hdl.handle.net/XXXXXX/XXXXXX>

Terms of use: <http://aisberg.unibg.it/doc/disclaimer.html>

Table of Contents

Introduction	1
1. Integrated Design Process and natural ventilation	5
1.1. The Integrated Design Process	5
1.2. Regulatory framework	9
1.2.1. European standard	10
1.2.2. US standards	12
1.2.3. Other countries	14
1.3. Natural ventilation as passive design solution for Net Zero Energy Buildings	15
1.3.1. Natural ventilation in cooling dominated climates	21
1.3.2. Natural ventilation in heating and cooling dominated climates	23
1.4. Barriers and constraints	26
Bibliography	31
2. Natural ventilation modelling	33
2.1. Physical principles	33
2.1.1. Stack effect	33
2.1.2. Wind pressure	36
2.1.3. Combination of wind and stack effect	37
2.2. Methods and tools for airflow modelling	39
2.2.1. Empirical models	40
2.2.2. Airflow network models	48
2.2.3. Zonal models	55
2.2.4. Computational Fluid Dynamics (CFD) models	56
2.3. Needs of development: methods and tools	59
Bibliography	60
3. Airflow network modelling in EnergyPlus	64
3.1. Theoretical background	65
3.2. Thermal and airflow zoning	68
3.3. Input objects	70
3.3.1. Simulation settings	70
3.3.2. Surface convection coefficients	71
3.3.3. External wind conditions	76

3.3.4.	External nodes	78
3.3.5.	Zones and surfaces.....	78
3.3.6.	Leakage components	79
3.3.7.	Wind pressure coefficients	88
3.3.8.	Control settings.....	90
3.4.	A modeling example: the new Technology Park in Bolzano	92
3.4.1.	Natural ventilation strategies	94
3.4.2.	EnergyPlus model to study airflows.....	95
	Bibliography	99
4.	Sensitivity analysis of natural ventilation design parameters.....	102
4.1.	Reference building	103
4.2.	Modelling method.....	104
4.3.	Parameter selection and variable range assessment.....	106
4.4.	Climate dependency.....	108
4.5.	The Elementary Effect method	110
4.6.	Results and discussion	114
	Bibliography	123
5.	Analysis of predicted and measured performance.....	125
5.1.	Methods	126
5.1.1.	Field study methods.....	127
5.1.2.	Environmental data measurement	130
5.1.3.	Early-design modelling method	130
5.1.4.	Uncertainty analysis method	133
5.1.5.	Improving the model	144
5.2.	Results.....	155
5.2.1.	Field study results	155
5.2.2.	Uncertainty analysis results	158
5.2.3.	Sensitivity analysis results.....	159
5.3.	Discussion and analysis	161
5.4.	Conclusions.....	168
	Bibliography	169
6.	Design procedure.....	171
6.1.	Pre-design phase	172
6.1.1.	Climate suitability analysis.....	173
6.1.2.	Constraints analysis	180

6.2. Schematic design	182
6.3. Design development	187
6.3.1. Detailing of natural ventilation.....	188
6.3.2. Control strategy definition.....	190
6.4. Construction documents	192
6.5. Summary and recommended guidelines	193
Bibliography	196
Conclusion.....	198
Publication List.....	201
Annex I	203

Table of Figures

- Figure 1-1. Figures of traditional design process (link) and integrated design process (right). Source: Leutgob K. [1.7]
- Figure 1-2. Design method focused on energy issues. Source: IEA Task 40/ECBCS Annex 52 [1.12]
- Figure 1-3. Energy balance of the analyzed case studies.
- Figure 1-4. Average U-values for wall, floor, roof and window and g-value of windows for the case studies.
- Figure 1-5. ENERPOS classroom with ceiling fans and vents allowing cross ventilation. Source: STC database.
- Figure 1-6. Interior view of the Pixel building with controlled high level windows. Source: STC database
- Figure 1-7. Cross section (link) and solar chimneys (right) of the ZEB at BCA. Source: STC database
- Figure 1-8. Green office solution set to face cooling challenges. Source: STC IEA T40/A52 database
- Figure 1-9. Solar XXI: light well for natural lighting and air exhausting. Vents connecting offices to the light well. Source: STC database
- Figure 1-10. Solar XXI BIPV-T system. Source: STC database
- Figure 1-11. Cross section of the building fire regulation plan with fire compartments, model zones and a scheme of the selected stack-driven cross ventilation configurations for the considered zones.
- Figure 2-1. Stack effect drivers. Source: <http://www.eng.upm.edu.my/>
- Figure 2-2. Pressure difference due to wind. Source: Lion L. [2.1]
- Figure 2-3. Pressure difference due to stack effect. Source: Lion L. [2.1]
- Figure 2-4. Natural ventilation modelling detail along the integrated design process.
- Figure 2-5. Schematic representation of ping-pong and onion approach. Source: (60)
- Figure 3-1. Airflow network schematic representation. Source: IBPSA-USA
- Figure 3-2. Schematic representation of relationship between zones and air paths. Source: IBPSA-USA
- Figure 3-3. Relationship among AirflowNetwork objects (right hand side) and associated EnergyPlus objects (link hand side). Source: Lixing G. [3.2]
- Figure 3-4. Airflow network control object with default settings.
- Figure 3-5. Vertical wall exterior convection model comparison depending on wind speed and surface roughness at a temperature difference of 10K between outdoor air and external wall surface when the façade is directed windward.
- Figure 3-6. Vertical wall interior convection model comparison at different temperature differences between air and wall interior surface. Image courtesy of Roberti F.

Figure 3-7. Horizontal slab interior convection models comparison at different temperature differences between air and wall interior surface. Image courtesy of Roberti F.

Figure 3-8. Decrease in wind speed as influenced by varieties of terrain roughness. Source:
http://www.stadtentwicklung.berlin.de/umwelt/umweltatlas/ed403_01.htm

Figure 3-9. Surface pressure coefficient as a function of wind incident angle for the Walton model and the Swami and Chandra model for side ratios $S = L_1/L_2$. Source: Deru M. et al. [3.25]

Figure 3-10. Building render. Source: CLEAA

Figure 3-11. Typical floor plan. Source: CLEAA

Figure 3-12. Building cross section. Source: CLEAA

Figure 3-13. Cross section of the building fire regulation plan with fire compartments, model zones and a scheme of the selected stack-driven cross ventilation configurations for the considered zones.

Figure 3-14. Section of the EnergyPlus geometry model in SketchUp with average airflow rates during summer season. Red and blue arrows represent respectively positive and negative airflow directions.

Figure 3-15. Natural volume flow rate frequency along the airflow network paths in the south office block.

Figure 4-1. Building SketchUp model and geometric characteristics.

Figure 4-2. Diurnal temperature swing and solar radiation of the three selected locations. EnergyPlus weather data [4.7].

Figure 4-3. Wind rose representing wind speed, direction and frequency in the analyzed climates from April to October during the whole day. EnergyPlus weather data [4.7]. Source: WRPLOT view

Figure 4-4. Trajectory examples in a 3-dimensional design space. Image courtesy of Filippi Oberegger U.

Figure 4-5. Combination of parameter values sample in a 3-dimensional design space. Image courtesy of Filippi Oberegger U.

Figure 4-6. Empirical distributions of $r = 20$ trajectories. Source: Saltelli et al. [4.8].

Figure 4-7. Sensitivity analysis methodology overview.

Figure 4-8. I Elementary Effect analysis results: influence on cooling need for Strategy A.

Figure 4-9. I Elementary Effect analysis results: mean and standard deviation of cooling need for Strategy A.

Figure 4-10. I Elementary Effect analysis results: influence on number of comfort hours for Strategy B.

Figure 4-11. I Elementary Effect analysis results: mean and standard deviation of comfort hours number for Strategy B.

Figure 4-12. II Elementary Effect analysis results: influence on cooling need for Strategy A.

Figure 4-13. II Elementary Effect analysis results: mean and standard deviation of cooling need for Strategy A.

Figure 4-14. II Elementary Effect analysis results: influence on number of comfort hours for Strategy B.

Figure 4-15. II Elementary Effect analysis results: mean and standard deviation of comfort hours number for Strategy B.

Figure 5-1. North –east side of the field study office.

Figure 5-2. Office layout and camera locations. Source: Dutton et al. [5.2]

Figure 5-3. Alameda office and AAMC1 weather station location. Source: Google Earth

Figure 5-4. Uncertainty analysis methodology overview.

Figure 5-5. Uncertainty analysis results with 27, 200 and 3000 samples.

Figure 5-6. Mean early design predicted percentage of window opening in front room, with indoor, outdoor, and comfort temperatures.

Figure 5-7. Measured percentage of window opening in front room, with indoor, outdoor and comfort temperatures.

Figure 5-8. Mean early design predicted percentage of window opening in back room, with indoor, outdoor and comfort temperatures.

Figure 5-9. Measured percentage of window opening in back room, with indoor, outdoor and comfort temperatures.

Figure 5-10. Alameda building as modeled in the wind tunnel with actual surroundings. Source: CPP engineering

Figure 5-11. Instrumented north-east room from the Alameda building. Pressure taps are visible around the perimeter of each window. Source: CPP Engineering

Figure 5-12. Measured wind pressure coefficient at pressure taps (101-108) along the window f8 and na2 perimeter over the simulation runs. Source: CPP Engineering

Figure 5-13. Measured wind pressure coefficient at pressure taps (109-116) along the window f6 and f7 perimeter over the simulation runs. Source: CPP Engineering

Figure 5-14. Measured wind pressure coefficient at pressure taps (301-308) along the window f2 and f3 perimeter over the simulation runs. Source: CPP Engineering

Figure 5-15. Measured wind pressure coefficient at pressure taps (309-316) along the window f4 and f5 perimeter over the simulation runs. Source: CPP Engineering

Figure 5-16. Measured wind pressure coefficient at pressure taps (501-508) along the door perimeter over the simulation runs. Source: CPP Engineering

Figure 5-17. Literature data sets and wind tunnel measured mean wind pressure coefficients for the north façade. Root mean square error (RMSE) are estimated by comparing literature data set with the wind tunnel measurements.

Figure 5-18. Literature data sets and wind tunnel measured mean wind pressure coefficients for the east façade. Root mean square error (RMSE) are estimated by comparing literature dataset with the wind tunnel measurements.

Figure 5-19. Literature data sets and wind tunnel measured mean wind pressure coefficients for the west façade. Root mean square error (RMSE) are estimated by comparing literature dataset with the wind tunnel measurements.

Figure 5-20. Measured and simulated airflow rates by the improved model in the front room.

Figure 5-21. Measured and simulated airflow rates by the improved model in the front room.

Figure 5-22. Measured and simulated airflow rates by the improved model in the back room.

Figure 5-23. Measured and simulated airflow rates by the improved model in the back room.

Figure 5-24. Frequency distribution of percentage of occupied hours when ACH met ASHRAE standard.

Figure 5-25. Standard Regression Coefficient of each input parameter considered.

Figure 5-26. Percentage of occupied hours when ASHRAE 62.1 requirements are met predicted by early design model, better estimated models and measured.

Figure 6-1. Overview of the proposed natural ventilation design method.

Figure 6-2. Mean hourly UHI intensity for a reference day in different European cities. Source: Kiesel K. et al. [6.3]

Figure 6-3. Design strategies for the Bolzano climate. Source: Climate consultant 5.4

Figure 6-4. Wind speed, direction and frequency analysis for Bolzano from 1st April until 31st October. Source: WRPLOT

Figure 6-5. Natural ventilation strategies and configuration thermal comfort performance. Categories are defined in EN 15251:2008 – Table 1.

Figure 6-6. Psychrometric scatter plot which indicates temperature and humidity levels through the summer period if a constant air change rate of 0.3 is provided.

Figure 6-7. Psychrometric scatter plot which indicates temperature and humidity levels through the summer period in case of stack and wind driven cross ventilation.

Figure 6-8. ACH frequency in the building zones during night (from June to September) due to the natural ventilation. Source: Belleri et al. [1.27]

Figure 6-9. Relationship between inlet and outlet opening area of the central stack in the new Technology Park building calculated by LoopDA.

Acknowledgements

Apart from the efforts of myself, the success of any research depends largely on the encouragement and guidelines of many others.

I would like to show my greatest appreciation to my super supervisor Roberto Lollini for his trust, guidance, precious suggestions and support (both technical and psychological).

I would also like to express my gratitude to Prof. Marengo for having trusted me and having offered me this opportunity.

I would like to thank EURAC for funding my research activities and for feeding my hunger of knowledge. In this regard I have to thank all the past and present EURAC collaborators for the precious technical support, the certain enthusiasm and the many ‘sweet’ moments spent together. The guidance and support received from all the EURAC collaborators was vital for this thesis.

I will forever be thankful to my overseas mentor Spencer Dutton for the precious and enthusiastic collaboration and the time spent editing my horrible English.

My special thanks to Davide for having been the best doctorate mate (and driver) I could ever had, to Giulia for having shared house, desktop, food.... and a lot of happy and funny moments with me and to Andreas for the music and the wise advices.

Last but not least, I would like to thank who has been my family, who still is my family and will always be (just because of that) and all the friends who became part of the big family.

The path to becoming a doctor is littered with distractions. I’d like to thank those distractions for making me the person I am.

to my parents

Abstract

Natural ventilation is widely applied to new building design as it is an effective passive measure to reach the Net Zero Energy target. However, the lack of modelling guidelines and integrated design procedures that include technology solutions using passive design strategies to exploit climate potential, frustrate building designers who prefer to rely on mechanical systems.

Within the existing natural ventilation modelling techniques, airflow network models seem the most promising tool to support the natural ventilation design as they are coupled with the most widely used building energy simulation tools. This PhD work provides methods to integrate natural ventilation in the whole building design and to improve natural ventilation predictability overcoming some of the barriers to its usage during early-design-stages, such as model zoning, input data estimation, model reliability and results uncertainty.

A sensitivity analysis on parameters characterizing different natural ventilation strategies has been performed on a reference office building model considering key design parameters that cannot be clearly specified during early-design-stages. The results underline the most important parameters and their effect on natural ventilation strategies in different climate types.

The airflow network modelling reliability at early stage design phases has been tested by comparing early-design-stage model results with output results from a detailed model as well as with measured data of an existing naturally ventilated building.

Results underline the importance of an optimized control strategy and the need of occupant behaviour studies to define better window opening control algorithms to be included in building dynamic simulation tools. Early-design-stage modelling caused an overestimation of natural ventilation performances mainly due to the window opening control standard object implemented in building dynamic simulation tools, which assume all the windows within the same zone are operated at the same way.

With sufficient input data (identify in the research work), airflow network models coupled with building energy simulation tools can provide reliable informative predictions of natural ventilation performance.

Finally, natural ventilation design guidelines are proposed to explain how existing design tools and methods can be applied within the whole design process, taking into account technology solutions for triggering the natural ventilation.

Introduction

The potential benefits of natural ventilation in terms of energy consumption, thermal comfort, indoor air quality and operating costs, especially under moderate climates have drawn the attention of building designers and contractors. After the entry into force of the new EPBD directive 31/2010/EU, natural ventilation has been increasingly applied as passive solution to achieve the Zero Energy target¹.

Several prior studies [1.1][1.2][1.3][1.4][1.5][1.6] led to the development of several guidelines for natural ventilation design that provide rules of thumb to support natural ventilation design in the conceptual design phase.

As new design strategies have been put forward, including more ambitious uses of night cooling and, most recently, hybrid combinations of natural and mechanical ventilation, these publications and especially the rules of thumb contained within them have quickly become dated. Nevertheless, the more general fundamental strategies presented remain valid and the associated guidelines useful.

The majority of these studies conclude with general guidance that is not possible to simulate effectively natural ventilation performance in building. The only exception being the study by NIST [1.1] that develops a comprehensive design methodology that includes multi-zone airflow network modelling, but does not include building energy simulation.

More specific energy design and modelling procedures, considering the use of dynamic simulation tools within the integrated design process, are needed to push the implementation of passive design techniques.

¹ The general definition of Zero Energy Building is a grid connected, energy efficient building which offsets or nearly offsets its energy demand by generating energy on site. Within the IEA Task 40 research project a common definition framework for Net ZEBs has been established. Please refer to Sartori et al. 2012 for the balance calculation method used. Energy demand and supply have been weighted in terms of primary energy. Energy demand for heating, cooling, built-in lighting, ventilation, domestic hot water and appliances has been taken into account in the balance calculation. Only energy produced on site by renewable energy sources has been taken into account in the balance calculation.

The objective of this PhD Thesis is the enhancement of the existing integrated design methods to define natural ventilation concepts.

As natural ventilation design affects building shape, architectural and urban decisions, both for the building and the surroundings, this work focuses in particular on early-design-stages when the definition of ventilation strategies is more effective.

Available building simulation tools, such as EnergyPlus, ESP-r, IES, TAS and TRNSYS, allow users to integrate building energy models with multi-zone airflow models providing quantitative information on natural ventilation performance both in terms of energy use and indoor environmental comfort. Thanks to this feature, these tools can be used to support early design decisions, which have the highest influence on building energy performance. However, building simulation models have to cope with the low detail level of information available at early-design-stage.

From the description of the research objectives the basic question of this research can be formulated as: *How to support the natural ventilation design of Net Zero Energy Buildings?*

A standardized procedure should be defined and based on parametrical and quantitative analysis to test results robustness and to identify the main sources of uncertainty within the input parameters. The result presentation should be attractive and clear to ease the communication with the decision makers.

The procedure should also define the appropriate model resolution for each design stage, according to the detail level of information required and being aware of the results uncertainty.

Therefore, more specific research questions should be formulated:

- *How can we use dynamic simulation tools in a simplified way to predict airflows in buildings?*
- Airflow network models imply assumptions on pressure distribution on the building facades and building interaction with the internal airflows. Additional design costs and time consuming activities would be needed to properly assess the airflow network input parameters. *How to assess the thermal-airflow model reliability in*

airflow prediction when accurate estimation of input data is not feasible?

- *Which is the impact of building design parameters on natural ventilation performance?*

The intention is to provide a modelling method which could be used at the early stages of building design. Since the details of the building needed for airflow estimation cannot be known until the project is well advanced, the method has to be able to cope with the less information possible.

In order to limit the scope of this study, the focus is directed at office buildings, but the results can be extended to other non-residential building typologies. Despite the defined use pattern, office building design can be very complex due to functionality, flexibility, efficiency and comfort needs. Furthermore, office buildings vary greatly in shape, and hence cover a variety of different natural ventilation concepts.

The thesis is organized as follows.

Chapter 1 identifies the role of natural ventilation within the existing design procedures and the regulatory framework. Design strategies adopted by existing Net Zero Energy Buildings (Net ZEBs) and involving natural ventilation are here described. Barriers and constraints to natural ventilation design have been identified and discussed.

Chapter 2 reviews the existing natural ventilation modelling techniques and tools.

Chapter 3 gives user guidelines for the EnergyPlus airflow network.

Chapter 4 presents a sensitivity analysis on different natural ventilation strategies performance in a reference office building considering key design parameters that cannot be clearly specified during early-design-stages.

Chapter 5 analyses the airflow network modelling reliability at early-design-stage by comparing predicted ventilation rates of an early-design-stage model with the one of a model with improved input data and measured data of an existing naturally ventilated building.

Chapter 6 tries to bring together the topics discussed in the preceding chapters that are of direct relevance to the design process, to explain

how airflow network modeling can be used within the whole design process.

Annex I contains data sheets about products relative to natural ventilation strategy implementation available on the market in order to give an overview of the available technology to practically implement natural ventilation concepts, analyse the demand of innovation of the existing products and their modelling feasibility.

1. Integrated Design Process and natural ventilation

The entry into force of the EPBD directive 31/2010/EU and the issuing of the Commission Delegated regulation n. 244/2012 require new building design approaches to reach the Zero Energy target. The building design strategy resulting from this framework promotes a whole building approach to define solution sets able to face the climate challenges (heating, cooling or both). While case studies have clearly shown that Net Zero Energy Buildings can be created using existing technologies and practices, most experts agree that the skills of a multidisciplinary design team and an Integrated Design Process (IDP) become indispensable to the implementation of solution sets.

This chapter reviews the state-of-the-art of the existing integrated design process procedures and guidelines considering the role of natural ventilation and how the present standards and building codes regulate, influence or restrict the design of natural ventilation addressing barriers and constraints.

1.1. The Integrated Design Process

“The Integrated Design Process is a method for realizing high performance buildings that contribute to sustainable communities. It is a collaborative process that focuses on the design, construction, operation and occupancy of a building over its complete life-cycle. The IDP is designed to allow the client and other stakeholders to develop and realize clearly defined and challenging functional, environmental and economic goals and objectives. The IDP requires a multidisciplinary design team that includes or acquires the skills required to address all design issues flowing from the objectives. The IDP proceeds from whole building system strategies, working through

increasing levels of specificity, to realize more optimally integrated solutions.”²

The IDP work team consists of individual figures (i.e. contractor, architect, engineer, constructor, sponsor and users), whose specific expertise, if effectively integrated, allows defining, analysing and evaluating different design solutions and their possible interactions. The choices are taken from the team through a participatory decision making process.

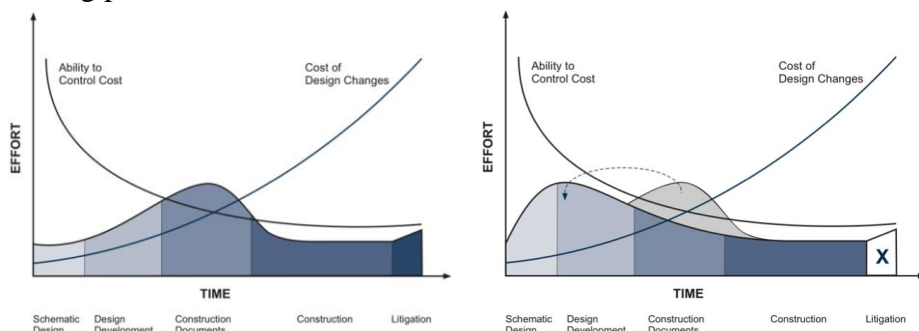


Figure 1-1. Figures of traditional design process (left) and integrated design process (right). Source: Leutgob K. [1.7]

Figure 1-1 shows the difference between a traditional approach and an integrated design process in terms of work load for building designers. The main advantage of the IDP is, that design decisions are taken at a time, when the cost does influence only design changes and not the overall construction cost. Based on past experiences [1.7], the IDP can lead to some advantages compared to a traditional design process. Design effort and costs could be 5 - 10% higher during the early design phases because more expertise and know-how are required. Building costs could be 5 - 10% more than those of a building designed following the traditional method. However, costs of the later design phases could be 5 - 10% lower, operational costs could be 70 - 90% lower and costs due to building faults could be 10 - 30 % less because of better planning and better follow up during construction.

² Excerpt from “The Integrated Design Process: Report on a National Workshop held in Toronto in October 2001.” March 2002

Existing literature about IDP reports general approaches about design process methods (how to work in team, what consider, when and who), design evaluation methods (evaluation of different design solutions, design criteria) and design strategy methods (which solutions to apply). These methods and the respective tools have been described and reviewed within the INTEND project [1.8] and the IEA Annex 44 [1.9]. The International Energy Agency has developed within Task 23/Subtask B the first international IDP guideline [1.10]. It is a comprehensive interactive guideline on how to manage the whole design process, from the design team selection to building operation and maintenance.

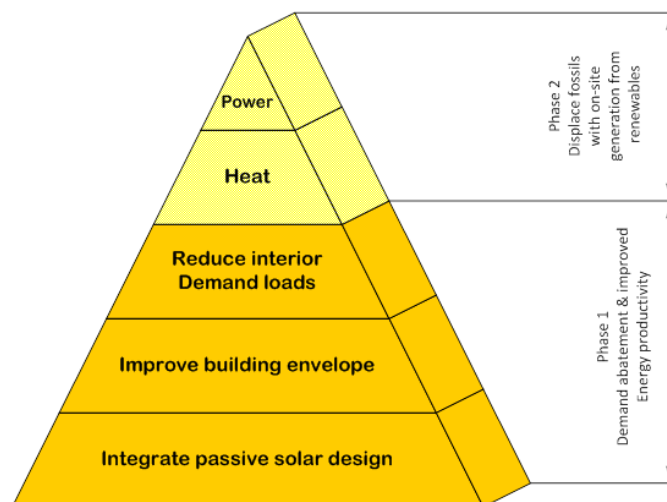


Figure 1-2. Design method focused on energy issues. Source: IEA Task 40/ECBCS Annex 52 [1.12]

More recently the BC Green Building Roundtable developed the Roadmap to the Integrated Design Process [1.11] to overcome the barriers that the roundtable sees as preventing IDP from being widely practiced. The document provides a comprehensive guide for IDP facilitators, as well as novice and seasoned participants. Simply stated, the guide outlines what the integrated design process is, how it works, and how to implement such a process.

Focusing on energy issues, the existing IDP methods generally agree on the design method summarized in the following steps (Figure 1-2):

1. use of passive solutions to minimize the energy need;
2. use of energy efficient systems to minimize the energy demand;
3. generation of power and heat from renewable energy sources.

A more detailed IDP definition is challenging, especially for non-residential buildings which often require a customized approach and considerable design effort.

Natural ventilation is always mentioned among the passive design strategies, even though no pragmatic design procedure has been yet implemented.

Smart-ECO project [1.13] collects, among others, examples of innovations that promote natural ventilation in buildings acknowledging that the correct design of natural ventilation and its interaction with architecture and mechanical systems requires a thorough integrated approach and detailed analyses of the natural phenomena occurring in the building (dynamic energy simulation tools, CFD if required, etc.).

Guideline developed within the INTEND project consider ventilation as one of the six central themes of the process [1.14]. Ventilation issues are also part of the energy engineer/modeller guide, a comprehensive overview on how to enhance the design team's understanding of design opportunities and constraints throughout each design step [1.15].

Detailed design procedures for naturally ventilated non-residential buildings are rarely described in literature and none of them considers it as integrated in the whole design process. As these studies are quite old, none of them deepens the issue of simulation tools to support natural ventilation design.

Several prior studies provide guidance on natural ventilation design [1.1][1.2][1.3][1.4][1.5][1.6]. The majority of these studies conclude with general guidance that is not specific to using building simulation to model natural ventilation performance. The one exception being the study by NIST [1.1] that develops a comprehensive design methodology that includes multi-zone airflow network modelling, but does not integrate it in the whole building energy simulation process.

The CIBSE Application Manual on natural ventilation in non-domestic buildings [1.3] provides detailed information on how to implement a decision to adopt natural ventilation. The manual focuses on the development of the design strategy, the integration of ventilation components in the building systems and provides rules of thumb for dimensioning, introducing natural ventilation simple modelling techniques.

The National Institute of Standards and Technologies (NIST) adapted the previous version of the CIBSE guidelines to US commercial buildings [1.1]. NIST also developed design tools to analyse the climate suitability (see par. 6.1.1) and to size openings through the loop design method (see par. 2.2.2).

A more recent study [1.16] considers the natural ventilation as part of the building design and integrates it within the whole building system by defining a decision support framework for the design of natural ventilation in non-residential buildings. It is though a qualitative study and no quantitative evaluation of the interactions between design parameters and energy performance is presented. The study also reports lessons learned from recently built naturally ventilated buildings.

1.2.Regulatory framework

By 2020 many countries will impose the nearly or net zero energy requirement. Building airtightness will implicitly become a mandatory point of attention, as well as energy efficient ventilation systems will become mandatory. The use of natural ventilation to improve thermal comfort and/or reducing cooling need (ventilative cooling) and to assure indoor air quality will significantly increase.

Existing CEN standards consider natural ventilation mainly as a measure to assure indoor air quality and not as a passive cooling strategy. One of the objectives of the “IEA ECBCS Annex 62 Ventilative cooling”, started in 2014, is to give guidelines for integration of ventilative cooling in energy performance calculation methods and regulations.

At present ventilation standards and guidelines define ventilation rates in non-industrial buildings to meet indoor air quality requirements. The required ventilation rates should be also based on health requirements related to the level of exposure. This is one of the goals of the HealthVent project³ attempting to define health-based ventilation guidelines for Europe.

Building codes and standard requirements are not mentioned by any of the existing IDP guidelines.

This paragraph is a summary of the codes sections relevant to natural ventilation across various countries. Above all that, other acts, codes, standards or recommendations not directly related to ventilation, comfort and energy (e.g. fire safety, acoustics..) may represent a barrier to natural ventilation systems. Barriers and constraints to natural ventilation design are discussed in par. 1.4.

1.2.1. European standard

The standard EN 15242: 2007⁴ specifies a direct method for calculating the airflow through open windows and a method for calculating the required opening of a given window as a proportion of its total area, taking into account wind turbulence, wind speed, stack effect along the height of the window, inside and outside temperature and user behaviour.

The standard EN 15243: 2007⁵ defines procedures to calculate temperatures, sensible loads and energy demands for rooms by hourly and simplified calculation methods.

Both the standards are under revision to rearrange the contents according to the EPBD recast.

The standard EN 15251: 2008⁶ establishes ventilation rates requirements to meet comfort requirements on building occupants. In

³ <http://www.healthvent.byg.dtu.dk/>

⁴ EN 15242: 2007. Ventilation for buildings — Calculation methods for the determination of air flow rates in buildings including infiltration.

⁵ EN 15243: 2007. Ventilation for buildings - Calculation of room temperatures and of load and energy for buildings with room conditioning systems.

⁶ EN 15251: 2008. Indoor environmental input parameters for design and assessment of energy performance of buildings addressing indoor air quality, thermal environment, lighting and

non-mechanically cooled buildings criteria for the thermal environment are specified differently from those with mechanical cooling during the warm season, because the expectations of the building occupants and their adaptation to heat stress are strongly dependent on external climatic conditions.

In case of naturally ventilated non-residential buildings, the Italian standard UNI TS 11300-1⁷ to evaluate the energy performance of buildings recommends to use the design ventilation rates of the UNI 10339:2008⁸. For different aims from design, i.e. indoor air quality satisfaction, the standard suggests to refer to EN 15251:2008 and UNI EN 13779:2007⁹, even though natural ventilation systems are not covered by this standard.

The Italian D.Lgs 311/06 at the Annex I, comma 9 requires to best exploit climate conditions and indoor spaces layout to favour natural ventilation strategies. Mechanical systems should be used in case natural ventilation could not be efficient.

Danish building regulation allows in general terms to take into account the effect of ventilative cooling, but does not specify how. Be10, the Danish compliance tool, allows users to input a ventilation rate value for ventilative cooling, but does not assist them in determining the value. It also does not take into account thermal comfort improvements due to elevated air velocity. Danish standard DS 447 specifies requirements for natural ventilation systems among others and also includes ventilative cooling expressed as free cooling, night cooling, passive cooling, cooling by means of natural ventilation and elevated air velocities effect.

Cooling demand in the Dutch building regulations NEN8088 accounts for passive night cooling, presence of windows and natural supply air systems.

acoustics.

⁷ UNI TS 11300-1. Energy performance of buildings – Part 1: Evaluation of energy need for space heating and cooling.

⁸ UNI 10339:2008. Impianti aeraulici a fini di benessere.

⁹ EN 13779:2007. Ventilation for non-residential buildings – Performance requirements for ventilation and room-conditioning systems.

Austrian national code B8110-3 (2012) on the prevention of summer overheating ventilation flow through windows is taken into account in the dynamic heat balance calculation according to EN ISO 13791 by applying a simplified formula which depends on temperature difference between inside and outside.

Part F of the UK building regulation focuses on ventilation for IAQ purposes. Ventilation to control thermal comfort is not controlled under the building regulation. Ventilative cooling is considered as part of energy performance according to the latest proposed changes (2013) of the Part L of the regulations, based on the EPBD recast.

CIBSE Guide B2 (2001) establishes the required ventilation rates to satisfy indoor air quality requirements.

The CIBSE Applications Manual AM10 – Natural Ventilation for Non Domestic Buildings is the main guidance used in the UK. The criteria for design is to not exceed 28°C for more than 1% annual occupied hours, based on an ideal summer design temperature of $25 \pm 3^\circ\text{C}$. Unlike the International Mechanical Code (IMC)¹⁰, there is no minimum operable window area requirement; rather the application manual provides design guidance and strategies to apply in order to meet the maximum overheating hours requirement. Compliance has to be documented through energy modelling software.

1.2.2. US standards

The IMC is the most popular mechanical code adopted and used in the United States. Chapter 4 of the IMC addresses ventilation and provides requirements for both natural and mechanical ventilation. Under natural ventilation, the minimum required area of operable window is based on building area being ventilated. The minimum opening area to the outdoors shall be 4% of the floor area being ventilated. Adjoining spaces without direct access to the outdoors must be provided with an unobstructed opening to an exterior space, sized at 8% of the floor area

¹⁰ The International Mechanical Code (IMC) is a convention concentrating on the safety of heating, ventilation and air conditioning systems, published by the International Code Council (ICC). It is used as the basis for the mechanical code of several countries.

of the interior space, but not less than 2.3 m². Operable openings shall be readily accessible to building occupants whenever the space is occupied.

The Uniform Mechanical Code (UMC) includes the same natural and mechanical ventilation requirements as the IMC but further requires that naturally ventilated spaces are located within 7.6 m of operable wall or roof openings to the outdoors.

The California Title 24 (Energy efficiency standards for non-residential buildings) requires that naturally ventilated spaces shall be permanently open to and within 6 m of operable wall or roof openings to the outdoors, the opening area of which is not less than 5% of the conditioned floor area of the naturally ventilated space.

ASHRAE Standard 62.1 specifies the minimum ventilation rates and IAQ level that will be acceptable to human occupants and minimize the potential for adverse health effects but does not address thermal comfort. For naturally ventilated spaces, Standard 62.1 provides requirements for minimum opening areas and maximum distances from opening areas (8 m) similar to the UMC requirements. In addition to the UMC requirements, Standard 62.1 requires local user control/access to operable windows/roofs and specifies minimum separation distances between air intakes and potential contamination sources.

The 2010 update of Standard 62.1 added new requirements, including a requirement that natural ventilation systems be combined with mechanical ventilation systems, with a few exceptions. Also added are limitations on floor areas that can be naturally ventilated based on the ceiling height and three ventilation configurations: single sided, double sided and corner openings.

ASHRAE standard 55 identifies the factors of thermal comfort and the process for developing comfort criteria for a building space and the occupants of that space. Standard 55 considers combinations of different personal and environmental indoor space factors that will result in thermal environmental conditions that are acceptable to at least 80% of the occupants. Personal factors include clothing and activity level, and environmental factors include humidity, temperature, thermal radiation and air speed at steady state conditions. For naturally

ventilated spaces, the standard provides a broader range of acceptable indoor air temperatures based on monthly outdoor temperatures. This broader range of acceptable indoor temperatures is based on field experiments that demonstrate different thermal responses for naturally ventilated spaces than mechanically cooled spaces due to different thermal experiences, occupant perception, local control and accessibility. While Standard 55 assumes steady state conditions, it is very rare to encounter steady state conditions in real buildings. In naturally ventilated buildings, occupants can better adapt to a higher temperature or larger range of acceptable temperatures by having access to operable window controls and by being able to react to the changing conditions.

The LEED rating systems are not a design guide and do not provide criteria for natural ventilation, however it does reference ASHRAE Standards and CIBSE Application Manuals that provide design criteria for natural ventilation. The LEED NC rating system contains prerequisites and credits in the Environmental Quality (EQ) section and credits under the Energy and Atmosphere (EA) section that could potentially be achieved by utilizing a natural or mixed mode ventilation strategy.

1.2.3. Other countries

Within the PERENE (ENERgy PERFORMANCE of Buildings in French) project a document was developed based on experience and local skills to help the design of low energy buildings in the French tropical island of La Reunion [1.17]. Cross ventilation is one of the mandatory requirements to get a low energy building in that climate context. The document gives recommendation about minimum façade porosity, minimum opening surface per room area and indoor spaces organization.

Part F4 Light and Ventilation of the Building Code of Australia provides the requirements for natural light and natural ventilation. The prescriptive requirements are similar to the IMC requirements for minimum opening area based on floor area being ventilated. The total minimum opening size shall not be less than 5 % of the floor area of the

room required to be ventilated. For ventilation borrowed from adjoining rooms, the window, opening, door or other device has a ventilating area of not less than 10 % of the floor area of the room to be ventilated, measured not more than 3.6 m above the floor and the adjoining room has a window, opening, door or other device with a ventilating area of not less than 10% of the combined floor areas of both rooms.

1.3.Natural ventilation as passive design solution for Net Zero Energy Buildings

Within the IEA Task 40 research project on Net Zero Energy solar Buildings worldwide national experts investigated whole building solution sets for Net ZEBs.

For solution set we mean the combination of passive, energy efficiency and active solutions able to achieve a Net Zero Energy performance. For instance, natural ventilation can be used as passive approach to reduce cooling need and to provide better thermal comfort, mainly in combination with advanced envelope and solar shadings.

Thirty well documented, existing Net ZEBs have been categorized by building typologies (residential, office and educational buildings) and by the climate challenges the design team had to face with:

- heating dominated (HD)
- heating and cooling dominated (HCD)
- cooling dominated (CD).

The climate classification method here applied identifies the biggest space conditioning challenge faced by the building taking into account not only the climate conditions but also the activity in the building and its architectural consistency, depending on typology [1.18]. The idea behind this new climate classification is that in buildings with high internal heat gains (office, commercial and school buildings) designers can face challenges that do not follow closely the external climate conditions.

Among the eighteen non-residential buildings analysed, it was observed that natural ventilation is used in most of the buildings that have to face

with cooling challenges. The dataset is small because one of the requirements was the availability of monitored data, but it is really an indicator of the relatively modest number of monitored buildings worldwide which claim Net ZEB status.

This section analyses the use of natural ventilation as part of a solution set to reach the Net Zero Energy target.

In the analysed case studies natural ventilation has been designed to reduce cooling needs and improve thermal comfort. Indoor air quality issues are beyond of the scope of the IEA Task 40 project. Table 1-1 reports the case studies within the category non-residential that use natural ventilation to face cooling challenges.

Four of them are located in a cooling dominated climate. The remaining six buildings are located in a mixed heating and cooling dominated climate.

Table 1-1. Naturally ventilated non-residential buildings within the IEA Task 40 case studies (edu.= educational).

Project	Location	Climate	Bld type	n. of stores	Net floor area [m ²]	S/V
 Enerpos	France - La reunion	CD	edu.	3	681	0.57
 Ilet du centre	France - La reunion	CD	office	5	310	11.1
 Pixel	Australia	CD	office	4	1085	0.46
 ZEB_BCA Academy	Singapore	CD	edu.	3	4500	nd
 Circe	Spain	HCD	office	2	1743	0.52

Project	Location	Climate	Bld type	n. of stores	Net floor area [m ²]	S/V
 <p>Green office</p>	France	HCD	office	8	21807	0.53
 <p>Limeil Brevannes school</p>	France	HCD	edu.	3	2935	nd
 <p>Meridian</p>	New Zealand	HCD	office	4	5246	0.21
 <p>Pantin primary school</p>	France	HCD	edu.	4	3560	0.36
 <p>Solar XXI</p>	Portugal	HCD	office	3	1500	0.40

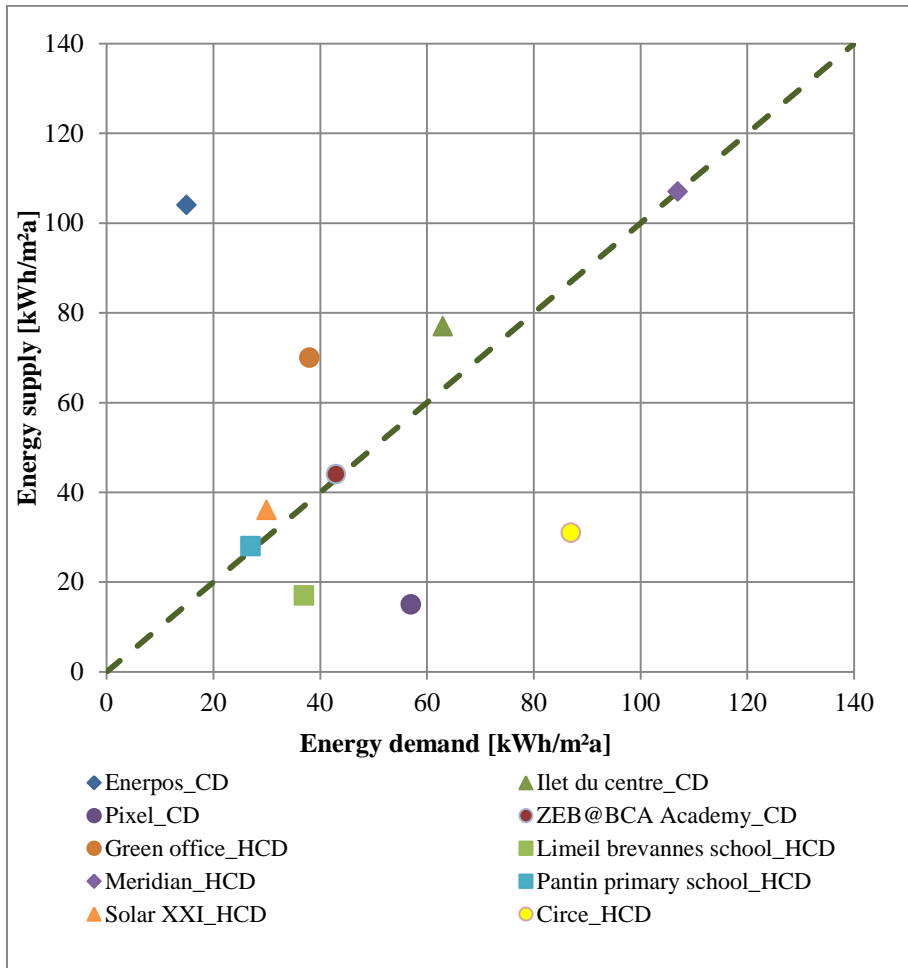


Figure 1-3. Energy balance of the analyzed case studies.

As shown in Figure 1-3, three buildings have a negative balance because their energy demand is more than the energy produced on site. Table 1-2 summarizes the solution sets applied to each case study to face cooling challenges. It can be generally noticed that if natural ventilation is exploited during the day, no cooling plant is needed. Pixel, Meridian and Circe building use night ventilation to reduce cooling need over the following day and thermal comfort during the day is assured by cooling plant.

Table 1-2. Solution sets applied to the case studies to face cooling challenges.

Building	Enerpos	Ilet du centre	Pixel	ZEB @ BCA	Green office	Limeil Brevannes school	Meridian	Pantin primary school	Solar XXI	Circe
Climate	CD	CD	CD	CD	HCD	HCD	HCD	HCD	HCD	HCD
sun shading										
night cooling										
evaporative cooling										
cross ventilation										
stack ventilation										
solar chimney										
green roof/facade										
ground cooling										
ceiling fans										
cooling plant										

Figure 1-4 shows the averaged envelope elements U-values and window g-values applied to the each case study.

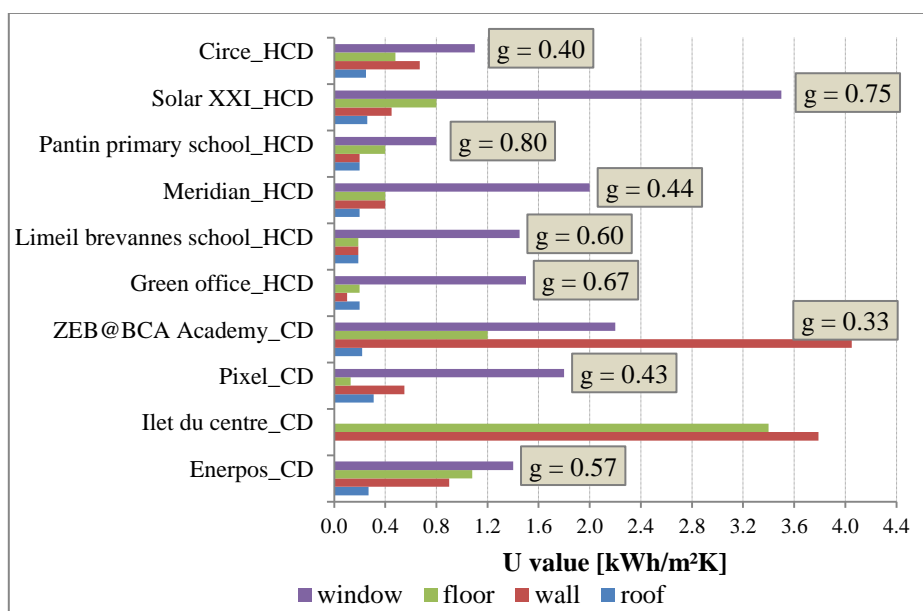


Figure 1-4. Average U-values for wall, floor, roof and window and g-value of windows for the case studies.

1.3.1. Natural ventilation in cooling dominated climates

In a cooling dominated climate the combination between sun shading, presence of vegetation, natural cross ventilation, ceiling fans and efficient lighting/electric equipment seems to be the best solution set. Among the four buildings located in cooling dominated climate, two of them, the Enerpos (La Reunion) and the Ilet du Centre (La Reunion) apply this solution set and does not need any cooling plant. Figure 1-5 shows one of the classrooms in the ENERPOS building where opposite windows and vents positions allow natural cross ventilation. The two buildings follow the design guidelines for French buildings in tropical climate developed within the PERENE Reunion (PERformances ENergétiques des bâtiments à La Réunion) project [1.17]. They also reach easily the Net Zero Energy balance thanks to the roof mounted PV system.



Figure 1-5. ENERPOS classroom with ceiling fans and vents allowing cross ventilation. Source: STC database.

The PIXEL¹¹ building design is mainly focused on daylighting solution. Therefore it has an extensive glazed surface protected by a complex system of solar shadings studied to allow daylighting, avoiding at the same time glare situations. This causes high solar gains

¹¹ <http://www.pixelbuilding.com.au/>

and the need of more complex active solutions: an active mass cooling system and an Underfloor Air Distribution (UFAD) with air heat recovery. High levels windows to the north and west facades are operated at night in summer by the Building Management System (Figure 1-6). These windows open for passive night cooling to flood the office floors with cool night air so that the exposed ceiling absorbs that cool, thus reducing the requirement for hydraulic cooling in the morning at start-up.



Figure 1-6. Interior view of the Pixel building with controlled high level windows.
Source: STC database

At the Building and Construction Academy¹² ZEB in Singapore the principle of solar chimney ventilation is used to increase air speed and improve thermal comfort in the school hall and classrooms. Air in the chimney expands under heating from the sun and being relatively lighter, it rises, allowing cooler air to enter the building from the fenestrations (Figure 1-7). This pull effect is complemented further by the push effect from the ambient wind. During a typical hot day, surface temperature of the solar chimney can reach up to 60°C, while the air within can achieve temperature of 47°C and speed of 1.9 m/s. This leads into one to two hours positive temperature time lag in the

¹² <https://www.bca.gov.sg/zeb/>

classroom, a higher air speed reaching a maximum of 0.49 m/s, and an average air change rate per hour of 9 ACH in the afternoon. An extraction fan is installed in each chimney to provide the extraction when natural stack effect is not functioning. Offices are cooled through chiller plants and cooling tower.

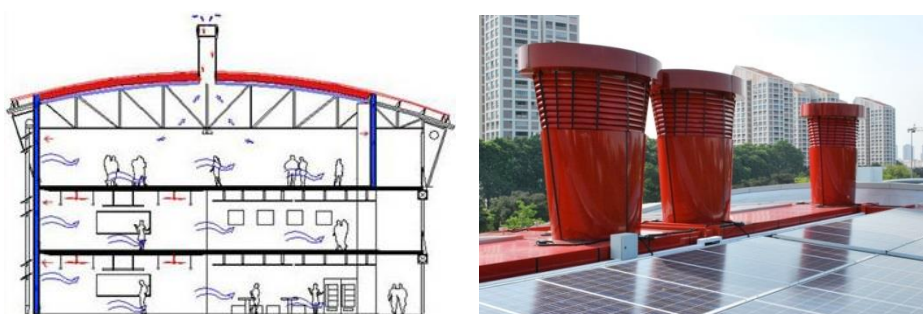


Figure 1-7. Cross section (link) and solar chimneys (right) of the ZEB at BCA.
Source: STC database

As shown in the graph in Figure 1-4, buildings located in cooling dominated climates have higher opaque envelope U-values than buildings located in heating and cooling dominated climates and g-values are lower than 0.6 to reduce the solar heat gains. In all the cases particular care has been taken to the microclimate to reduce the heat island effect: green roof, green facade and plants around the building.

1.3.2. Natural ventilation in heating and cooling dominated climates

Among the six naturally ventilated non-residential buildings facing both heating and cooling challenges in the database, two of them are educational buildings and the rest are office buildings.

Thanks to the exploitation of ventilative cooling and helped by the occupation patterns (typically schools are not occupied during summer period), educational buildings does not need any cooling plant.

Both Jean-Louis Marquèze school in Limeil-Brevannes (France) and the primary school in Pantin (France) meet comfort and cooling requirements by means of a combination of diurnal cross ventilation and night cooling with high thermal mass.

Office building needs a more complex solution set due to the higher internal heat gains and the most extensive use.

The solution set implemented in the Green Office Meudon¹³ building in Paris to face cooling challenges exploits fully the natural ventilation potential. The façade is divided into different parts which play different roles. Figure 1-8 shows the modular fenestration of the building: a fixed glazed part with outside shadings, a smaller operable window allows fresh air direct inlet and a shaft beside the window allows stack effect natural ventilation and passive cooling control. The biggest fixed glazed part allows daylighting and outside view. Direct ventilation can be activated by opening windows. The shafts connect all the floors allowing stack effect ventilation and their opening can be modulated to control air speed. Over summer nights the shafts are left completely opened to maximize night flush cooling. There is no false ceiling in order to allow ceiling thermal mass activation. Ceiling fans can be activated by users to improve thermal comfort. During winter the building is mechanically ventilated with heat recovery.

The façade function dissociation concept has been also applied in the Nicosia town hall in Cyprus [1.19] and as a retrofit solution for the Net Zero Energy Retrofit 2020 Testbed at the Cork Institute of Technology in Ireland [1.20].



Figure 1-8. Green office solution set to face cooling challenges. Source: STC IEA T40/A52 database

The Solar XXI office building in Portugal has a three floor stair well with an operable glazed part at the top for both natural daylighting and

¹³ <http://www.green-office.fr/en/realisations/meudon/overview>

air exhausting (Figure 1-9). The offices are connected to the light well through vents located above the doors. The natural ventilation is also used to extract heat from the façade integrated PV panels. Air inlet and outlet can be managed in different modes depending on the climate (Figure 1-10). When outdoor air temperature is significantly higher users can use ground cooling provided by the air entering the building through 32 buried pipes.

Building monitoring undertaken during summer 2007 showed that air temperature remains below 27°C over 95% of the observation period [1.21]. The air temperature difference between the lower floor and the upper floor reach 5°C during summer.

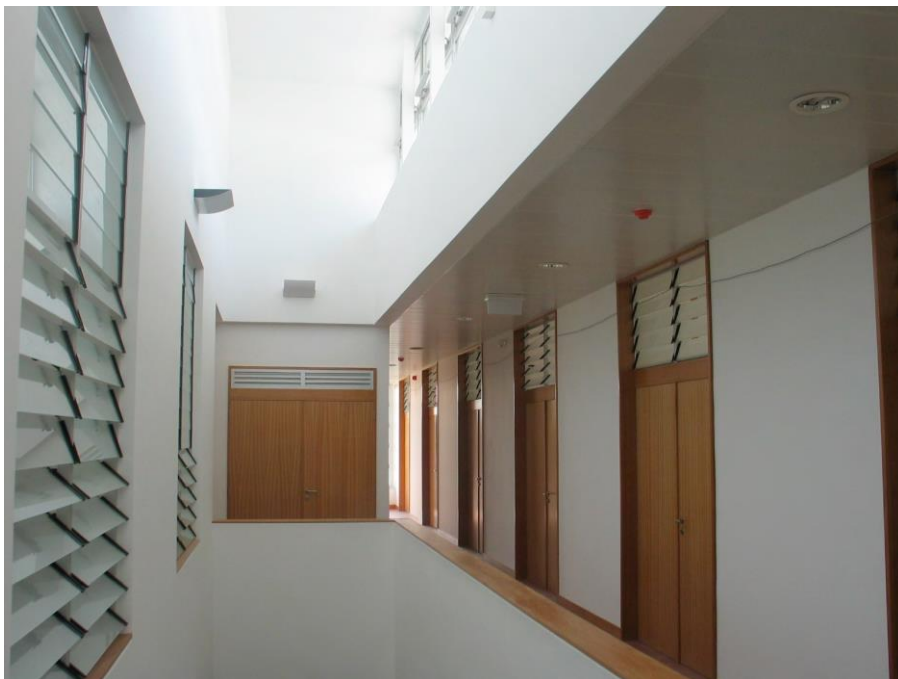


Figure 1-9. Solar XXI: light well for natural lighting and air exhausting. Vents connecting offices to the light well. Source: STC database

Envelope thermal transmittances (Figure 1-4) are more dependent on national regulations. Generally, for buildings located at middle-high latitudes U value for walls are between 0.1 and 0.4 kW/m²K. They are higher in Mediterranean climates and even higher in tropical climates,

especially when no cooling plant is installed. U values for roof is lower than $0.3 \text{ kW/m}^2\text{K}$ in every case study.

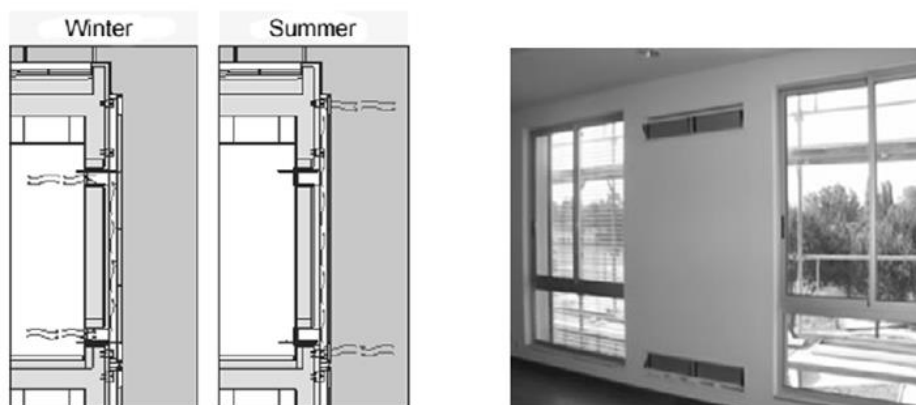


Figure 1-10. Solar XXI BIPV-T system. Source: STC database

1.4.Barriers and constraints

Barriers and constraints have been largely investigated in previous projects.

Within the European project NatVent, a survey was conducted across seven countries (Denmark, Switzerland, Norway, Belgium, Great Britain, The Netherlands and Sweden) to address the barriers that restrict the implementation of natural or simple fan-assisted ventilation systems in the design of new office buildings and in the refurbishment of existing such buildings [1.22]. A total of 107 interviews with architects, consultant engineers, contractors, developers, owners and the governmental decision makers responsible for regulations and standards were conducted to address their general knowledge, viewpoints, experience and perceived problems with natural ventilation systems in office type buildings, as well as understand the decisions taken in a specific building project.

The interviewees expect a higher user satisfaction and lower installation, running and maintenance costs in naturally ventilated buildings, but they recognize several advantages in mechanical ventilation systems in terms of cooling effectiveness, IAQ assurance and controllability. Their experience with designed naturally ventilated

buildings is significantly lower than with mechanically ventilated buildings. They also request for standard and guidelines improvements and for simple design tools that can be used in the early design process. Most of the interviewed architects and consultant engineers are paid for the detailed design according to a fixed fee, which is often a percentage of the construction costs, and are normally only paid a 'per hour rate' in the case of initial draft design or small specific design tasks. This may advantage mechanical ventilation, which takes less time to be designed and has higher installation costs.

Also more recent interviews to design professionals conducted across California within the CEC natural ventilation project [1.23] underline the higher design effort required for natural ventilation design compared to mechanical ventilation and the lack of design tools. The installation costs are now perceived as higher for natural ventilation rather than for mechanical ventilation because of the additional hardware for windows control and operation.

In fact, the designers are faced with many, and sometimes, conflicting requirements in the task of designing natural ventilation. In meeting the design need it is necessary to consider a wide range of criteria varying from building standards and regulations accomplishment to installation and maintenance.

Existing natural ventilation guides [1.2][1.24][1.25] address important design constraints, which can be summarized as:

- Building regulations and standards: as shown in par. 1.2, building regulations and standards are often prescriptive, in the sense that they specify the minimum ventilation rate or the minimum opening area. There is also strong correlation between standards covering the requirements for energy efficiency (air tightness) and comfort to those associated with other aspects of indoor air quality (e.g. health). Acoustics regulation and fire safety regulations can put constraints regarding the vent connections between different zones/rooms of between inside and outside. Products available on the market allows overriding these issues. A survey among 12 countries has been performed within HybVent project to identify paragraphs in acts, codes, standards or recommendations that may

represent a barrier to hybrid ventilation systems in office and educational buildings [1.26].

- Building type: commercial/office buildings are more densely occupied, polluted and have higher internal gains; school buildings are dominated by high occupant loads, very transient occupation and high levels of metabolic activity; shopping malls often enclose large open spaces and atria with high solar and internal gains which can be drivers for natural ventilation; hospitals need to control and filter fresh air to patient; food store need to control and filter fresh air to avoid fresh food contamination; residential buildings are occupied for longer period. There are also other problems related to user acceptability and building operation, like safety, undesired draught and presence of shadings.
- Local outdoor environment: aside the outdoor climate conditions, outdoor air quality issues and noise levels influence the design of natural ventilation systems. Ventilation systems cannot rely upon low-level inlets since the outdoor air at street levels may be contaminated and inlets will be shielded from winds. Furthermore, the use of natural ventilation in the urban environment should take into account the effect of surroundings on wind velocity and direction but also on outdoor temperatures (heat island effect).

It is also necessary to integrate the ventilation system itself into the overall design of the building, especially in relation to airtightness, room partitioning and accessibility. Since such a wide range of parameters is involved both from architectural and constructive point of view, a solution has to be found out through an integrated design process. Table 1-3 shows the building professionals role and the information sharing needs regarding natural ventilation within the integrated design process. It also gives an idea about the design constraints due to other important requirements fulfilment such as fire safety, acoustics and building structure.

Table 1-3. Role of every building professional within the natural ventilation IDP and information exchanges.

Building professionals	Task	Information needed	Information to be shared
Architect	Lower the architectural impact of the solution or integrate it into the design concept	<ul style="list-style-type: none"> – opening size and position – presence of chimneys, stacks, ducts and atria – connections within zones – users' needs 	<ul style="list-style-type: none"> – indoor spacing layout – architectural concept constraints
Structure engineer	Building structure design	presence of stacks, chimneys, ducts and other possible interferences with the building structure	building structure constraints
HVAC engineer	Users comfort Air quality Accomplishment with the standard requirements Plant sizing	<ul style="list-style-type: none"> – inlet location – cooling peak load – airflow rates – air velocity – indoor temperature and humidity 	<ul style="list-style-type: none"> – ventilation efficiency – cooling plant size – ducts size
Electric engineer	Building Management System programming Lighting and electric plant	<ul style="list-style-type: none"> – control strategy – sensors and actuators specification – users control needs 	BMS user manual
Energy specialist	Energy efficient building	<ul style="list-style-type: none"> – architectural concept constraints – building structure constraints – constructions – climate conditions – use pattern 	<ul style="list-style-type: none"> – energy consumption – cooling peak load – airflow rates – opening size and position – fan assist size – free cooling opportunities – control strategy – thermal zoning
Fire safety	Fire strategy	building plans	<ul style="list-style-type: none"> – fire compartments – escape routes
Acoustics specialist	Accomplishment with building acoustics regulations Privacy	<ul style="list-style-type: none"> – structural components – rooms connections through vents/ducts – surrounding traffic and noise – privacy needs 	<ul style="list-style-type: none"> – acoustic performance specification – acoustic zoning

	Protection against outdoor noise		
Users	Indoor environmental comfort	BMS user manual Natural ventilation user manual Maintenance plan	<ul style="list-style-type: none"> – use patterns and activities – control needs – privacy needs – safety needs – flexibility requirements – maintenance needs

The constraints found during the natural ventilation design of one of the new office buildings in the new Technology Park of Bolzano [1.27] and solved thanks to an IDP can be reported as example.

Figure 1-11 shows the cross section of the building fire regulation plan used to plan the natural ventilation strategies.

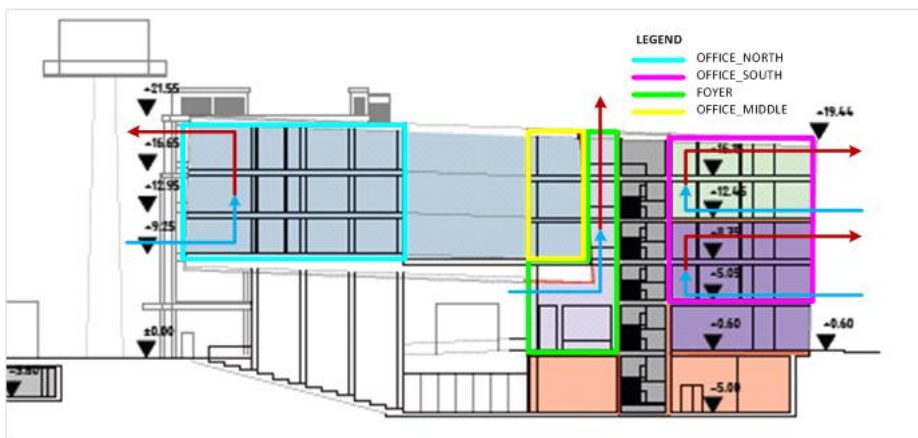


Figure 1-11. Cross section of the building fire regulation plan with fire compartments, model zones and a scheme of the selected stack-driven cross ventilation configurations for the considered zones.

The agreed solution balances performance needs with constraints given by fire regulations, acoustic comfort and user's needs, and to keep acceptable the architectural impact of the solution.

To maintain the indoor spaces layout flexibility it was not possible to plan ventilation shaft or stack devices and to estimate accurately the pressure drops due to the internal walls and vent size.

Furthermore, the plan of natural ventilation has to strictly comply with fire regulations and plans. The building is divided into fire compartments enclosed with a fire resistive construction that have to be by definition air tight or closable. A natural ventilation configuration that involves more fire compartments should use components with high fire resistance ratings. Due to the high additional costs it was decided to study a natural ventilation configuration for every fire compartment. Furthermore, acoustic problems due to air connections between offices and plans should not be neglected as the future users need privacy during the working hours.

Another constraint was about the architectural impact of the solutions. The monolithic block feature has to be maintained by reducing as much as possible the movable part in the façade, operable windows included.

Bibliography

- [1.1] Axley J. W. Application of Natural ventilation for US commercial buildings. GCR-01-820 NIST, 2001.
- [1.2] Allard F., Santamouris M. Natural ventilation in building design - A design handbook. 1998.
- [1.3] Natural ventilation in non-domestic buildings. Chartered Institution of Building Services Engineers. CIBSE guide AM10:2005.
- [1.4] Martin A., Fitzsimmons J. Guidance Note GN 7/2000: Making Natural Ventilation system work. Bracknell, Berkshire, UK : The Building Services Research and Information Association (BSRIA), 2000.
- [1.5] Martin A.J. Technical Note TN 11/95: Control of Natural Ventilation. The Building Services Research and Information Association (BSRIA), Berkshire, UK 1996.
- [1.6] Natural Ventilation in Non-Domestic Buildings. Garston, Watford, UK : Building Research Establishment, 1994.
- [1.7] Leutgöb K. Introduction to Integrated Design (ID). [Online] 05 23, 2013. http://www.e-sieben.at/en/projects/1210_matrid.php.
- [1.8] EU INTEND project. Mapping of previous integrated energy approaches. Part of work package no. 2 - task 2.1, 2009.
- [1.9] Andresen I., Kleiven T., Knudstrup M.A., Heiselberg P. Integrated Building Concepts - State of the art review. IEA Annex 44, 2006.
- [1.10] Löhnert G., Dalkowski A., Sutter W. Integrated Design Process - A guideline for sustainable and solar- optimized building design. Berlin/Zug : IEA task 23 "Optimization of Solar Energy Use in Large Buildings" - subtask B "Design process guidelines", 2003.

- [1.11] Busby Perkins+Will. Roadmap to the Integrated Design Process. 2010.
- [1.12] IEA SHC Task 40 / ECBCS Annex 52. Towards Net Zero Energy Solar Buildings (NZEBS). <http://www.iea-shc.org/task40/index.html>. [Online]
- [1.13] Smart-ECO. WP3 Innovation, Deliverable 4 - Innovation supporting the vision on sustainable buildings. 2009.
- [1.14] INTEND project. A guide to Integrated Energy Design. Some principles of low energy buildings. www.intendesign.com. [Online] 09 2009. [Cited: 05 12, 2011.]
- [1.15] Northwest Energy Efficiency Alliance (NEEA). Integrated energy engineering and performance modeling into the design process. [Online] 2011.
http://www.betterbricks.com/graphics/assets/documents/Performance_Modeling_FINAL-WEB.pdf.
- [1.16] Zaho Y. A decision support framework for design of natural ventilation in non-residential buildings. Virginia Polytechnic Institute and State: PhD Thesis, 2007.
- [1.17] Garde F., David M., Adelard L., Ottenwelter E. Elaboration of thermal standards for french tropical islands: presentation of the PERENE project. Clima. Lausanne, 2005.
- [1.18] Cory S., Lenoir A., Donn M., Garde F. Formulating a building climate classification method. Building Simulation. Sydney, 2011.
- [1.19] Flourentzou F. Hybrid ventilation and cooling technics for the new Nicosia Townhall. 33rd AIVC Conference and 2nd TightVent Conference. Copenhagen, 2012.
- [1.20] Cork Institute of Technology (CIT). ZERO 2020 Energy. [Online] 2013.
<http://www.zero2020energy.com/>.
- [1.21] Oliveira Pano M. J. N., Goncalves H. J. P. Solar XXI building: Proof of concept or a concept to be proved? Renewable Energy, 2011.
- [1.22] Aggerholm S. Perceived barriers to natural ventilation design of office buildings. Annual AIVC conference. Oslo, 1998.
- [1.23] CEC Natural ventilation project. UC San Diego. <http://ssi.ucsd.edu/>. [Online] 2010.
http://ssi.ucsd.edu/index.php?option=com_content&view=article&id=460&Itemid=2.
- [1.24] Liddament M. A guide to energy efficient ventilation. AIVC, 1996.
- [1.25] Santamouris M., Wouters P. Building ventilation. The state of the art. London : Earthscan, 2006.
- [1.26] Delsante A., Arvid Vik T. Hybrid ventilation - State of the art review. IEA-ECBCS Annex 35, 1998.
- [1.27] Belleri A., Castagna M., Lollini R. Natural night ventilation as passive design strategy for a Net Zero Energy office building. Improving Energy Efficiency in Commercial Buildings. Frankfurt, 2012.

2. Natural ventilation modelling

First step to develop a design procedure is to understand physical principles and to document existing modelling methods and tools assessing capabilities, gaps, needs and problems in the context of natural ventilation performance prediction. Existing tools range from simple empirical formulas to complex dynamic simulation environments. Their applicability at a certain design stage depends on the required input data detail level and output data accuracy. Therefore, needs of development of current tools and modelling techniques are addressed in this chapter.

2.1. Physical principles

Natural ventilation relies on natural forces: wind and air temperature differences generate pressure gradients between outdoor and indoor or between different internal zones. Air flows through openings and cracks from outdoor to indoor if pressure gradient is positive and exit if pressure gradient is negative. The indoor/outdoor pressure difference depends on the magnitude of driving mechanisms and from characteristics of openings and cracks in building envelope. Wind and buoyancy forces are extremely variable, depending on weather conditions and building's and openings' layout.

2.1.1. Stack effect

Hydrostatic pressure of air masses located inside and outside a building causes the stack pressure. Hydrostatic pressure distribution depends on air density and height above a reference point. Density is function of barometric pressure, temperature and humidity, even if humidity influence is generally negligible.

In not conditioned buildings, indoor air, usually warmer than outdoor air, tends to flow out from upper openings and recalls external fresh air from lower openings, as shown in Figure 2-1. Temperature differences generate air density differences and consequently a pressure gradient; air flows to restore pressure equilibrium condition. Vertical pressure distribution depends from air density and height above ground level.

$$p(z) = p_0 - \rho \cdot g \cdot z \quad \text{Equation 2-1}$$

where

$$\begin{aligned} p_0 &= \text{atmospheric pressure at } z = 0 \text{ [Pa]} \\ \rho &= \text{air density at } z \text{ level and } T \text{ temperature [kg/m}^3\text{]} \\ g &= \text{gravity acceleration [m/s}^2\text{]} \end{aligned}$$

In Equation 2-1 air density depends from temperature according to the relation in the Equation 2-2.

$$\rho = \rho_0 \frac{T_0}{T} \quad \text{Equation 2-2}$$

where

$$\begin{aligned} \rho_0 &= \text{air density at reference point level and temperature [kg/m}^3\text{]} \\ T_0 &= \text{reference temperature [273.15 K]} \\ T &= \text{temperature of } z \text{ level [K]} \end{aligned}$$

To exploit buoyancy forces in natural ventilation, outdoor temperature must be lower than indoor temperature. The different hydrostatic pressure distribution on internal and external building surfaces creates local horizontal gradients along the building height (see Figure 2-1). Neglecting vertical density gradient and considering an opening or crack at z height above a reference level, the stack pressure gradient is given by Equation 2-3.

$$\begin{aligned} \Delta p_s &= (\rho_o - \rho_i) \cdot g \cdot (z_{n.p.l.} - z) = \\ &= \rho_o \cdot \left(\frac{T_i - T_o}{T_i} \right) \cdot g \cdot (z_{n.p.l.} - z) \end{aligned} \quad \text{Equation 2-3}$$

where

ρ_o = outdoor air density [kg/m^3]

ρ_i = indoor air density [kg/m^3]

g = gravity acceleration [m/s^2]

T_o = outdoor temperature [K]

T_i = indoor temperature [K]

z = height of opening/crack above a reference level [m]

$z_{n.p.l.}$ = height of neutral pressure line above a reference level [m]

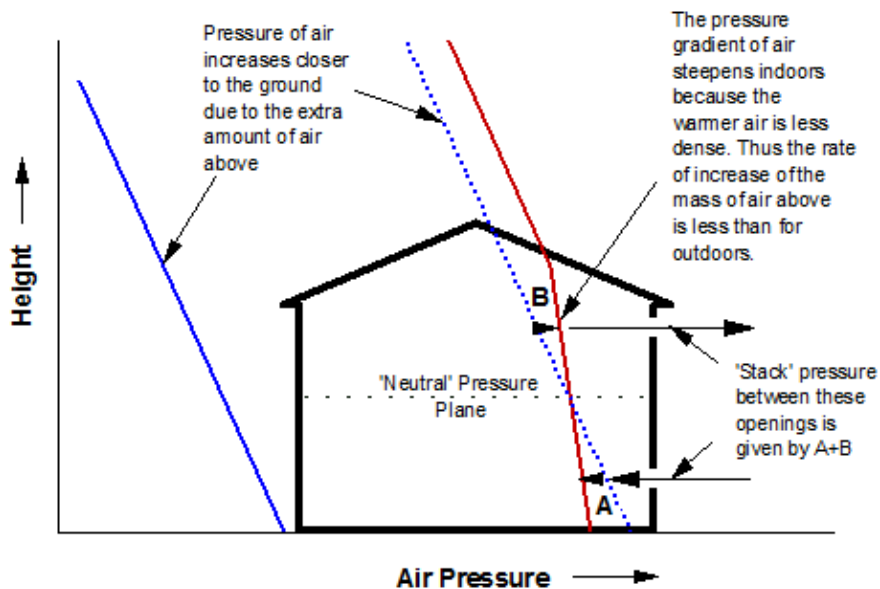


Figure 2-1. Stack effect drivers. Source: <http://www.eng.upm.edu.my/>

At the same height, if external pressure is higher than internal one, a positive difference of pressure acts on building external surface and the air tends to flow indoor. On the contrary, if external local pressure is lower than internal ones, air flows out from the building through openings and cracks. Stack pressure is proportional to the difference between internal and external temperature and to the distance from the neutral pressure level. At neutral pressure level the pressure difference is zero and therefore there is no air motion between outdoor and indoor. In absence of other driving forces, the neutral pressure level position depends on leakages area and distribution over the building and on interior layout. An accurate estimation of neutral pressure level ensures

correct fresh air paths. Especially if natural ventilation is used to improve the indoor air quality, it is important to place the neutral pressure line as high as possible, to ensure the inlet of fresh air from openings below.

If internal and external pressure distributions are known, the correct position of neutral pressure level can be calculated considering a null gradient of pressure. Generally fresh air inlet due to the stack effect in upper stores of buildings is low, but it can be increased by a chimney or by means of fans (hybrid ventilation).

2.1.2. Wind pressure

Wind creates overpressure on windward surfaces and depression on leeward surfaces, according to incidence direction, dimension and slope of building surface and presence of obstructions in the surroundings. The pressure on building envelope drives the airflow through openings and cracks, from pressure zones to depression ones. Pressure difference between internal and external air due to wind is given by Equation 2-4.

$$\Delta p_w = 0.5 \cdot C_p \cdot \rho_o \cdot v^2 \quad \text{Equation 2-4}$$

where

Δp_w = difference of pressure due to wind effect [Pa]

C_p = wind pressure coefficient []

ρ_o = outdoor air density [kg/m³]

v = local wind speed [m/s]

Starting from weather data, a wind speed profile can be estimated. Correction factors relate the wind speed recorded by the weather station, to the local wind speed, depending on terrain type and height above ground.

The wind pressure coefficients allow representing the effectiveness of wind power on building surfaces. It depends on wind incidence angle on façade and building geometry; in general, windward façades have positive wind pressure coefficient values and leeward façades have negative wind pressure coefficients. The pressure coefficient are defined as the ratio of static pressure to dynamic pressure at a given

point on the façade. Equation 2-5 gives the wind pressure coefficient at height z for a given wind direction θ .

$$c_p(z, \theta) = \frac{p_z - p_0}{\Delta p_w(z)} \quad \text{Equation 2-5}$$

where

p_z = static pressure at height z on the building façade [Pa];

p_0 = static reference pressure [Pa];

Δp_w = dynamic pressure due to the wind at height z [Pa].

Wind pressure coefficients evaluation approaches are described in paragraph 3.3.7.

The standard approach to exploit wind driven ventilation is to design horizontal flow paths according to main wind directions (cross ventilation). However strategies of vertical ventilation can benefit from wind forces by using chimneys with wind catcher or by combining wind and stack effects.

2.1.3. Combination of wind and stack effect

In real applications, building airflows are driven from a combination of wind and thermal effects. Depending on weather conditions and building operation, wind forces can prevail against buoyancy forces and vice versa. Total pressure difference across each leakage at z level is given by the Equation 2-6.

$$\Delta p_t = 0.5 \cdot C_p \cdot \rho_o \cdot v^2 + \rho_o \cdot \left(\frac{T_i - T_o}{T_i} \right) \cdot g \cdot (z_{n.p.l.} - z) \quad \text{Equation 2-6}$$

where

Δp_t = total difference of pressure [Pa]

C_p = wind pressure coefficient []

v = local wind speed [m/s]

$z_{n.p.l.}$ = height above ground of normal pressure line [m]

z = height of opening/crack above a reference level [m]

ρ_o = outdoor air density [kg/m^3]

g = gravity acceleration [m/s^2]

T_o = outdoor temperature [K]
 T_i = indoor temperature [K]

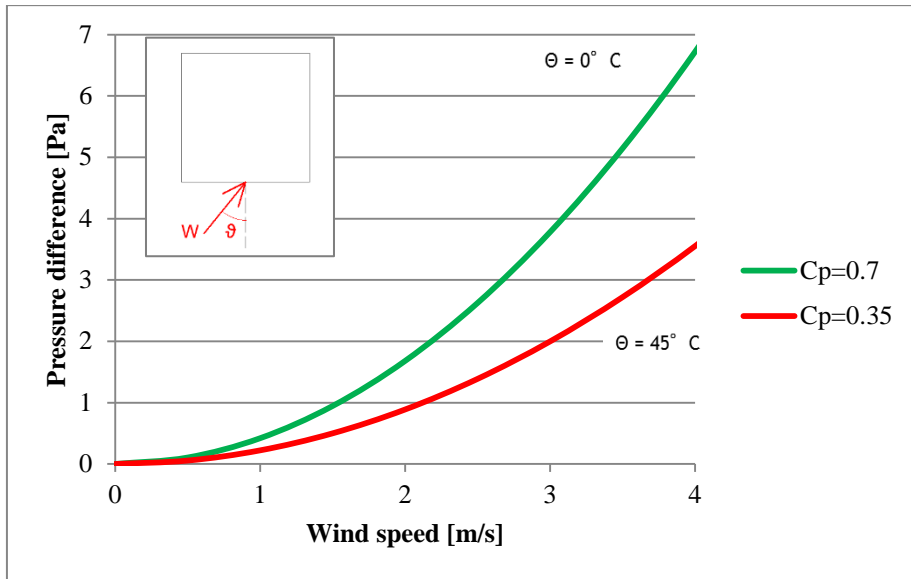


Figure 2-2. Pressure difference due to wind. Source: Lion L. [2.1]

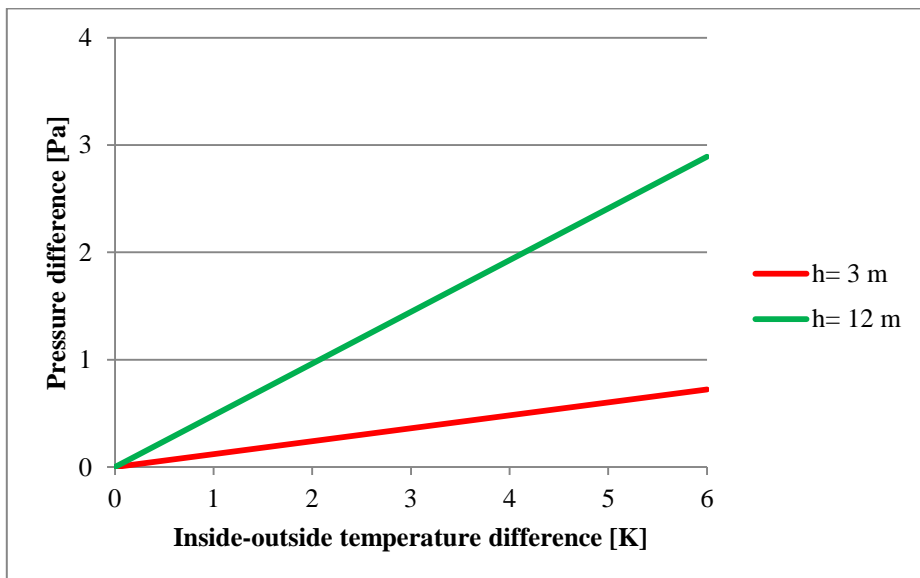


Figure 2-3. Pressure difference due to stack effect. Source: Lion L. [2.1]

Figure 2-2 shows pressure difference generated by incident wind on the surface of a square plant building totally exposed, in function of the

local wind speed. Two typical values of pressure coefficients are considered corresponding to wind incident angle θ of 0° ($C_p = 0.7$) and 45° ($C_p = 0.35$). Figure 2-3 shows pressure difference due to stack effect when openings height difference is 3 m, typical inter-floor distance, and 12 m, four stores total height, at different inside-outside temperature differences.

2.2.Methods and tools for airflow modelling

Until very recently, natural ventilation systems were designed based on local or regional traditions, empirical studies, and fundamental but incomplete theoretical models.

In the last years modelling tools have been developed to carry out one or more of the following tasks:

- Evaluate ventilation rates through the whole building and/or through each opening;
- Simulate air flow patterns through the whole building and/or in each room;
- Size the ventilation components;
- Evaluate indoor temperatures and calculate comfort parameters;
- Select the control strategy that maximizes energy efficiency, indoor air quality and thermal comfort;
- Verify the accomplishment of minimum standard requirements for indoor air quality and thermal comfort.

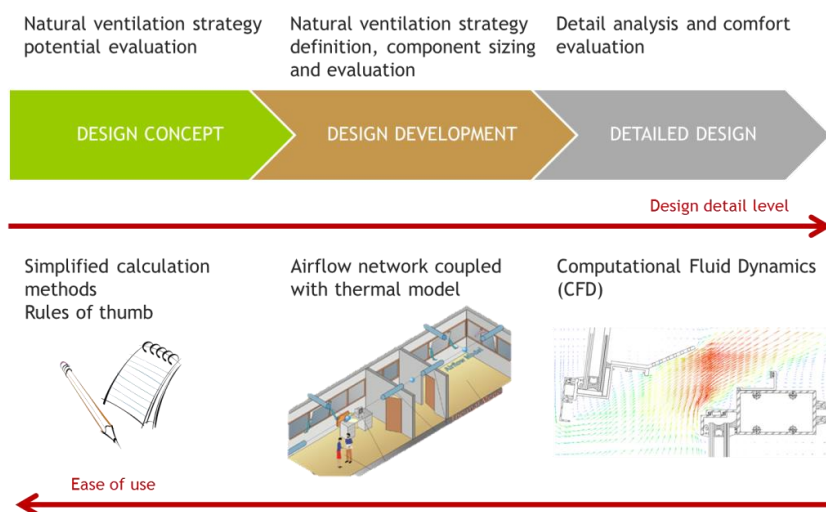


Figure 2-4. Natural ventilation modelling detail along the integrated design process.

As building design is characterized by different detailed design levels, airflow model with different resolution are used to support the decision-making process.

The available airflow models are commonly divided into four categories:

- Empirical models
- Nodal model or airflow network models
- Zonal model
- Computational Fluid Dynamic

A review of the available methods for airflow modelling can be found in existing literature [1.2][2.2][2.3][2.4]. The following paragraphs try to summarize these findings.

2.2.1. Empirical models

Empirical models are basically static correlations derived analytically or experimentally to predict ventilation airflow rates for simple opening configuration. Because of their easy application, they are used in early-design-stages to pre-size components. In literature empirical methods are grouped in two categories, depending on their output results: air flow rate and opening sizes and air speed into the building. As they

refer to a limited number of case studies or to more detailed model simplifications, they are based on specific assumptions.

Table 2-1. Existing empirical model to estimate airflow rates. W=wind driven, B= buoyancy driven, W&B = Wind and buoyancy driven.

Openings nr	Configuration	Equation	Reference
1	W	$Q = \pm C_D A \sqrt{U^2 - \left(\frac{2\gamma P_a}{\rho V}\right) \omega}$ <p>where Q = ventilation flow rate C_D = discharge coefficient γ = polytrophic exponent, 1.4 for adiabatic flows and 1.0 for isothermal flows</p>	Pulsation theory derived through wind tunnel testing [2.5]
1	B	$q_B = \frac{1}{3} A C_d \sqrt{\frac{ T_{in} - T_{out} H g}{(T_{in} + T_{out})/2}}$	Derived analytically by Warren P.R. et al. [2.6]
1	W	$q_w = 0.025 A v_{w,ref}$	Wind tunnel tests and full-scale experiments in 2 real buildings [2.6]
1	W&B	$q_{bw} = \frac{1}{2} A \sqrt{C_1 + (C_2 v_{w,ref}^2) + (C_3 H T_{in} - T_{out})}$	33 measurements on a full-scale building [2.7]

Openings nr	Configuration	Equation	Reference
1	W&B	$q_{bw} = A \sqrt{C_1 C_p v_{w,ref}^2 + C_2 H \Delta T + C_3 \frac{\Delta C_{p,opening} \Delta T}{v_{w,ref}^2}}$ <p>with</p> $\Delta C_{p,opening} = 9.1894 \cdot 10^{-9} \cdot \varphi^3 - 2.626 \cdot 10^{-6} \cdot \varphi^2 - 0.0002354 \cdot \varphi + 0.113$ <p>where C_1, C_2 and C_3 are empirical coefficients</p>	Wind tunnel test and 48 full-scale measurements on real buildings [2.9]
1	W	$Q = CAU$ <p>where C = airflow coefficient varies depending on geometry and wind incidence direction A = opening area U = wind speed</p>	Semi-analytical model [2.8] and [2.10]
1	B	$Q = \frac{C_d A}{3} \sqrt{gh \frac{\Delta T}{T_{out}}}$ <p>where h = height of the opening</p>	Semi-analytical model [2.8]

Openings nr	Configuration	Equation	Reference
1	W&B	$U_m = \sqrt{C_1 U_{10}^2 + C_2 h \Delta T + C_3}$ <p>where U_{10} = reference wind speed measured at the height of 10 m C_1 = wind constant (0.001) C_2 = buoyancy constant (0.0035) C_3 = turbulence constant (0.01)</p> $Q = \frac{1}{2} A U_m$	Measurements on the lowest floor apartmentsof three buildings in different climates [2.11]
4*	W&B	$q_w = C_d \cdot A_w \cdot v_w \cdot C_{p,1} - C_{p,2} ^{0.5}$ $q_B = C_d \cdot A_B \cdot \left(\frac{2 \cdot T_{in} - T_{out} \cdot h g}{[(T_{in} + T_{out})/2]} \right)^{0.5}$ <p>where</p> $\frac{1}{A_w^2} = \frac{1}{(A_1 + A_2)^2} + \frac{1}{(A_3 + A_4)^2}$ $\frac{1}{A_B^2} = \frac{1}{(A_1 + A_3)^2} + \frac{1}{(A_2 + A_4)^2}$	Two openings on each side [2.12]
2	B	$q = C_d \sqrt{A^* \frac{\rho_o - \rho_i}{\rho} g h}$ $A^* = \sqrt{2} A_t A_b / \sqrt{A_t^2 + A_b^2}$ <p>where A_t = area at the top of the stack A_b = area at the bottom of the stack</p>	Fully mixed model [2.13]

Openings nr	Configuration	Equation	Reference
2	B	$q = C_d A^* \sqrt{\frac{T_i - T_o}{T_o}} g(h - h_c)$	Emptying water-filling box model [2.14]
2	B	$q = C_d A^* \sqrt{\left[\frac{T_b - T_o}{T_o} g h_c + \frac{T_t - T_o}{T_o} g(h - h_c) \right]}$ $T_t = \frac{E}{\rho c_p q} + T_o$ $T_b = \lambda(T_t - T_o) + T_o$ <p>where</p> $\lambda = \left[\frac{q \rho c_p}{A_t} \left(\frac{1}{\alpha_f} + \frac{1}{\alpha_r} + \frac{1}{\alpha_c} \right) + 1 \right]^{-1}$ <p> α_f = convective heat transfer coefficient at floor α_r = radiative heat transfer coefficient α_c = convective heat transfer coefficient at ceiling </p>	Emptying air filling box model I [2.15]
2	B	$q = C_d A^* \sqrt{\left(\frac{1}{2} g h \frac{T_b - T_o}{T_o} + \frac{1}{2} g h \frac{T_t - T_o}{T_o} \right)}$	Emptying air filling box model II [2.15]
2+	B	$Q = C_d A \sqrt{2 g \Delta H_{NPL} (T_i - T_o) / T_i}$ <p>where ΔH_{NPL} = height from midpoint of lower opening to neutral pressure level [m]</p>	Semi analytical model [2.8]

Other analytical models that take into account buoyancy sources, geometry and position are:

- Buoyancy driven natural ventilation induced by two buoyancy sources [2.16];
- Buoyancy driven natural ventilation induced by a heat source distributed uniformly over a vertical wall [2.17];

- Buoyancy driven natural ventilation in an enclosure with two stacks and a heat source uniformly distributed over the floor [2.18];
- Natural ventilation of a room with distributed based heating and vents at multiple levels [2.19].

Non-dimensional methods allow quick and easy manual calculation avoiding the need of detailed and time-consuming numerical simulations; they can be used to identify important parameters and check the sensitivity of the design to possible changes. Li Y. and Delsante A. [2.20] present non-dimensional graphs to calculate ventilation flow rates and air temperatures, and to size ventilation openings in a single-zone building with two openings when no thermal mass is present. Both fully assisting and fully opposite wind solutions are taken into account. The model also includes solar radiation and heat conduction losses through the building envelope. Etheridge D. [2.21] also proposes the use of non-dimensional graphs to determine the size and the position of openings and estimate air flow rates. The graphs are generated from both theoretical models and experimental methods. ASHRAE method defines a more general equation to estimate the bulk air flow rate in a single zone building by the Equation 2-7.

$$Q = A \sqrt{a\Delta T + bv_{met}^2} \quad \text{Equation 2-7}$$

where Q = bulk airflow rate [m^3/h];
 A = total effective leakage area [cm^2];
 a = stack coefficient [$\text{m}^6/\text{h}^2\text{cm}^4\text{K}$];
 ΔT = indoor-outdoor temperature difference [K];
 b = wind coefficient [$\text{m}^4\text{s}^2/\text{h}^2\text{cm}^4$];
 v_{met} = meteorological wind speed [m/s].

The stack coefficient a is defined depending on the number of building stores, as in Table 2-2.

Table 2-2. Stack coefficients a. Source: ASHRAE [2.8]

<i>Number of building stores</i>	<i>a [m⁶/h²cm⁴K]</i>
1	0.00188
2	0.00376
3	0.00564

The wind coefficient *b* depends on the number of stores and the shielding class, as in Table 2-3.

Table 2-3. Wind coefficient b. Source: ASHRAE [2.8]

<i>Shielding class</i>	<i>1 storey</i>	<i>2 storeys</i>	<i>3 storeys</i>
No obstructions	0.00413	0.00544	0.00640
Light local shielding	0.00319	0.00421	0.00495
Moderate local shielding	0.00226	0.00299	0.00351
Heavy shielding	0.00135	0.00178	0.00209
Very heavy shielding	0.00041	0.00054	0.00063

Indoor air velocity is important to verify comfort conditions as air velocity increases body's convective heat exchange improving comfort conditions at high indoor temperatures. The Givoni method allows to estimate the indoor air speed. The correlation in Equation 2-8 is given by experimental results on a square floor zone with the same opening area on the upwind and on the downwind façade.

$$v_i = 0.45 \cdot (1 - e^{-3.48x}) \cdot v_{ref} \quad \text{Equation 2-8}$$

where

- v_i = average indoor air temperature [m/s];
- x = opening to wall ratio [];
- v_{ref} = reference external wind speed [m/s].

Graca G.C. [2.22] developed a model to calculate indoor air speed in the jet and the recirculation zone in cross ventilated rooms while knowing the inlet air flow rates. Considering the maximum air velocity in front of the opening calculated as in Equation 2-9.

$$v_{max} = \frac{q_{in}}{A_{inlet} c_d} \quad \text{Equation 2-9}$$

where

q_{in} = inlet flow rate [m^3/s];

A_{inlet} = inlet area [m^2];

c_d = discharge coefficient for flow through an aperture [-].

The air velocity of the main air jet (v_{jet}) is calculated as in Equation 2-10.

$$v_{jet} = 1.56 \cdot v_{max} \cdot c_d \cdot \sqrt{\frac{A_{inlet}}{A_{cross}}} \quad \text{for } 1/3 < C_L < 11 \quad \text{Equation 2-10}$$

where

$$C_L = \frac{2D_{room}}{W_{room} - W_{inlet}}$$

A_{cross} = cross sectional area of the main jet flow in the room [m^2];

D_{room} = room depth [m];

W_{room} = room width [m];

W_{inlet} = inlet width [m].

The air velocity in the recirculation area (v_{rec}) is calculated as in Equation 2-11.

$$v_{rec} = v_{jet} \cdot C_{RJ} \cdot \sqrt{\frac{D_{room}}{A_{inlet}^{0.5}}} \quad \text{Equation 2-11}$$

where

$$C_{RJ} = \begin{cases} 0.191 & \text{for } 1/3 < C_L < 4 \\ 0.104 & \text{for } 4 < C_L < 11 \end{cases}$$

As regards ventilative cooling, natural ventilation performance is related also to cooling load prediction. Thermal mass effect directly influences cooling loads and therefore more complicated methods such as frequency domain thermal network models are needed to develop simplified methods and tools.

Balaras C.A. [2.23] identified 16 simplified design methods for calculating cooling loads and indoor air temperature of a building taking into account thermal mass effects. The paper categorizes the models by inputs, outputs and restrictions on their level of accuracy or other design limitations.

2.2.2. Airflow network models

Airflow network models have been developed to more quickly solve airflows throughout a building. They represent the building with one or more well-mixed zones, assumed to have a uniform temperature and a pressure varying hydrostatically, connected by one or more airflow paths. Each airflow path is mathematically described using the Bernoulli equation. A matrix of the equation is constructed and numerically solved. Convergence is reached when the sum of all mass flow rates through all components approaches zero within the tolerance band specified [1.2]. The most widely used airflow network modelling tools are COMIS [2.24] and CONTAM [2.25]. As both tools are based on the same theoretical model, no significant difference has been noted among them.

Airflow network models can be coupled to dynamic simulation models to evaluate the whole building performance, taking into account the thermal mass effect as well. ESP-r has a built-in network model [2.26]. Existing tool features and coupling approaches have been analysed in Table 2-4.

Because of their simplicity, airflow network models have some important limitations, which are:

- heavily dependency on coefficients like wind profile exponent, wind pressure coefficients and discharge coefficients;
- temperature distribution within air volumes (e.g. stratification) cannot be determined;

- local surface convection determination is limited by the insufficient resolution;
- turbulent fluctuations of wind pressures are neglected;
- air speed in rooms cannot be calculated.

Zhai J. et al. [2.27] performed airflow models evaluations by comparing predicted airflow from EnergyPlus, CONTAM and ESP-r airflow network models with measured airflow in laboratory experiments across 8 defined scenarios at steady conditions. They concluded that all the models yielded similar predictions, which are within 30% error for the simple cases evaluated.

The worst results are obtained for buoyancy driven single-sided, wind driven cross ventilation and combined buoyancy and wind driven natural ventilation configuration, whereas buoyancy driven cross ventilation error is less than 10%. It is well known that airflow network models cannot generally well represent single-sided ventilation, as it is mainly driven by turbulent fluctuations of wind pressures, neglected in nodal models [2.3].

Table 2-5 reports some of the tools developed or under development to support early-design-stage modelling.

Zhai J. et al. [2.27] further document and analyse natural/hybrid ventilation models, which are not as widely used as the previous mentioned ones and are mainly developed for in-house study:

- CHEMIX, developed at CSIRO Building Construction and Engineering in Australia [2.28];
- AIOLOS, developed under the ALLTENER Energy Programme [1.2];
- PASSPORT-Air, developed under PASCOOL research programme [2.29];
- SIMulator of Building And Devices (SIMBAD) developed by CSTB [2.29].

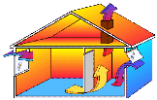


Among the above cited tools, the SIMBAD toolbox is the one still available as Matlab/Simulink component library dedicated to the modelling and dynamic simulation of fully equipped buildings at small time steps. It is then particularly useful to design and evaluate controllers and control strategies.

The software tool LoopDA [2.31] applies the loop equation design method developed by Axley J. [1.1] to a multi zone model. Compared to the airflow network model, the equations are reversed.

Equations are written for the changes of pressure along airflow paths within the building, defined as loops from the inlet to the exhaust and back to the inlet again. The sum of the pressure changes around any loop must equal zero at every time step. The resulting loop equations define combinations of system component sizes that will provide desired ventilation flow rates given specific environmental design conditions.



Therefore, instead of defining the physical characteristics of the flow components (opening area and position) and calculate airflow through them, the loop equation method requires the user to define the design airflow rates through the components and determines the physical characteristics of the components to provide the required flow rates.



Table 2-4: Most widely used airflow model.

Tool	Developer	Link to other tools	Coupling approach ¹⁴	Output	Particular features
<p>COMIS</p> 	<p>LBNL</p> <p>IEA Annex 23</p>	<p>EnergyPlus</p> <p>Trnsys (Trnflow)</p>	<p>Ping-pong coupling with EnergyPlus [2.32]</p> <p>Onion coupling with Trnsys</p>	<ul style="list-style-type: none"> – airflows due to infiltration or natural ventilation; – interactions of the HVAC system, ducts, and exhaust hoods and fans. 	<p>Variable air density model allowable.</p> <p>Ability to apply a density gradient on each side of the opening.[2.33]</p>
	NIST	Trnsys	Onion coupling with Trnsys. It could either be integrated in Type 56 or be included in the model as a separate Type. [2.34]	<ul style="list-style-type: none"> – airflows due to infiltration or natural ventilation; – interactions of the HVAC system, ducts, and exhaust hoods and fans; – air contaminant concentration; – user exposure. 	<p>Graphical interface for data input and result viewer.</p> <p>Fully coupled multizone CFD model [2.25]</p> <p>CONTAM does not allow the user to modify the wind speed reference height. [2.33]</p>
<p>mfs</p> 	ESRU	ESP-r	Various way of coupling possible [2.35]	<ul style="list-style-type: none"> – airflows due to infiltration or natural ventilation; – velocity at connections; – air contaminant concentration; 	<p>Poor representation of single-sided ventilation. Bidirectional flow can be approximated with a pair of airflow openings.</p> <p>Different wind profile options available. It has a built-in pressure coefficient database.</p>

¹⁴ Refer to par. 2.2.2.1 for a description of the existing coupling approaches.

Table 2-5. Other available tools for natural ventilation early-design-stage.

Tool	Model	Developer	Output	Particular features
	Loop equation method [2.31]	NIST	size ventilation airflow components of natural and hybrid ventilation systems	The equations are re-written to form physical closed loops around which the sum of the pressure changes must equal zero. They can be used also as “reverse” method.
	Multi zone model [2.36]	EPFL	<p>Time variation over a typical day of:</p> <ul style="list-style-type: none"> – Neutral pressure level visualization – Air flow rate common to all zones – Mean zone air temperatures – mean zone surface temperatures – Ventilation cooling rate for each zone 	<p>It cannot:</p> <ul style="list-style-type: none"> – calculate multi path air movement, simulate periods much longer than 1 day; – include interactions with neighbouring zones other than by the ventilation rate of the common flow path; – directly take into account solar gains (they has to be scheduled); – directly simulate wind induced natural ventilation (it is assumed that the worst case for cooling purposes is the case without wind); – model multi-layer wall elements (it is assumed that the thermal effect of the surface layer dominates),; – model thin walls (the thermal storage effect of thin walls may be overestimated).

Tool	Model	Developer	Output	Particular features
	Single zone model integrated to a monozone heat balance model for office type buildings [2.37]	Danish Building Research Institute SBI [2.38]	<ul style="list-style-type: none"> – Hourly indoor temperature – Maximum and minimum airflow rate during working hours 	<p>The thermal model is only used in the summer for the calculation of the indoor air temperature and the internal surface temperature in the building. In winter the temperatures are set to 20°.</p> <p>No heat losses through ground floor.</p> <p>All internal structures and surfaces have the same temperature.</p>
	Multizone airflow model	Environmental Design Solutions Ltd	<ul style="list-style-type: none"> – airflows due to infiltration or natural ventilation; – indoor temperatures 	<p>It automatically generates airflow network.</p> <p>It can import/export from CAD models.</p>
CoolVent	Multizone airflow model	MIT [2.39]	<ul style="list-style-type: none"> – airflows due to infiltration or natural ventilation; – internal temperatures 	<p>The model allows time-varying thermal conditions for a typical day of a month (based on weather data), accounting for the effects of thermal mass, and night cooling.</p> <p>The model does not account for radiative heat transfer between the internal zone surfaces.</p> <p>Solar radiation through roof openings is not taken into account.</p>

2.2.2.1. Thermal – airflow model coupling

Common dynamic simulation tools give the user the possibility to either couple or decouple the thermal model with the airflow model. The first option becomes fundamental to predict passive cooling performance, where a higher ventilation rate can avoid overheating [2.35] and improve thermal comfort. Although for winter ventilation design the airflow can be considered uncoupled from the thermal behaviour of the building, for summer natural ventilation a coupled model become fundamental [2.3].

Different ways exist to avoid computationally intractable fully coupled models [2.35]: in the ping-pong approach, the thermal model uses the results of the airflow model at the previous time step and vice versa; in the onion approach thermal and airflow model iterate within one time step until satisfactory small error estimates are achieved.

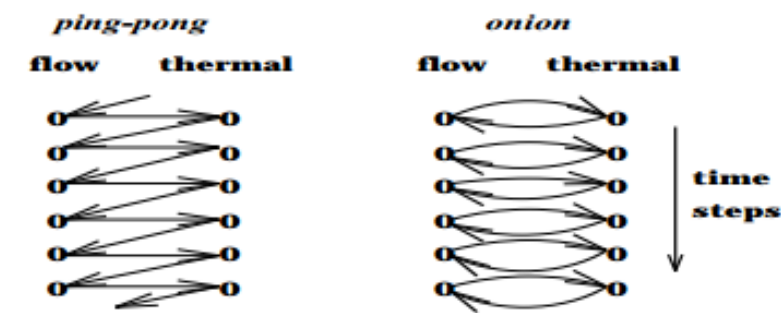


Figure 2-5. Schematic representation of ping-pong and onion approach. Source: (60)

Hensen [2.35] found out that the ping-pong approach may lead to substantial errors if combined with a large time step (equal or more than an hour), and the onion approach will have implications on computation time if combined with a short time step (less than an hour).

EnergyPlus is coupled to the COMIS airflow model through a ping-pong approach [2.32], Trnsys adopts an onion approach with both COMIS and CONTAM airflow models [2.34], whereas in ESP-r different coupling approaches are available to be selected by the user [2.35].

Zhai et al. [2.40] also compared measured indoor temperatures of three naturally ventilated buildings with detailed EnergyPlus model output data. The EnergyPlus model performed excellently for simple and well defined cases, but less accuracy is observed in cases with complex geometry. Due to the lack of available information (on site measured weather data, measured volume flow rates, level of thermal mass, effective area and discharge coefficient of openings, wind pressure coefficient data), it was not possible to assess the accuracy of model coupling.

2.2.3. Zonal models

Zonal models are considered intermediate models between airflow networks and CFD, as they divide the bounded space into a number of smaller control volumes to calculate velocity and temperature field within the zone. These models have been initially developed for mechanical systems to study the interaction between the terminal unit and the rest of the room. Later they were used to study temperature stratification and airflow velocity within the room. Zonal models are of particular interest to obtain information as temperature stratification, thermal interaction with cold façade, draft and thermal radiation performances.

A review of the zonal models developed can be found in Megri et al. 2007 [2.41]. They generally assume that the temperature is uniform within the zone and the pressure varies hydrostatically. Mass (Equation 2-12) and thermal energy (Equation 2-13) conservation equations are applied to each zone.

$$\sum \dot{m}_{ij} = 0 \quad \text{Equation 2-12}$$

$$\sum \dot{m}_{ij} C_p T = 0 \quad \text{Equation 2-13}$$

where \dot{m}_{ij} is the rate of mass flow from zone i to zone j.

The mass flow across zones interfaces is in most models calculated using the power law equation (Equation 2-14).

$$\dot{m}_{ij} = C \Delta P_{ij}^{\beta} \quad \text{Equation 2-14}$$

where C is a constant flow coefficient and β is the exponent flow coefficient.

The underlying problem with this equation is that for $\Delta P = 0$ there is no flow rate, which is valid for steady flow through an opening in a wall, but not generally for flow in a bounded space [2.42].

The velocity field is independent of the pressure field and is obtained by application of the momentum equation.

To date, there is no commercial program or software based on the zonal modelling approach, limiting the possibility to use this kind of models for design purposes.

2.2.4. Computational Fluid Dynamics (CFD) models

CFD aims at solving the Navier-Stokes equation (Equation 2-15, Equation 2-16, Equation 2-17), which are based on treating the fluid as a continuum. Navier-Stokes equations are based on conservation of mass, momentum and energy for not viscid and incompressible fluid. They describe the unsteady three-dimensional motion of air in terms of instantaneous velocities, temperature (or density) and pressure at a point. The building is divided into control volumes and the equations are solved for every mesh element, using iterative solutions.

$$\rho \left(\frac{\partial u}{\partial t} + u \frac{\partial u}{\partial x} + v \frac{\partial u}{\partial y} + w \frac{\partial u}{\partial z} \right) = \quad \text{Equation 2-15}$$

$$= -\frac{\partial P}{\partial x} + \mu_o \left(\frac{\partial^2 u}{\partial x^2} + \frac{\partial^2 u}{\partial y^2} + \frac{\partial^2 u}{\partial z^2} \right) =$$

$$= \rho \left(\frac{\partial v}{\partial t} + u \frac{\partial v}{\partial x} + v \frac{\partial v}{\partial y} + w \frac{\partial v}{\partial z} \right) =$$

$$= -\frac{\partial P}{\partial y} + \mu_o \left(\frac{\partial^2 v}{\partial x^2} + \frac{\partial^2 v}{\partial y^2} + \frac{\partial^2 v}{\partial z^2} \right) = \quad \text{Equation 2-16}$$

$$= \rho \left(\frac{\partial w}{\partial t} + u \frac{\partial w}{\partial x} + v \frac{\partial w}{\partial y} + w \frac{\partial w}{\partial z} \right) = \quad \text{Equation 2-17}$$

$$= -\rho g - \frac{\partial P}{\partial z} + \mu_o \left(\frac{\partial^2 w}{\partial x^2} + \frac{\partial^2 w}{\partial y^2} + \frac{\partial^2 w}{\partial z^2} \right)$$

The viscosity μ_o is assumed to be uniform. The velocity components are u, v and w in the x, y, and z directions respectively and P denotes the pressure.

The primary applications of CFD to design natural ventilation are:

- the calculation of velocity and temperature fields in rooms and buildings;
- the calculation of envelope flows;
- the calculation of surface wind pressure distributions;
- whole field calculations;
- the calculation of the flow characteristics of openings.

Important modelling issues are the choice of calculation domain and the associated grid, the boundary conditions settings and the convergence requirements.

Grid density, shape and orientation have to be defined carefully. Regions of high spatial gradient need higher density of the grids. The orientation of the grids has to be set considering the local flow direction. In case of external CFD, the external flow domain needs to be large enough, such that the results are nominally independent of its size. Modeler should be experienced enough to decide how to refine the mesh for solving local gradients.

Boundary conditions have to be specified at the surfaces of the domain and at the internal solid surfaces. The accuracy of results depends strongly by the accuracy of boundary conditions. External CFD is easier to set, because boundary conditions regard only wind characteristics. Detailed information about the domain are needed otherwise the long calculation time is not rewarded by mediocre results. CFD simulations provide the users with a large amount of information that can be handled with the desired spatial and temporal resolution. Given the long calculation time and the high dependency on boundary condition, CFD simulations are commonly used in the later stages of design. Due to the high effort both from computational than from output post-processing point of view, it is practically counter-

productive to use transient CFD to predict natural ventilation strategies within the whole building.

Most of the CFD codes used in practice are commercial programs where the source code is not available to the users and with many more applications than natural ventilation design. ANSYS Fluent (2) is the most widely used software.

DesignBuilder software [2.44] performs both internal and external steady CFD analysis. Temperatures, heat flows and flow rates previously calculated by EnergyPlus can be seamlessly used to provide boundary conditions simply by specifying the time/date of the CFD analysis. Grids are automatically generated from model geometry and boundary conditions to promote optimal solution convergence.

CONTAM was recently enhanced to incorporate CFD capabilities for both internal and external environmental analysis [2.45] by coupling with CFD0, a CFD software tool with an indoor zero-turbulence model [2.46]. The external link to CFD0 calculates wind pressure coefficients for each building leakage path and for a defined range of wind directions. The link to CFD0 allows to embed a CFD zone in a CONTAM network model by iteratively exchanging boundary conditions such as airflow rate, air pressure and contaminant concentrations. The internal CFD zone enables the detailed calculation of air and contaminant concentrations within a space of a building for which the well-mixed assumption is insufficient, handling the remaining rooms with the well-mixed assumption. The external CFD link predicts distributions of wind pressures and contaminant concentrations outside a building to simulate their effect on indoor air flows.

Thermal domain and detailed airflow domain can also be coupled to achieve better results because the two can exchange boundary conditions [2.47].

ESP-r has its own CFD module able to predict non-stable mixed (turbulent, laminar and transitional) flows within 2D/3D domains [2.48]. It is one of the earliest coupled CFD and network models. Boundary conditions are automatically defined at each time step by interaction with the building and airflow network.

Later studies conducted by Srinivas T. [2.49], Yuan J. [2.50] and Jayaraman B. [2.51] showed that coupling a CFD model with a multi zone model allows to obtain more realistic predictions of airflow and contaminant transport in buildings with large spaces.

CFD coupling is still under development for some tools. The network method is much more mature and more commonly used.

2.3.Needs of development: methods and tools

As reported in the par. 1.4, interviews to building professionals [1.23] identified the need of more specific energy design procedures, tools and modelling techniques.

Since natural ventilation relies on natural driving forces (i.e. wind and temperature difference), variable and hardly predictable, traditional simplified design tools are typically too limited to be useful even during early-design-stages because of the strict base assumptions. Natural ventilation design would be better supported by dynamic simulation tools, based on suitable models. Due to the complexity of these tools, the lack of knowledge and measured data, the natural ventilation strategy proposals have often no engineering analysis base. Dynamic simulation tools require expert to assess input data about airflow as no exhaustive database is available.

Moreover, Net Zero Energy Buildings design requires a whole building simulation approach to analyse design solutions interactions and optimize the whole building solution set. The ventilative cooling design should be supported by coupled thermal-airflow models to take into account the building physics interaction between convection, conduction and radiation phenomena. A lot of information about the building are needed to use those kind of models. Therefore, Building Integration Modelling (BIM) techniques are closely related to the integrated design concept as it enhances the information exchange within the design team.

The following needs of development have been identified:

- to cope with the level of information data available at a given design stage by proving results robustness through parametric

analysis;

- to add new features/types for new solutions and technologies modelling;
- to improve usability by developing structured guidelines for performance assessment, development of program specific and general courses on airflow modelling and simulation;
- to increase interoperability by exchanging information in a more efficient way within the design team;
- to validate theoretical models by comparing experimental/monitoring data with simulation results and calibrate building models.

Bibliography

- [2.1] Lion L. Natural ventilation in existing school buildings: the case study of Lavis school. Università degli Studi di Trento, Master Thesis, 2012.
- [2.2] Delsante A., Vik T. A. Hybrid ventilation. State-of-the-art review. s.l. : IEA Annex 35 Hybvent, 1998.
- [2.3] Caciolo M., Marchio D., Stabat P. Survey of the existing approaches to assess and design natural ventilation and need for further developments. 11th International IBPSA Conference.. pp. 220-227. Glasgow, 2009
- [2.4] Zhai J., Krarti M., Johnson M.H. Assess and implement natural and hybrid ventilation models in whole-building energy simulations. ASHRAE TRP-1456 : Department of Civil, Environmental and Architectural Engineering, University of Colorado, 2010.
- [2.5] Cockroft J.P., Robertson P. Ventilation of an enclosure through a single opening. Building and Environment 11, pp. 29-35, 1996.
- [2.6] Warren P.R. Dubrovnik. Ventilation through openings on wall only. International Conference Heat and Mass transfer in buildings, 1977
- [2.7] Phaff H., De Gids W. Ventilation rates and energy consumption due to open windows: a brief overview of research in the Air Infiltration review 4. Netherlands, 1982.
- [2.8] ASHRAE Handbook of Fundamentals, 2009.
- [2.9] Larsen T.S. Natural ventilation driven by wind and temperature difference. Aalborg University: PhD thesis, 2006.
- [2.10] Yamanaca T., Kotani H., Iwamoto K., Kato M. Natural, wind-forced ventilation cause by turbulence in a room with a single opening. International Journal of Ventilation 5, pp. 179 – 187, 2006

- [2.11] Phaff J.C., De Gids W.F., Ton D.V., van der Ree, Schindel L.M. The ventilation of buildings: investigation of the consequences of opening one window on the internal climate of a room. Delft, Netherlands, 1980.
- [2.12] CIBSE Guide - Volume A, Design data. Chartered Institution of Building Services Engineers, 1986.
- [2.13] Andersen K. T. Theoretical considerations on natural ventilation by thermal buoyancy. ASHRAE Transactions 101, pp. 1103–1117, 1995.
- [2.14] Linden P.F., Lane-Serff G.F., Smeed D.A. Emptying filling boxes: the fluid mechanics of natural ventilation. Journal of Fluid Mechanics 212, pp. 309-335, 1990.
- [2.15] Li Y. Buoyancy-driven natural ventilation in thermally stratified one-zone building. Building and Environment 35, pp. 207-214, 2000.
- [2.16] Cooper P., Linden P.F. Natural ventilation of an enclosure containing two buoyancy sources. Journal of Fluid Mechanics 311, pp. 153-176, 1996.
- [2.17] Chen Z. D., Mahoney J. Natural ventilation in an enclosure induced by a heat source distributed uniformly over a vertical wall., Building and Environment 36, pp. 493-501, 2001
- [2.18] Chenvidyakarn T., Woods A. W. Multiple steady states in stack ventilation. Building and Environment, pp. 399-410, 2005.
- [2.19] Fitzgerald S.D., Woods A.W. Natural ventilation of a room with vents at multiple levels. Building and Environment 39, pp. 505-521, 2004.
- [2.20] Li Y., Delsante A. Natural ventilation induced by combined wind and thermal forces. Building and Environment 36, pp. 59-71, 2001.
- [2.21] Etheridge D.W. Non-dimensional methods for natural ventilation design. Building and Environment 37, pp 1057-1072, 2001.
- [2.22] Graca G.C. Simplified models for heat transfer in rooms. University of California, San Diego: PhD Thesis, 2003.
- [2.23] Balaras C.A. The role of thermal mass on the cooling load of buildings. An overview of computational methods. Energy and Buildings 24, pp 1-10, 1996.
- [2.24] Warren P. Multizone Airflow Modelling (COMIS). Summary of IEA Annex 23, 1996.
- [2.25] Walton G.N., Dols W.S. CONTAM - User guide and program documentation. NISTIR 7251, 2010.
- [2.26] Hensen J.L.M. On the thermal interaction of building structure and heating and ventilating system. PhD Thesis: Eindhoven University of Technology, 2001.
- [2.27] Zhai J., Krarti M., Johnson M.H. Assess and implement natural and hybrid ventilation models in whole-building energy simulations. ASHRAE TRP-1456. Department of Civil, Environmental and Architectural Engineering, University of Colorado, 2010.

- [2.28] Heinrich, C.A. The CSIRO - SGTE - THERMODATA package for the thermodynamic computations at BMR Overview: Geochemical applications, BMR extensions of data base and species index, installation at BMR. Bureau of Mineral Resources, Geology and Geophysics (1987). URI: <http://www.ga.gov.au/metadata-gateway/metadata/record/14170/>.
- [2.29] Daskalaki E., Santanouris M., Allard F., PASSPORT-Air, a network air ventilation tool. Passive cooling workshop, pp. 183-192, University of Athens, 1995.
- [2.30] CSTB. Simbad Building and HVAC Toolbox. [Online] 2010. [Cited: 10 18, 2013.] <http://www.simbad-cstb.fr/index.html>.
- [2.31] Dols W.S., Emmerich S.J. LoopDA - Natural ventilation design and analysis software. NISTIR 6967 : National Institute of Standard and Technology, 2003.
- [2.32] Huang J., Winkelmann F., Buhl F., Curtis P., Fischer D., Liesen R., Taylor R., Strand R., Crawley D., Lawrie L. Linking the COMIS multizone airflow model with the EnergyPlus building energy simulation program. Proceedings of building simulation, pp. 1065-1070. Kyoto, 1999.
- [2.33] Hensen J. Performance evaluation of network airflow model for natural ventilation. s.l. : ASHRAE, 2012.
- [2.34] McDowell T. P., Emmerich S. J., Thornton J. W., Walton, G. N. Integration of airflow and energy simulation using CONTAM and Trnsys. ASHRAE Transactions - Annual Meeting. pp. 1-14. Kansas City, 2003.
- [2.35] Hensen J.L.M. Modelling coupled heat and airflow: Ping-pong vs onions. Proceedings of the 16th AIVC Conference "Implementing the Results of Ventilation Research". pp. 253-262. Palm Springs, 1995.
- [2.36] Flourentzos F., Van Der Maas J., Roulet C.A. Lesocool Manual. Lausanne : EPFL LESO-PB, 2006.
- [2.37] Svensson C., Aggerholm S. The NatVent programme 1.0 Fundamentals. Danish Building Research Institute SBI, 1998.
- [2.38] BRE. NatVent EU project. <http://projects.bre.co.uk/natvent/>. [Online] 1994.
- [2.39] Menchaca-B. M. A., Glicksman P. CoolVent: a multizone airflow and thermal analysis simulator for natural ventilation in buildings. Third national conference if IBPSA-USA. pp. 132-139. Berkeley, 2008.
- [2.40] Zhai Z. J., Johnson M.-H., Krarti M. Assessment of natural and hybrid ventilation models in whole-building energy simulations, Energy & Buildings 43, pp. 2251 – 2261, 2011.
- [2.41] Megri A.C., Haghighat F. Zonal modelling for simulating indoor environment of buildings: review, recent developments and applications. HVAC&Research vol.13, nr 6, pp. 887-905, 2007.
- [2.42] Etheridge D. Natural ventilation of buildings. Theory, measurement and design. John Wiley and Sons, 2012.

- [2.43] ANSYS Fluent Flow Modeling Simulation Software. ANSYS - Simulation Driven Product Development. [Online] 2013.
<http://www.ansys.com/Products/Simulation+Technology/Fluid+Dynamics/Fluid+Dynamics+Products/ANSYS+Fluent>.
- [2.44] DesignBuilder CFD. DesignBuilder - Building design, simulation and visualisation. [Online] 2010.
<http://www.designbuilder.co.uk/content/view/40/61/>.
- [2.45] Wang L., Dols S.W., Chen Q. An introduction to the CFD capabilities in CONTAM 3.0. Fourth National Conference of IBPSA-USA. pp. 490-496. New York, 2010.
- [2.46] Chen Q., Xu W. A zero-equation turbulence model for indoor airflow simulation. *Energy and Buildings* 28, pp. 137-144, 1998.
- [2.47] Ery Djunaedy. External coupling between building energy simulation and computational fluid dynamics. TU Eindhoven, 2005.
- [2.48] ESRU. ESP-r: Computational Fluid Dynamics. Energy Systems Research Unit - University of Strathclyde. [Online] [Cited: 10 20, 2013.]
http://www.esru.strath.ac.uk/Programs/ESP-r_capabilities/cfd.html.
- [2.49] Srinivas T. Evaluation and enhancement of computational techniques in indoor air quality analysis. Halifax, Nova Scotia : Dalhousie University: PhD Thesis, 2001.
- [2.50] Yuan J., Srebric J. Improved prediction of indoor contaminant distribution for entire buildings. New Orleans, Louisiana, 2002. The 2002 ASME International Mechanical Engineering Congress and Exposition. p. 8.
- [2.51] Jayaraman B., Lorenzetti D., Gadgil A. Coupled model for simulation of indoor airflow and pollutant transport. Berkeley, California : Lawrence Berkeley National Laboratory, 2004.

3. Airflow network modelling in EnergyPlus

As discussed in par. 2.2.2, the airflow network model in EnergyPlus allows analysing airflows and pressure differences throughout the building zones, driven by external wind, stack effect and also mechanical pressures (fans). Thanks to the coupling with the EnergyPlus building simulation tool, the airflow network is a useful design tool to compare ventilation strategies and configurations and optimize control strategies taking into account the whole building design solution set performance.

However, improvements in its usability are needed, which include more detailed modelling guidelines.

This chapter presents the EnergyPlus – airflow network modelling features and input data collection and assessment, including zoning criteria and control settings. The present guidelines are focused on natural ventilation modelling only, contaminant transport and mechanical air distribution system modelling are here not considered.

Table 3-1. List of the EnergyPlus airflow network modelling capabilities and limitations.

Can do	Cannot do
Air flow through cracks in exterior or interzone surfaces.	Air circulation and/or air temperature stratification within a thermal zone.
Air flow through cracks around windows and doors when closed.	Pollutant transport cannot currently be modelled.
Natural ventilation (i.e., air flow through open or partially open exterior windows and doors).	
Zone level control of natural ventilation (all windows/doors in a zone that are defined with a component opening object have identical controls).	
Individual surface control of natural ventilation for a subsurface (window,	

Can do	Cannot do
door, or glassdoor).	
Modulation of natural ventilation to prevent large zone air temperature swings.	
Interzone air flow (i.e., air flow through open interzone windows and doors, and through cracks in interzone surfaces).	
Dependence of air flow on buoyancy effects and wind pressure.	
Dependence of wind pressure on wind speed, wind direction and surface orientation.	
Bi-directional flow through large openings.	

3.1.Theoretical background

The EnergyPlus model is linked through the airflow network object to the COMIS model. In the COMIS/EnergyPlus link, COMIS is called each time step by the EnergyPlus program by means of an onion coupling approach (refer to par. 2.2.2.1). Using inside and outside temperatures and the wind pressure distribution at the beginning of a time step, COMIS calculates air flows through cracks and large openings (such as open windows) between outside and inside and from zone to zone. These are then used by the EnergyPlus thermal calculation to determine surface temperatures and zone air temperatures for that time step (which are then used in the next time step to calculate new air flow values, and so on).

The building is represented with one or more well-mixed zones, assumed to have a uniform temperature and a pressure varying hydrostatically, connected by one or more airflow paths. Each airflow path is mathematically described using the Bernoulli equation. A matrix of the equation is constructed and numerically solved. Convergence is reached when the sum of all mass flow rates through all components approaches zero within the tolerance band specified.

Zones are connected by various airflow paths, forming a network of “nodes” (zones) and “resistances” (linkages). The network can be solved by specifying external climate conditions (temperature, humidity, wind velocity and directions), climate-envelope interactions (wind pressure on the facade) and engineering models for resistances.

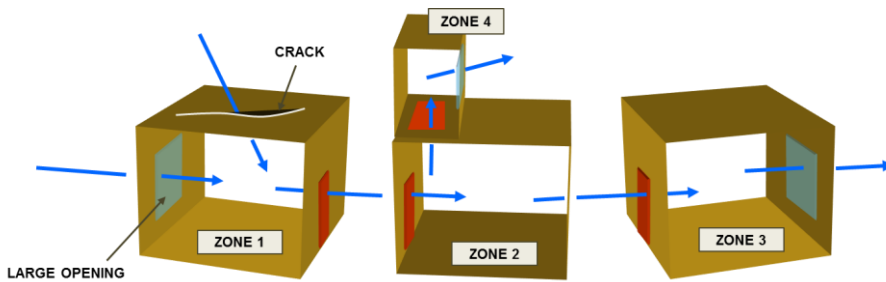


Figure 3-1. Airflow network schematic representation. Source: IBPSA-USA

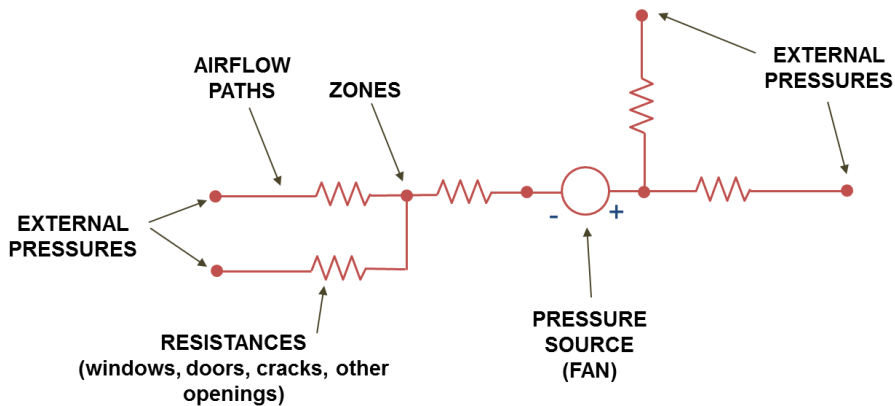


Figure 3-2. Schematic representation of relationship between zones and air paths. Source: IBPSA-USA

The calculation procedure consists of three sequential steps:

1. Pressure and airflow calculations
2. Node temperature and humidity calculations
3. Sensible and latent load calculations

The pressure and airflow calculations determine pressure at each node and airflow through each linkage given wind pressures and forced airflows. Based on the airflow calculated for each linkage, the model then calculates node temperatures and humidity ratios given zone air

temperatures and zone humidity ratios. Using these node temperatures and humidity ratios, the sensible and latent loads from duct system conduction and leakage are summed for each zone. The sensible and latent loads obtained in this step are then used in the zone energy balance equations to predict HVAC system loads and to calculate the final zone air temperatures, humidity ratios, and pressures. Further details on the calculation procedure and linkage models can be found in the EnergyPlus Engineering reference [3.1].

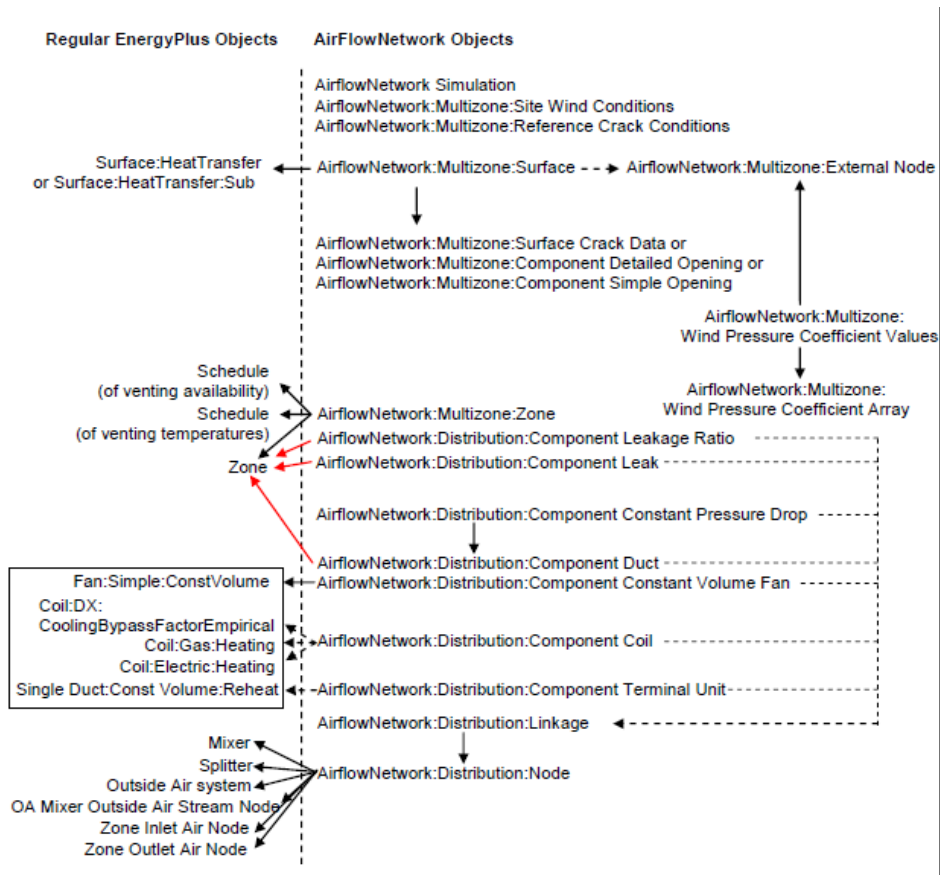


Figure 3-3. Relationship among AirflowNetwork objects (right hand side) and associated EnergyPlus objects (link hand side). Source: Lixing G. [3.2]

Figure 3-3 shows the relationships among “AirflowNetwork:Multizone” objects and between “AirflowNetwork:Multizone” objects and regular EnergyPlus objects.

Much of the information needed for the airflow network is automatically extracted from the building description for thermal modelling. These include zone volume, height, building surfaces geometry and orientation, weather data and terrain type.

3.2. Thermal and airflow zoning

When translating real building geometry into an energy model, simplifications will need to occur. The trick is understanding the right simplifications to make, that will not compromise the integrity of the model.

Thermodynamically, only exposed surface area, orientation, and tilt matter when modeling heat transfer surfaces. When modeling building geometry and exterior surfaces, it does not always matter that the actual building shape is maintained as long as the same exposed surface area, tilt and azimuth are maintained and the surfaces are assigned to the appropriate thermal zone. This one fact allows for many simplifications.

There are a few simple criteria that should be followed when zoning an energy model, in order to ensure an accurate representation of the actual systems, and also to meet all loads within the energy model:

1. Usage: any rooms that are combined into a single thermal zone should have similar internal loads (people, lights, equipment) and usage schedules. For example, it would not be appropriate to combine a high density, variable occupancy conference room and a regular occupied office space within the same thermal zone.
2. Thermostat: any rooms that are combined into a single thermal zone should have the same heating and cooling setpoints and the same thermostat schedules.
3. Solar gains: any rooms that are combined into a single thermal zone should have similar solar gains. Modellers should consider shading when zoning according to solar exposure. For perimeter zones with glazing openings, there should be at least one thermal zone for each façade orientation.

4. Perimeter areas: perimeter areas should be zoned separately from interior spaces, with a depth of perimeter zoning typically within 3 and 5 meters from the exterior wall. This is important as the heating and cooling requirements can vary greatly.
5. Distribution system: since the entire zone will be assigned to one system type, modellers should only combine rooms that will be served by the same type of HVAC system.

In case of airflow modelling additional criteria must be considered:

6. Zone volume: the total volume of enclosed spaces matters if ventilation rates are specified in terms of air changes per hour (ACH). EnergyPlus automatically calculates the zone volume from the zone geometry given by the surfaces that define the zone. If the calculated volume significantly differs from the zone air volume, the volume to be used in airflow calculation can be specified in the Zone object.
7. Airflow paths: zone heat gains and height, or difference of height between zones, determine the node pressure of the airflow network. Thermal stratification situations should be considered when zoning the model.
8. Linkages: linkages represent flow resistances. Combining zones connected through openings involved in the defined airflow path causes an overestimation of the ventilation rates as the flow resistances due to those openings are not taken into account.

Therefore, building airflow zoning can be more detailed than building thermal zoning. Thermal zones can be divided into more zones depending on the planned airflow paths and linkages. However, EnergyPlus does not distinguish between thermal and air nodes and they have both to be specified as thermal zones.

Even though it is not recommended to divide high spaces into “virtual” subzones to represent temperature stratification, in early-design-stage modelling this approximation could be acceptable as less time consuming than a CFD simulation. Even though this approach has not been independently experimentally validated, similar approaches has

been used in prior studies conducted by Hensen J. et al. [3.3] and Baharvand E. [3.4] and experimentally validated for the specific case.

3.3.Input objects

This paragraph describes the most relevant input objects and provides some default settings references and recommendations.

3.3.1. Simulation settings

The airflow network controls allow to switch on and off the airflow network and the natural ventilation and active air distribution system by selecting:

- “MultiZoneWithDistribution”: airflow calculations include the impact of active air distribution systems;
- “MultiZoneWithoutDistribution”: only natural air flows are modelled;
- “MultizoneWithDistributionOnlyDuringFanOperation”: airflow calculations include the impact of active air distribution systems only when fan is operating;
- “NoMultizoneOrDistribution”: airflow network model is switched off and any simplified natural ventilation model (ZoneInfiltration:*, ZoneVentilation:*, ZoneMixing and ZoneCrossMixing objects) specified in the input file is performed.

The airflow network controls also determine whether the wind pressure coefficients are input by the users or surface averaged. For further information about wind pressure coefficients, please refer to par. 3.3.7. Default values for convergence criteria are reported in Figure 3-4.

Field	Units	Obj1
Name		AFN
AirflowNetwork Control		MultizoneWithoutDistribution
Wind Pressure Coefficient Type		Input
AirflowNetwork Wind Pressure Coefficient Array Name		EVERY45DEGREES
Height Selection for Local Wind Speed Calculation		ExternalNode
Building Type		LowRise
Maximum Number of Iterations	dimensionless	500
Initialization Type		LinearInitializationMethod
Relative Airflow Convergence Tolerance	dimensionless	0.0001
Absolute Airflow Convergence Tolerance	kg/s	0.00001
Convergence Acceleration Limit	dimensionless	-0.5
Azimuth Angle of Long Axis of Building	deg	
Ratio of Building Width Along Short Axis to Width Along		1

Figure 3-4. Airflow network control object with default settings.

The simulation time step may be an important source of uncertainty. Zhai J. et al. [2.27] performed a sensitivity analysis to investigate the effect of the ping-pong coupling (see par. 2.2.2.1) between EnergyPlus and the Airflow Network module varying the simulation time step from 1 min to 1 hour. The results show that time steps of 1 min, 6 min, and 15 min provides practically identical solutions, while time step of 1 h produces significantly different results, indicating that the sequential passing of information between such long time steps affects the prediction. Therefore 15min time steps is considered to be reasonable to the coupling of airflow and thermal models.

3.3.2. Surface convection coefficients

As previous studies on the performance of night ventilation strategies to cool the building structure found out a high sensitivity to surface convection coefficients ([3.5][3.6][3.7]), a digression on their calculation is here needed even though the convection coefficient settings are not part of the airflow network EnergyPlus objects, but they are part of the general EnergyPlus settings.

In the simulation parameters section of EnergyPlus users can select which model equations or values to apply for the exterior convection coefficients calculation. There are five models based on ASHRAE correlations and different flat plate measurements: SimpleCombined, TARP, MoWitt, DOE-2 and AdaptiveConvectionAlgorithm.

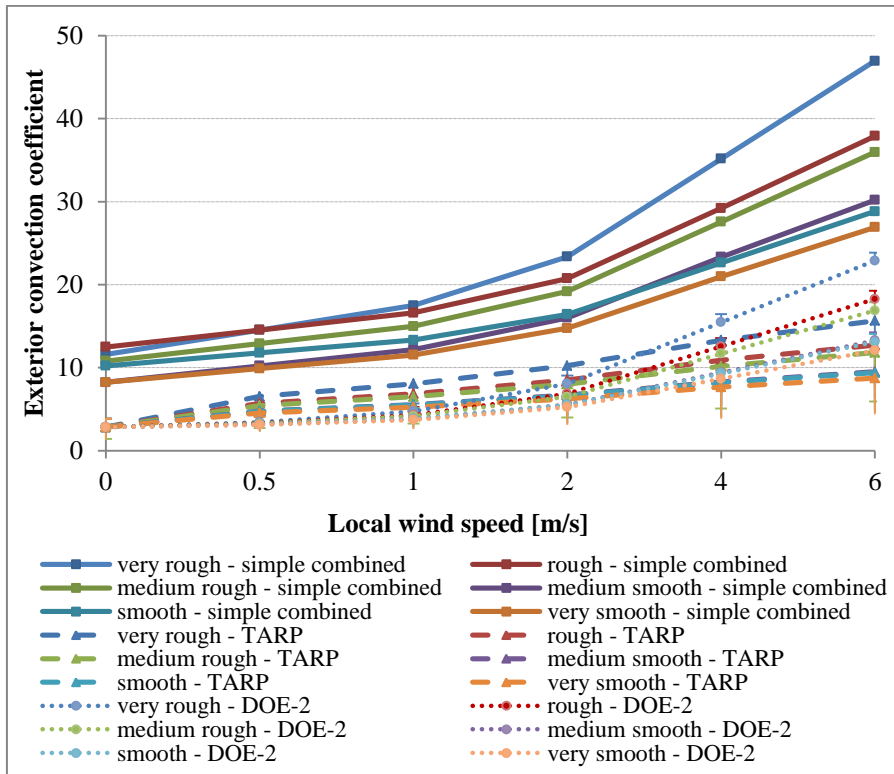


Figure 3-5. Vertical wall exterior convection model comparison depending on wind speed and surface roughness at a temperature difference of 10K between outdoor air and external wall surface when the façade is directed windward.

Simple combined model [2.8] returns higher values as also radiation to sky, ground and air is included in the exterior convection coefficient, whereas all other algorithms yield a purely convective heat transfer coefficient. MoWitt model can be applied only to very smooth vertical surfaces as it is based on measurements taken at the Mobile Window Thermal Test (MoWiTT) facility [3.8]. DOE-2 model [3.9] is a combination of MoWitt and BLAST [3.10]. TARP model [3.11] is very similar to BLAST and detailed convection models. The adaptive convection algorithm [3.12] assigns default equations to surfaces depending on their outside face classification, heat flow direction and wind direction.

The graph in

Figure 3-5 compares the exterior convection coefficients for a vertical surface calculated by TARP and DOE-2 model depending on wind

speed and surface roughness, assuming a temperature difference of 10K between outdoor air and external wall surface. DOE-2 and TARP model returns similar results for low wind speeds. At higher wind speeds DOE-2 is more affected by wind speed than the TARP one. Internal convection coefficients can be assigned independently at every surface of the model and depend on the zone use, zone airflow regime and surface orientation and heat flow direction. EnergyPlus includes five models to determine the interior convection coefficients: TARP, Simple, CeilingDiffuser, TrombeWall and Adaptive ConvectionAlgorithm.

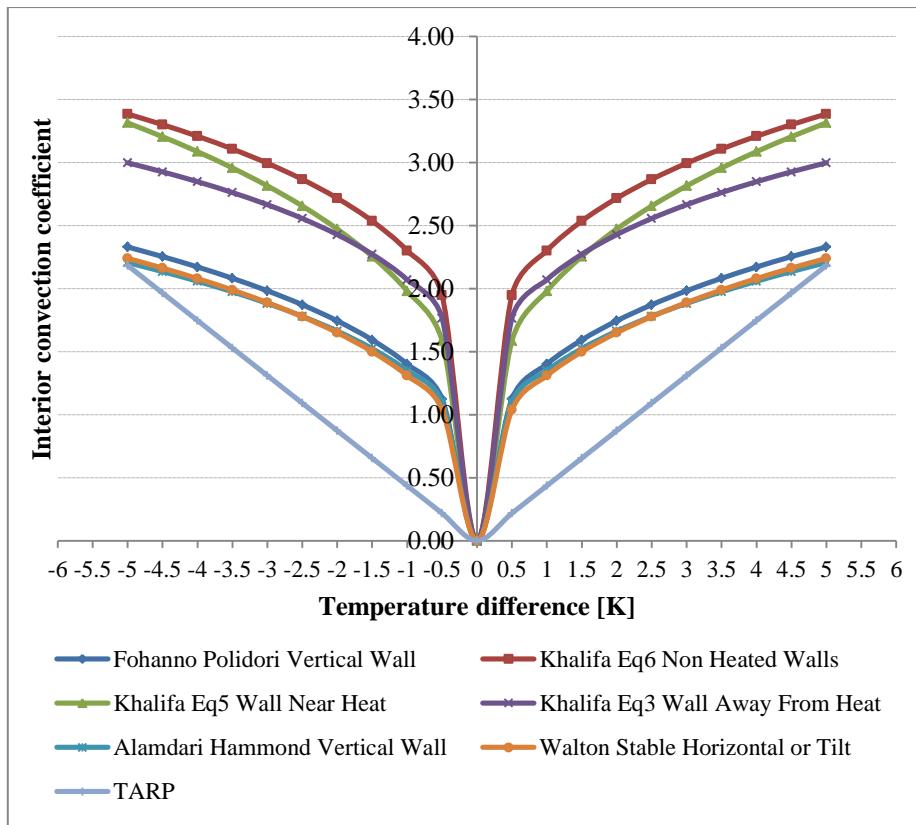


Figure 3-6. Vertical wall interior convection model comparison at different temperature differences between air and wall interior surface. Image courtesy of Roberti F.

TARP algorithm [3.11] is based on ASHRAE equations for natural convection heat transfer coefficients in the turbulent range for large, vertical plates and correlates the heat transfer coefficient to the surface orientation and the difference between the surface temperature and the zone air temperature.

The Simple convection model uses constant coefficients for different heat transfer configurations: vertical surface ($h = 3.076$), horizontal surfaces with enhanced convection model ($h = 4.040$) and with reduced convection model ($h = 0.948$), tilted surfaces with enhanced convection model ($h = 3.870$) and with reduced convection model ($h = 2.281$). The coefficients are also taken from (88).

The CeilingDiffuser algorithm is based on empirical correlations developed by Fisher D.E. and Pedersen C.O. [3.13] which use air change rate as correlating parameter.

The Trombe wall algorithm is used to model convection in a "Trombe wall zone", i.e. the air space between the storage wall surface and the exterior glazing. This convection model is based on the correlations from ISO 15099 applied for the convection between glazing layers in multi-pane window systems.

The adaptive convection algorithm [3.12] assigns default equations to surfaces depending on the zone airflow regime and the surface orientation and heat flow direction. The convection models are selected by the algorithm depending on the zone air flow regime.

The graph in Figure 3-6 compares the TARP interior convection model for vertical wall with some of the models for vertical walls included in the adaptive convection algorithm: Walton Stable Horizontal or Tilt, Fohanno Polidori Vertical Wall, Alamdari Hammond Vertical Wall, Khalifa Eq3 Wall Away From Heat, Khalifa Eq5 Wall Near Heat, Khalifa Eq6 Non Heated Walls.

Walton G.N. et al. [3.10] developed an equation to calculate the surface convection coefficient by fitting curves from various sources. Stable refers to the direction of heat flow and the associated buoyancy relative to the surfaces, meaning that the natural tendency is to retard flow in the sense that rising warmer air, or falling cooler air, is driven against the surface.

Fohanno-Polidori [3.14] and Alamdari-Hammond [3.15] equations determine interior convection coefficient for vertical wall in simple buoyancy flow conditions depending on temperature difference between surface and air and on ceiling height.

Khalifa A. [3.16] conducted experiments in test chambers and developed correlations for convectively heated zones and applies to vertical surfaces located away from the heat source (Eq3), near the heat source (Eq5) and to not heated walls (Eq6).

In simple buoyancy flow conditions and for temperature differences greater than 0.5 K the calculated interior convection coefficients may range from 1 to 2.5 according to the adaptive convection algorithm equations. Lower values are predicted by the TARP algorithm. Interior convection coefficient values between 2 and 3.5 are predicted for surfaces located in convectively heated zones.

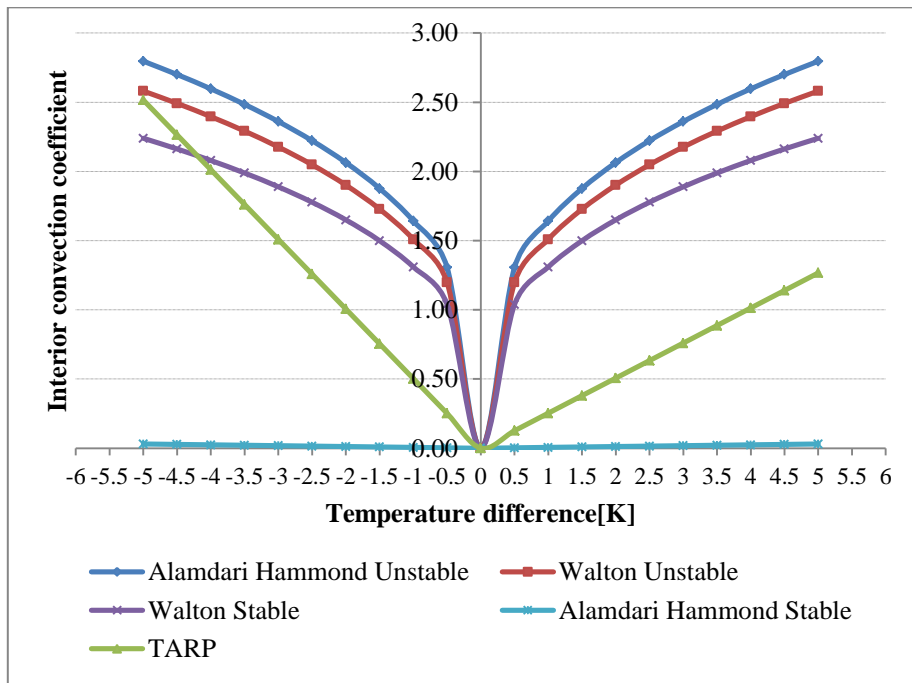


Figure 3-7. Horizontal slab interior convection models comparison at different temperature differences between air and wall interior surface. Image courtesy of Roberti F.

The graph in Figure 3-7 compares the TARP interior convection model for a horizontal surface with some of the models for vertical walls included in the adaptive convection algorithm: Alamdari Hammond Stable Horizontal, Alamdari Hammond Unstable Horizontal, Walton Unstable Horizontal and Walton Stable Horizontal.

Alamdari-Hammond [3.15] developed equations for horizontal surface in stable thermal situation and in a buoyant thermal situation (unstable). The interior convection coefficient predictions in stable conditions are significantly lower than in the other cases.

Walton model is applicable to both horizontal and tilted surfaces as the equations require the tilt angle of the surface as input. The Walton model is a component of the overall TARP algorithm.

It is also possible to override the convection coefficients on the inside of any surface by using the “SurfaceProperty:ConvectionCoefficients” object in the input file to set the convection coefficient value on the inside of any surface or the Energy Management System actuators that are available for overriding convection coefficients values. These options can also include schedules that control values over time. Specific details are given in the EnergyPlus documentation [3.17].

3.3.3. External wind conditions

EnergyPlus converts wind velocity weather data through numerical method that considers the differences between the weather station location and the building site, according to Equation 3-1.

$$V_z = V_{met} \left(\frac{\delta_{met}}{Z_{met}} \right)^{a_{met}} \left(\frac{Z}{\delta} \right)^a \quad \text{Equation 3-1}$$

where

- V_{met} = wind velocity at the EnergyPlus default weather station [m/s];
- V_z = measured wind speed [m/s];
- Z_{met} = EnergyPlus default wind sensor height (10 m) [m];
- δ_{met} = EnergyPlus default wind speed profile boundary layer thickness (270 m) [m];
- Z = wind sensor height above ground [m];
- δ = wind speed profile boundary layer thickness for the terrain surrounding the on-site weather station [m];

α_{met} = EnergyPlus default wind speed profile exponent (0.14) [-];
 α = wind speed profile exponent for the terrain surrounding the on-site weather station [-].

Terrain type field in the building object associates different values of wind speed profile exponent and height. Five different terrain type are included in the EnergyPlus model (Table 3-2).

Further wind velocity profiles can be set using the Site:WeatherStation object. The wind speed profile coefficients can be calculated using CFD modelling of the weather station terrain.

Terrain type does not affect wind directions. The only way to adjust wind directions according to the urban surroundings is to modify directly the weather file.

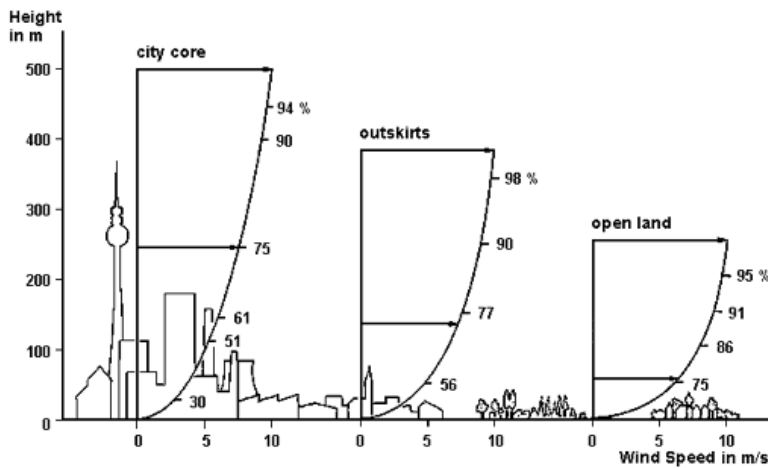


Figure 3-8. Decrease in wind speed as influenced by varieties of terrain roughness.
 Source: http://www.stadtentwicklung.berlin.de/umwelt/umweltatlas/ed403_01.htm

Table 3-2. Wind speed profile coefficients. Source: ASHRAE [2.8]

Terrain type	Terrain description	Exponent, α	Boundary layer thickness, δ (m)
Country	Flat, open country	0.14	270
Suburbs	Rough, wooded country, suburbs	0.22	370
City	Towns, city outskirts, centre of large cities	0.33	460
Ocean	Ocean, Bayou flat country	0.10	210
Urban	Urban, Industrial, Forest	0.22	370

3.3.4. External nodes

Every surface considered in the airflow network has to be associated to an external node which define environmental conditions outside of the building depending on the specified height of the node. These conditions include wind speed that varies depending on the height of the node according to the defined wind speed profile and wind pressure coefficients and can be highly dependent on the building geometry.

External nodes play an essential role in the modelling of stack effect where ventilation rates are also driven by pressure differences due to height difference between inlet and outlet.

3.3.5. Zones and surfaces

Zones and surfaces involved in the airflow network, such as windows, vents and surfaces containing cracks, have to be connected to the thermal model through the “AirflowNetwork:Multizone:Zone” and the “AirflowNetwork:Multizone:Surface” objects.

In order to establish an airflow network, each “AirflowNetwork:Multizone:Zone” object must have at least two surfaces defined with “AirflowNetwork:Multizone:Surface” objects, so that air can flow from one zone into other zones (or to outdoors) through the network (air mass flow conserved). In addition, for all “AirflowNetwork:Multizone:Surface” objects facing the same Zone, at least two different environments must be defined for the other side of these surfaces (e.g., an external node and an adjacent zone, two adjacent zones, or two external nodes).

Surface inputs may be a time consuming task as every surface involved in the airflow network must be added as a new object. To save input effort and calculation time, in case of multiple windows or doors with similar shadowing and daylighting located on the same surface and operated at the same time, it is recommendable to use the Multiplier field in the “FenestrationSurface:Detailed” object. The total airflow across the surface is equal to the airflow based on the surface geometry multiplied by the subsurface multiplier.

In the thermal model, the window vertices specified in the geometry should be referred only to the glazed part of the window and do not include the frame area. Frame and dividers are added as window properties. This should be considered in the opening factors definition. Adjacent surfaces do not have to be entered twice in the airflow network model. This would cause the air flow through the surface to be counted twice.

Each external surface has to be related to a leakage component (simple, detailed or horizontal opening, effective leakage area or crack) and connected to an external node of the airflow network (see par.3.1).

Ventilation control mode and schedules can be defined either at zone level (all the zone's operable windows and doors are operated at the same time and in the same way) or at surface level (each zone's operable window and door can be controlled in a different way). Par. 3.3.8 reports more on control settings.

It is assumed that the air flow through a window opening is unaffected by the presence of a shading device such as a shade or blind on the window. Also, the calculation of conductive heat transfer and solar gain through a window or door assumes that the window or door is closed. Cui S. et al. [3.18] analysed the impact on the modification of optical characteristics of glazed surfaces on thermal condition and natural lighting due to opening windows, concluding that this secondary effect should be considered in case of large south-oriented glazed surfaces in temperate climates, where natural ventilation can be dominant.

3.3.6. Leakage components

A linkage used in the Airflow Network model has two nodes, inlet and outlet, and is linked by a component which has a relationship between airflow and pressure.

All the linkages can be led back to the general form of the power law model (Equation 3-2).

$$Q = C[f(\Delta P)]^n \quad \text{Equation 3-2}$$

where ΔP is the pressure difference between inlet and outlet node of the network and C and n are defined constants.

Three component types are available for openings:

- Simple opening
- Detailed opening
- Horizontal opening

Details about the relationship between airflow and pressure for the above mentioned components are available in the EnergyPlus Engineering reference [3.1].

Simple and detailed opening allow modelling air flow moving simultaneously in two different directions depending on stack effects and wind conditions. Airflow network model allows bi-directional flow only for vertical openings. The simple opening component assumes the pressure difference across the opening is a function of height varied from opening bottom to top, so that two-way flow may be obtained if appropriate. The detailed opening component assumes both the pressure difference across the opening and air density are a function of height, so that three-way flow may be obtained. The air density is assumed to be a linear function of height.

In the detailed window object users can also specify opening type and different sets of opening factor data.

Horizontal opening component can be linked only to interzone surfaces. The best modelling technique for horizontal openings is to put a crack object in a horizontal surface and use a large air mass flow coefficient. Crack flow is assumed to be uni-directional in any given timestep, but can reverse flow direction from timestep to timestep.

Infiltrations can be modelled in a detailed way by linking crack or effective leakage area objects to surfaces.

The relationship used to calculate air flow rate through cracks is expressed as Equation 3-3.

$$Q = c_T c_Q \Delta P^n \quad \text{Equation 3-3}$$

where

Q = air mass flow [kg/s];

c_Q = air mass flow coefficient [kg/s @ 1 Pa];

c_T = reference condition temperature correction factor [-];

ΔP = pressure difference across crack [Pa];
 n = air flow exponent [-].

As regards openings, the program generates automatically four cracks around the perimeter of the window or the door. Air mass flow coefficient and exponent in Equation 3-3 have to be specified in the opening object. In this case, the air mass flow coefficient is normalized by component perimeter length and the temperature correction factor is not used.

The relationship between airflow and pressure used to define the Effective Leakage Area (ELA) is expressed as Equation 3-4.

$$\dot{m} = A_L \cdot C_D \sqrt{2\rho} \cdot (\Delta P_r)^{0.5-n} (\Delta P)^n \quad \text{Equation 3-4}$$

where

\dot{m} = air mass flow rate [kg/s]
 A_L = effective leakage area [m²]
 ρ = air density [kg/m³]
 ΔP_r = reference pressure difference [Pa]
 ΔP = pressure difference across this component [Pa]
 C_d = discharge coefficient [dimensionless]
 n = air mass flow exponent [dimensionless]

The distribution of air leakage paths and component air leakage characteristics should be known. Data about leakage characteristics based on component leakage tests can be found in existing literature [3.19][3.20][3.28]. NISTIR 6585 report [3.20] also contains whole building air leakage characteristics based on whole building pressurization tests. The AIVC calculation techniques [3.28] present a summary of air leakage characteristics of building components gathered from standards, recommendation and codes of practice.

3.3.6.1. Blower door test

The leakage area in small to medium buildings is most commonly determined through the use of blower door tests, which result in the

flow coefficient c and the flow exponent n in the power law equation (Equation 3-5).

$$Q = c(\Delta P)^n \quad \text{Equation 3-5}$$

where

- Q = airflow rate [m^3/s];
- c = flow coefficient [$\text{m}^3/(\text{s}^n)$];
- n = flow exponent [-].

The measured airflow rate at a reference pressure can be converted to an equivalent or effective air leakage area by using Equation 3-6 reported from chapter 16 in ASHRAE Handbook [2.8].

$$A_L = 10000 Q_r \frac{\sqrt{\rho/2 \Delta p_r}}{c_D} \quad \text{Equation 3-6}$$

where

- A_L = equivalent or effective air leakage area [cm^2];
- Δp_r = reference pressure difference [Pa];
- Q_r = predicted airflow rate at Δp_r (from curve fit to pressurization test data) [m^3/s];
- ρ = air density [kg/m^3];
- c_D = discharge coefficient.

Blower door tests usually report an overall airtightness values for the whole building. The simplest way to use these results is to apply the total effective leakage area derived from the blower door test evenly over the exterior envelope surface area of the building model.

Air leakage area at one reference pressure can be converted to air leakage area at another reference pressure difference according to Equation 3-7.

$$A_{r,2} = A_{r,1} \left(\frac{c_{D,1}}{c_{D,2}} \right) \left(\frac{\Delta P_{r,2}}{\Delta P_{r,1}} \right)^{n-0.5} \quad \text{Equation 3-7}$$

where

- $A_{r,1}$ = air leakage area at reference pressure difference $\Delta P_{r,1}$ [cm^2];
- $A_{r,2}$ = air leakage area at reference pressure difference $\Delta P_{r,2}$ [cm^2];
- $c_{D,1}$ = discharge coefficient used to calculate $A_{r,1}$ [-];

$c_{D,2}$ = discharge coefficient used to calculate $A_{r,2}$ [-];
 n = pressure exponent [-].

Air leakage at one reference pressure difference can be converted to airflow rate at some other reference pressure difference according to Equation 3-8.

$$Q_{r,2} = \frac{C_{D,1}A_{r,1}}{10\,000} \sqrt{\frac{2}{\rho}} (\Delta p_{r,1})^{0.5-n} (\Delta p_{r,2})^n \quad \text{Equation 3-8}$$

Flow coefficient c in Equation 3-5 may be converted to air leakage area according to Equation 3-9.

$$A_L = \frac{10000\,c}{C_D} \sqrt{\frac{\rho}{2}} (\Delta p_r)^{n-0.5} \quad \text{Equation 3-9}$$

Air leakage area can be converted to flow coefficient c in Equation 3-5 according to Equation 3-10.

$$c = \frac{c_D A_L}{10\,000} \sqrt{\frac{2}{\rho}} (\Delta p_r)^{0.5-n} \quad \text{Equation 3-10}$$

3.3.6.2. Discharge coefficient

The discharge coefficient is required as input in airflow models and is defined by Equation 3-11.

$$c_d = \frac{q}{A} \sqrt{\frac{\rho}{2\Delta p}} \quad \text{Equation 3-11}$$

where

q = volume flow rate across the opening [m^3/s];
 A = defined open area [m^2];
 ρ = air density [kg/m^3];
 Δp = airflow difference across the opening [Pa].

The Equation 3-11 is applied to openings installed in a surface that separates two much larger spaces in still-air conditions, with uniform and equal densities. In practice flows through openings are generated and influenced by wind and buoyancy forces. The wind modifies the

external flow field, whereas the buoyancy forces cause different air densities.

The discharge coefficient is a fixed property of an opening and it is generally evaluated in still-air conditions. It is a function only of the shape of the opening and the Reynolds number. However, when an opening is installed in an envelope, the actual discharge coefficient may differ from the still-air one due to installation effects. In particular, the installation effects depend primarily on the magnitude of V/u_m (typical values range from 1.5 to 9), where V is the cross flow velocity and u_m is the spatial mean velocity through the opening:

- if $V/u_m < 1$ the effect is small;
- if $V/u_m > 5$, the discharge coefficient can be reduced by 50% or more.

Table 3-3 reports the opening classification and the flow characteristics developed by Etheridge D. [2.42]. As Etheridge D. stated, the installation effects are negligible for air vents and small windows (opening type 2) in case of low velocity ratio and for large stacks (opening type 3) in case of inward flow only.

It is to underline that these effects are only present when wind is present and they can be reduced by considering the following facts:

- the presence of buoyancy will increase u_m and decrease V/u_m ;
- in any given building, one half of the flow will be outward. If the outflow is through stacks or chimneys, wind effects will be reduced;
- there are likely to be some openings that lie in a wake region where V is small;
- there are likely to be long openings as well as sharp-edged ones.

Sensitivity studies showed that airflow predictions are linearly dependent on the value of the discharge coefficient [2.33] and therefore they imply directly proportional results uncertainty. Johnson M. et al. [3.29] compared airflow network predictions with measured airflow values and found that the discrepancy in the predicted value is due to inaccuracy in the discharge coefficient, which was an estimated value.

Karava P. et al. [3.21] reviewed the current literature and found that a discharge coefficient dependent only on opening shape is an invalid simplification as it varies considerably with façade porosity, opening configuration, Reynolds number, wind incidence angle, local geometrical and airflow conditions, opening height and temperature differences. Larger differences have been shown in cross ventilation cases, especially at small porosities (less than 15%).

Heiselberg P. et al. [3.22] showed that the discharge coefficient for a window opening cannot be regarded as a constant and it varies considerably both with the opening area, the window type and the temperature difference and that the use of a constant value can lead to serious errors in the prediction of airflow capacity. As much as opening angle is smaller the uncertainty is higher, because leakages along all other sides of the opening account for a relative large part of the opening area. Table 3-4 reports some of the discharge coefficient values estimated by past studies depending on opening type and flow regime.

Table 3-3. Opening type classification and discharge coefficient (c_d) relations. Source: Etheridge D. [2.42]

Type	Size	A/A_w^* (%)	L/d_h^{**}	Description	Still-air c_d -Re and Δp -q characteristics	Flow direction	Examples
1	Small	<0.1	wide range	adventitious	C_d depends strongly on Re_o $\frac{1}{c_d^2} = C \frac{L}{Re_o d_h} + D$ $\Delta p = a q^2 + b q$	unidirectional flow	crack in door and window frames
2	Small	<2	<2	purpose-provided, short	C_d =constant $\Delta p = a q^2$	unidirectional flow	air vents, small windows
3	Large	not relevant	>5	purpose-provided, long	$\frac{1}{c_d^2} = C \frac{L}{Re_o^{0.25} d_h} + D$ $\Delta p = a q^2 + b q^{1.75}$ For $Re_o > 2000$ approx.	unidirectional flow	chimneys, stacks, ducts
4	Large	<20	<2	purpose-provided, short	Still-air C_d probably not relevant.	bidirectional flow	large open windows, internal doors
5	Very large	>50	<2	purpose-provided, short	Still-air C_d probably not relevant.	flow affects external envelope flow when wind present	large open windows, external doors

* Ratio between the area of the opening (A) and the wall area of the space ventilated by the opening (A_w)

** Aspect ratio (L is the length of the opening in the flow direction and d_h is the hydraulic diameter)

Table 3-4. Value of discharge coefficient found in existing literature.

Cd value	Flow regime	Opening type	Assessment method	Reference
0.71	Still air	Sharp-edged orifice	Wind tunnel	Chiu Y.H. et al. [3.23]
0.1 – 0.7	Effect of freestream wind speed	(flush to the wall)		
0.1 – 0.5	Still air	Long opening		
0.1 – 0.4	Effect of wind with upward flow	(chimney)		
0.2 – 0.5	Effect of wind with reversed flow			
0.65	stack driven ventilation	Sharp-edged opening	analitical	ASHRAE Handbook [2.8]
$C_d = 0.40 + 0.0045(T_i - T_o)$	wind driven/diagonal winds			
0.25-0.35	wind driven/perpendicular winds			
0.5-0.6				
$\begin{cases} \frac{C_z}{C_{zo}} = \left(\frac{Re}{Re_c}\right)^{0.333} & Re < 18000 \\ C_{zo} = 0.66 & Re \geq 18000 \end{cases}$	Varying turbulent effects	Square shaped openings – variable opening diameter and wall porosity	Wind tunnel	Chia R. et al. [3.24]

3.3.7. Wind pressure coefficients

Wind pressure coefficients are used to calculate wind-induced pressures on each façade surface during simulations and are defined as the ratio of static pressure to dynamic pressure at a given point on the façade (Equation 2-5).

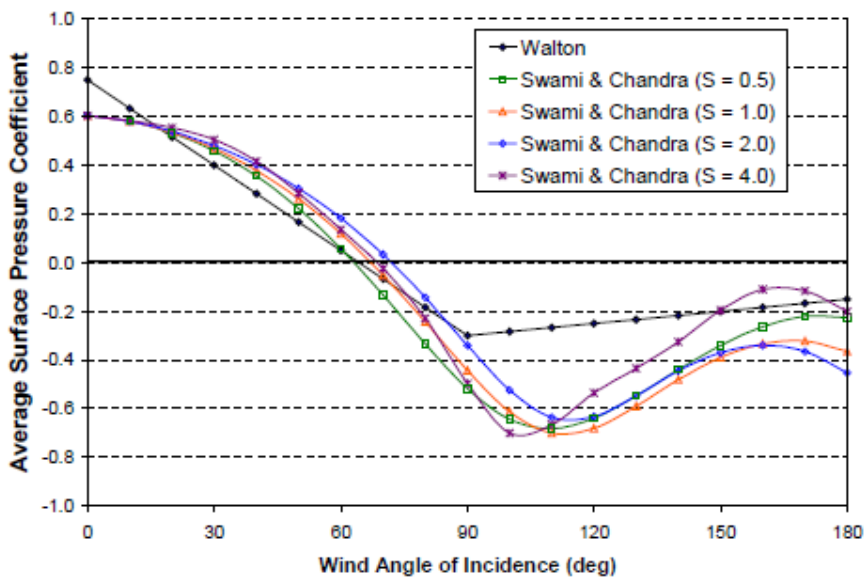


Figure 3-9. Surface pressure coefficient as a function of wind incident angle for the Walton model and the Swami and Chandra model for side ratios $S = L_1/L_2$. Source: Deru M. et al. [3.25]

Wind pressure coefficient values depend on wind direction and node position on the building façade. In EnergyPlus users can specify wind pressure coefficients for up to 36 wind directions. The program automatically interpolates wind pressure coefficient values according to the wind direction at every time step defined in the weather file.

Wind pressure coefficients are related to external node/surfaces. If building north axes is different from true north, wind pressure coefficient array should be adjusted to the building orientation.

For instance, if the building main axes is rotated 30 degrees relative to true north, the wind pressure coefficient array should be changed from

[0, 45, 90, 135, 180, 225, 270, 315] to [30, 75, 120, 165, 210, 255, 300, 345].

They can be evaluated in detail through different approaches:

- full-scale measurements;
- reduced-scale experiments in wind tunnels;
- computational fluid dynamics (CFD) simulations.

However these approaches are not suitable to early stage design simulations as they are time-consuming activities and would require additional costs.

EnergyPlus includes an algorithm to calculate surface averaged coefficients [3.26] for four vertical facades and roof. It should be used for rectangular shaped buildings only by specifying the side ratio. Surface-averaged wind pressure coefficients should be avoided when more openings per façade are present as the magnitude of their uncertainty is high [3.27].

Other analytical models and database are available for different building geometry.

The Air Ventilation and Infiltration centre (AIVC) database [3.28] is based on the interpolation of data from published material. Wind pressure coefficient datasets are available for high and low-rise buildings with different exposure conditions and with different length to width ratio.

The Tokyo Polytechnic University (TPU) aerodynamic web database [3.30] is based on wind tunnel experiments on 12 test cases including low and high rise buildings with varied eaves.

The ASHRAE Handbook provides data for low-rise and high-rise buildings, presenting examples of the distribution of wind pressure coefficient values over the façade.

The Dutch institution TNO developed a web-based application called Cp generator [3.31] based on systematic performed wind tunnel tests and on published results of on-site tests performed by several research organizations. Users have to write an input form with c_p coordinates and obstacle geometry and distance from the building.

In par. 5.1.5 a comparison between wind pressure coefficients gathered from existing literature dataset with the one estimated by wind tunnel measurements is presented for a case study.

3.3.8. Control settings

Opening factors control in the EnergyPlus Airflow Network model can be set by:

- using the predefined ventilation control mode;
- programming with the energy management system.

3.3.8.1. Ventilation control mode

Ventilation control modes can be applied at zone or surface level. All the openings in a thermal zone are operated in the same way, unless the ventilation control mode is applied at surface level.

Ventilation availability schedule defines when the natural ventilation is allowed.

Predefined natural ventilation control mode are:

NoVent:	All of the zone's operable windows and doors are closed at all times independent of indoor or outdoor conditions. Venting availability schedule is ignored in this case.
Temperature:	All of the zone's operable windows and doors are opened if $T_{zone} > T_{out}$ and $T_{zone} > T_{set}$ and venting availability schedule allows venting.
Enthalpy:	All of the zone's operable windows and doors are opened if $H_{zone} > H_{out}$ and $T_{zone} > T_{set}$ and venting availability schedule allows venting.
Constant:	Whenever the venting availability schedule allows venting, all of the zone's operable windows and doors are open, independently of indoor or outdoor conditions.

ASHRAE55Adaptive: All of the zone's operable windows and doors are opened if the operative temperature is greater than the comfort temperature (central line) calculated from the ASHRAE Standard 55-2010 adaptive comfort model and venting availability schedule allows venting.

CEN15251Adaptive: All of the zone's operable windows and doors are opened if the operative temperature is greater than the comfort temperature (central line) calculated from the CEN15251 adaptive comfort model and venting availability schedule allows venting.

Temperature and Enthalpy control mode require the input Ventilation Control Zone Temperature Set-point Schedule and the opening can be modulated according to the outdoor-indoor temperature/enthalpy. No modulation option is available for the ASHRAE55Adaptive control type.

AirflowNetwork:Multizone:Zone must be associated at EnergyPlus zone objects and can be associated to Schedules to control the ventilation availability.

3.3.8.2. **Energy Management System (EMS)**

To override the controls associated with the airflow network control modes, an Energy Management System (EMS) object can be used.

The EMS system of EnergyPlus can access output variables and use them as sensors to direct various type of control actions.

There are four Energy Management System objects within EnergyPlus that can be used: Sensor, Actuator, Program calling manager, and Program. It is recommended to have one object per zone that is being controlled to avoid any conflicting calculations.

Sensor: The sensor object defines what aspect of the model that is monitored. The monitored aspect has to be one of the defined output variables.

- Actuator: The actuator object defines what aspect of the model will be overridden (e.g. opening factor).
- Program Calling Manager: The program calling manager defines at what stage the EMS should be used during the energy calculation, and what Program should be calculated.
- Program: The program object is where the override calculation is included. The formula reads the sensor information and if the argument is ‘true’, the actuator object is overridden with the SET value provided. In this situation, the override values are set to either “on” (1) or “off” (0) within the operation schedule.

In case of natural ventilation modeling, the EMS is useful to control opening factors, which have to be set as actuators.

It is also possible to set schedule values for opening factors as output variables and sensors in the EMS and then set the actuated component (window/door opening factor) equal to the sensor (schedule value). This option would be useful if window operation data are available as in the case study presented in chapter 5. However, it has to be considered that sub-hourly schedules cannot be set in EnergyPlus.

Further information about the EMS and how it works is described in the EnergyPlus EMS application guide; included in the EnergyPlus documentation [3.17].

3.4.A modeling example: the new Technology Park in Bolzano

The project of the new Technology Park in Bolzano (Italy) aims at regenerating an old industrial area, where three main existing blocks listed as industrial historical buildings will be renovated and other new buildings will be built. For the new building, owner and design team have taken up the challenge to achieve the targets of Net Zero Energy Building and total primary energy index lower than 60 kWh/m²y. The

ambitious targets could be reached considering first of all the reduction of energy needs, in particular through passive solutions. Natural ventilation has been considered since the early-design-stages as a passive solution and the decision making process has been supported through dynamic simulation tools to quantify the energy savings.

The building is architecturally conceived as a black monolithic block with a nearly-square plant. It has five floors above ground and an underground floor. The main entrance is on the north side of the ground floor and on the south side there is the expo area. The upper floors will host offices, meeting and service rooms, whereas in the underground floor there will be several conference rooms. In the centre of the building and through the full height, a green patio is designed as a buffer zone to improve indoor comfort and daylighting. Figure 3-10 to Figure 3-12 show the architectural concept of the building.



Figure 3-10. Building render. Source: CLEAA

The envelope is a metal-glass façade with a solar shading system in the south façade and a black surface with different strips of horizontal windows in the other facades. The horizontal windows on north, east and west façade are positioned on the inner side of the external wall. In this way, the deep reveal due to the wall thickness and the low height of the windows work as a sun shading system and the glazed part of the façade will not be visible from the outside perspective.



Figure 3-11. Typical floor plan. Source: CLEAA



Figure 3-12. Building cross section. Source: CLEAA

3.4.1. Natural ventilation strategies

A climate suitability analysis and simplified airflow network transient simulations in CONTAM [1.27] allowed identifying a night stack driven cross ventilation as the most effective configuration that balances performances needs with constraints given by fire compartments, acoustic comfort and privacy needs in the offices during the working hours.

To increase the height difference between inlet and outlet openings, office zones (outlined in cyan blue and magenta in Figure 3-13) will be connected by floor vents. Inlet and outlet openings are automatically controlled top hung windows. The floor vents are closed during the working hours to avoid acoustic discomfort and maintain privacy between offices.

The foyer is directly connected to a lightwell and to the hall of every floor (outlined in green in Figure 3-13) and is ventilated through a stack driven cross ventilation to avoid overheating situations.

Due to safety reasons underground floor and expo areas are mechanically ventilated. A small office area in the central part of the building (outlined in yellow in Figure 3-13) is single-sided ventilated and connected with the green patio.

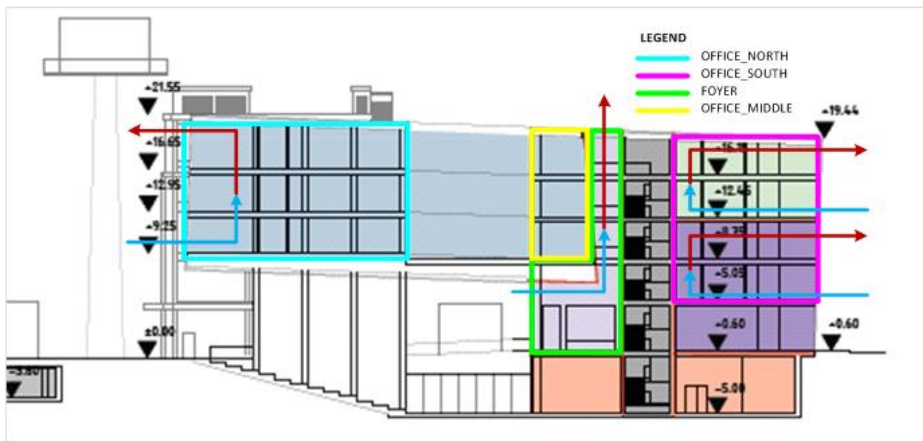


Figure 3-13. Cross section of the building fire regulation plan with fire compartments, model zones and a scheme of the selected stack-driven cross ventilation configurations for the considered zones.

3.4.2. EnergyPlus model to study airflows

The original EnergyPlus building model zoning has been re-thought to introduce an airflow network. Particular care has been taken to reduce computational time.

The building has been divided into thermal zones with the same temperature and pressures, occupation patterns, internal gains, major exposure, cooling setpoints. Thermal zones have been further on

Table 3-5) to support the building design. Horizontal window series and floor vents series have been modelled using multiplier as they have the same size and the same height from the ground level. In this way window shape effects are taken into account properly and less input objects are necessary to set window controls.

Table 3-5. Airflow network surface components area and height from the ground.

Zone group	Airflow network component name	Opening type	Height [m]	Area [m ²]	Nr of windows	Tot. opening area [m ²]
OFFICE_ SOUTH	01_INLET	Top hung window	7.5	0.65	16	10.40
	02_OUTLET	Top hung window	10.9	0.65	18	11.70
	03_INLET	Top hung window	14.6	0.54	26	14.04
	04_OUTLET	Top hung window	16.8	0.80	26	20.80
	12_FLOOR VENT	Horizontal opening	8.2	1.60	9	14.40
	34_FLOOR VENT	Horizontal opening	15.6	1.60	10	16.00
OFFICE_ NORTH	N_INLET	Top hung window	10.6	0.54	10	5.37
	N_OUTLET	Top hung window	19.0	0.74	10	7.39
	04_BUFFER	Top hung window	17.6	0.71	4	2.85
	02_BUFFER	Top hung window	11.7	0.71	4	2.85
	N23_FLOOR VENT	Horizontal opening	12.4	0.60	9	5.40
	N34_FLOOR VENT	Horizontal opening	16.1	0.60	9	5.40
BUFFER ZONE	BUFFER_INLET	Top hung window	21.5			8.00
	BUFFER_OUTLET	Top hung window	21.5			8.00

Zone group	Airflow network component name	Opening type	Height [m]	Area [m ²]	Nr of windows	Tot. opening area [m ²]
STACK	STACK_INLET	Top hung window	3.4	-	-	8.70
	STACK_OUTLET	Top hung window	22.0	-	-	8.70

An opening factor of 0.5 has been set for top hung window assuming a maximum opening angle of 45°.

This may cause inaccurate shadowing and daylight distribution inside the building, but the computation time decreases. However, daylight study was not one of the purposes of this simulation and opening area is only a small percentage of the whole glass area. For the same reason a full exterior solar distribution with no reflections has been set. Reflections would have required also no-convex zones, that would have meant setting more zones.

Energy Management System objects are used to introduce simple controls on windows and vents opening. Indoor and outdoor temperature variables have been set as sensors and venting opening factors as actuators. A program was written to activate natural night ventilation between 8 pm and 8 am if the following conditions are fulfilled:

- indoor temperature is higher than 24°C;
- indoor temperature is higher than outdoor dry bulb temperature;
- outdoor dry bulb temperature is higher than 10°C.

External nodes at each floor height and each facade have been set to take into account more accurately wind pressure conditions and model stack effects.

Floor vent interzone surfaces are linked to horizontal opening components with a 90° sloping pane angle. Horizontally pivoted detailed openings are used to model inlet and outlet top hung windows. An ideal loads air system template, with a cooling setpoint temperature of 26°C during working hours, has been implemented to evaluate

cooling loads without taking into account the plant system. Infiltration rates have been neglected, as the building tightness required by the local standard is restrictive (0.5 h^{-1} at 50 Pa) and will be proven by blower door test.

Simulations have been run from June to September. Average airflow network volume flow rates are shown in Figure 3-14. Simulation results of the base case model have showed that among the summer period the airflow direction do not always follow the airflow path in the positive direction: it works in the 86% of activation hours in the upper floors and in the 46% of activation hours in the lower floors. This could be due to the lower opening area in the 1st and 2nd floor. The graph in Figure 3-15 shows the airflow frequencies through the inlet-outlet components in the south office block. It could be noticed that low airflow rates are more frequent in the negative airflow direction.

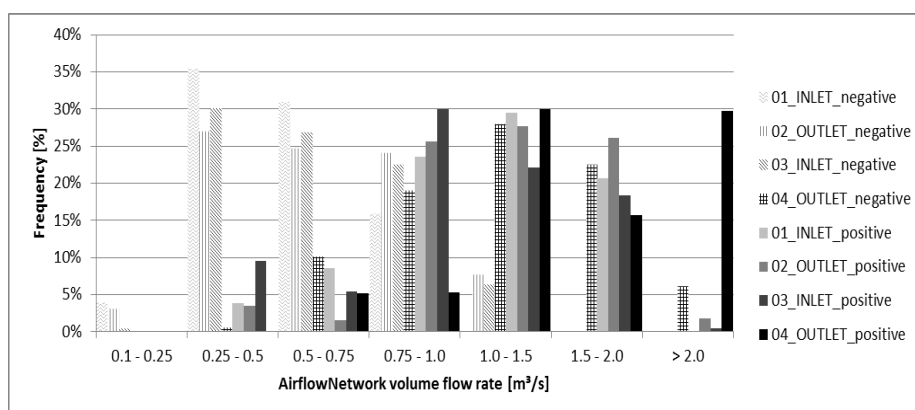


Figure 3-15. Natural volume flow rate frequency along the airflow network paths in the south office block.

Bibliography

- [3.1] EnergyPlus Engineering Reference. 2012.
- [3.2] Lixing Gu. Airflow network modeling in Energyplus. Building simulation, 2007.
- [3.3] Hensen J., Bartak M., Drkal F. Modeling and simulation of a double-skin facade system. ASHRAE transactions, Vol. 108, 2002.
- [3.4] Baharvand E. How to model a wall solar chimney? Complexity and predictability. TU Eindhoven: Master Thesis, 2010.

- [3.5] Breesch H. Natural night ventilation in office buildings. Gent University, Netherland : PhD Thesis, 2006.
- [3.6] Breesch H., Janssens A. Performance evaluation of passive cooling in office buildings based on uncertainty and sensitivity analysis. Energy and Buildings, 2010.
- [3.7] Artmann N., Manz H., Heiselberg P. Parameter study on performance of building cooling by night time ventilation. Renewable Energy 33, pp. 2589-2598, 2008.
- [3.8] Yazdanian M., Klems J. H. Measurement of the exterior convective film coefficient for windows in low-rise buildings. ASHRAE Transactions, Vol. 100 - Part 1. 1994, p. 1087.
- [3.9] DOE2.1E-053 source code. Lawrence Berkeley National Laboratory, 1994.
- [3.10] Walton G.N. Passive solar extension of the Building Loads Analysis and System Thermodynamics (BLAST) program. United States Army Construction Engineering Research Laboratory, 1981.
- [3.11] Thermal Analysis Research Program (TARP) Reference Manual. National Bureau of Standards NBSSIR 83-2655, 1983.
- [3.12] Beausoleil-Morrison I. The adaptive coupling of heat and air flow modeling within dynamic whole-building simulations. Glasgow: PhD Thesis. University of Strathclyde, 2000.
- [3.13] Fisher D.E., Pedersen C.O. Convective heat transfer in building energy and thermal load calculations. ASHRAE Transactions 103, 1997.
- [3.14] Fohanno S., Polidori G. Modelling of natural convective heat transfer at an internal surface. Energy and Buildings 38, pp. 548 – 553, 2006.
- [3.15] Alamdari F., Hammond G.P. Improved data correlations for buoyancy-driven convection in rooms. Building Services Engineering Research & Technology, pp. Vol. 4 - No.3, 1983.
- [3.16] Khalifa AJN. Heat transfer processes in buildings. University of Wales : PhD Thesis, 1989.
- [3.17] EnergyPlus v 7.2 Documentation. Input Output reference. 2012.
- [3.18] Cui S., Stabat P., Marchio D. Influence of natural ventilation on solar gains and natural lighting by opening windows. Building Simulation, pp. 10-17. Chambery, 2013.
- [3.19] Orme M., Leksmono N. Ventilation modeling data guide. IEA - AIVC, 2002.
- [3.20] Persily A. K., Ivy E.M. Input data for multizone airflow and IAQ analysis. NISTIR 6585, 2001.
- [3.21] Karava P., Stathopoulos T., Athienitis A. K. Natural ventilation openings - a discussion of discharge coefficients. Building for the Future: The 16th CIB World Building Congress. Rotterdam (NE), 2004.
- [3.22] Heiselberg P., Svendsen K., Nielsen P.V. Characteristics of airflow from open windows. Building and Environment 36, pp. 859-869, 2001.

- [3.23] Chiu Y- H., Etheridge D.W. External flow effects on the discharge coefficients of two types of ventilation opening. *Journal of Wind Engineering and Industrial Aerodynamics*, pp. 225-252, 2007.
- [3.24] Chia R. Chu, Chiu Y.-H., Yan-Jhih Chen, Yu-Wen Wang, C.-P. Chou. Turbulence effects on the discharge coefficient and mean flow rate of wind-driven cross-ventilation. *Building and Environment* 44, pp. 2064-2072, 2009.
- [3.25] Deru M., Burns P. Infiltration and natural ventilation model for whole-building energy simulation of residential buildings. NREL/CP-550-33698, 2003.
- [3.26] Swami M.V., Chandra S. Correlations for pressure distributions on buildings and calculation of natural ventilation airflow. *ASHRAE Transactions* 94, pp. 243-266, 1988.
- [3.27] Cóstola D., Blocken B., Ohba M., Hensen J.L.M. Uncertainty in airflow rate calculations due to the use of surface-averaged coefficients. *Energy and Buildings* 42, pp. 881-888, 2010.
- [3.28] Liddament M.W. Air infiltration calculation techniques. AIVC, 1986.
- [3.29] Johnson M.H., Thai Z., Krarti M. Performance evaluation of network airflow models for natural ventilation. *HVAC & Research*, 2012
- [3.30] Tokio Polytechnic University. Aerodynamic database for low-rise buildings. [Online] 2007. http://www.wind.arch.t-kougei.ac.jp/info_center/windpressure/lowrise/mainpage.html.
- [3.31] TNO Built Environment and Geosciences. TNO Web Applications. [Online] 2002. <http://cpgen.bouw.tno.nl/home/Default.asp>.

4. Sensitivity analysis of natural ventilation design parameters

EnergyPlus model with airflow network can be applied during early design phases to inform natural ventilation design and test whole solution sets performance, as it enables to simultaneously model building energy use, natural ventilation airflow, and occupant comfort. Often however many of the building design parameters that impact natural ventilation performance, are not defined during the early-design-stages. This uncertainty presents a significant challenge for simulation engineer when modelling potential ventilation strategies.

Parametric analysis can be used to some extent to give a range of potential outcomes given uncertainty in the model input parameters. However performing a parametric analysis that includes all of the unknown design parameters requires significant time and resources. Several prior studies [3.6] [4.1] [4.2] [4.3] have attempted to identify which simulation parameters have the most impact on building performance. These studies focused primarily on simulation variables such as convective and radiation heat transfer coefficient, ground reflectance, radiative fraction of internal gains etc. rather than the building design parameters that are likely to evolve throughout the design process. No prior studies have been identified that focus on the uncertainty in building energy models that are coupled with an airflow network model.

In order to provide guidance for designers of naturally ventilated non-residential buildings on the impact various design parameters have on natural ventilation performance, a sensitivity analysis on key design parameters that cannot be clearly specified during early-design-stages was performed in collaboration with the simulation research group at

the Lawrence Berkeley National Laboratory. The considered design parameters include, internal and solar gains, envelope characteristics and window geometry and opening type.

4.1.Reference building

The sensitivity analysis is performed on a four-storey office building north-south oriented, intended to be representative of a typical European medium sized office. The building layout is symmetric around the central stairway and services.

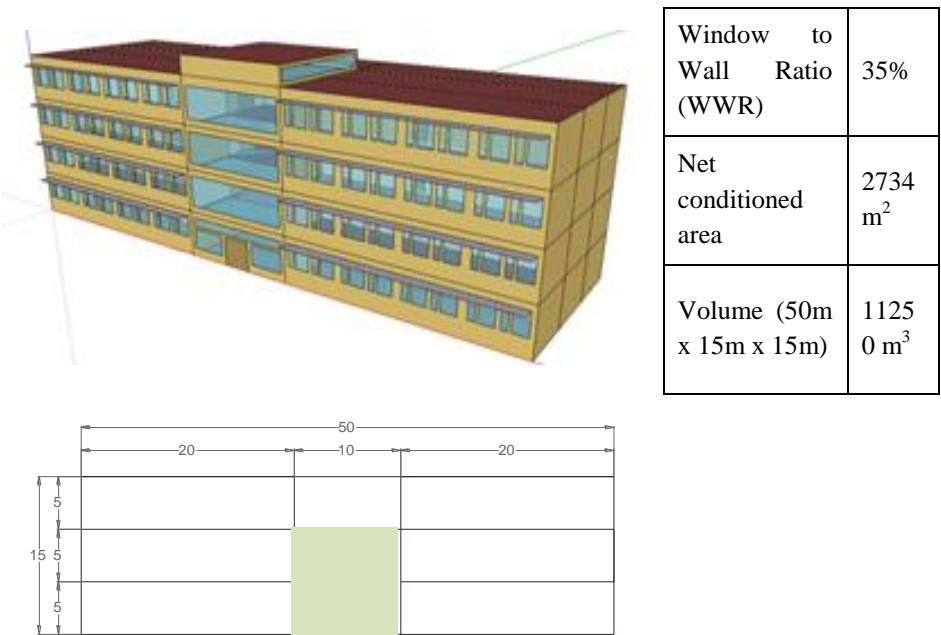


Figure 4-1. Building SketchUp model and geometric characteristics.

Figure 4-1 shows the building model in SketchUp and the plan view of one of the four storey. Each floor has four open plan office zones connected through vents to the stairwell passive stack. An opening at the ground floor and openings on the roof allow the stack effect.

Each window frame has two panes, the left one for natural ventilation and the right one for daylighting. Overhangs have been added to the south façade to reduce the solar gains during summer.

Automatically controlled windows have been added to the south and north façade. Vents between the hallways and the offices allow air movement even if the doors are closed.

4.2. Modelling method

We modelled two commonly used passive ventilation strategies using the multi-zone airflow network model with the EnergyPlus building energy simulation program: night stack driven cross ventilation, to reduce cooling needs (Strategy A), and wind driven cross ventilation during the day, to improve thermal comfort (Strategy B). In Strategy A, we assume windows are closed during office hours, and that cooling loads are met using mechanical cooling. Windows and vents open autonomously if the indoor temperature exceeds 26°C, allowing night-time free cooling through the stairwell passive stack. The modelled strategy varies the opening area depending on the inside-outside temperature difference, in order to reduce the possibly large fluctuations in temperature. We modelled stairwell passive stack as four vertically stacked zones connected to each other through cracks with large air mass flow coefficient and to the office floors through vents.

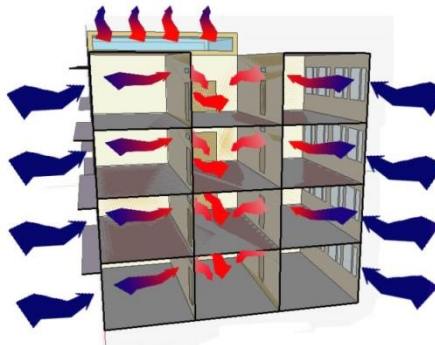
In Strategy B, we assume windows are operated during normal office hours by occupants based on their thermal comfort. When windows are in use, ventilation cooling is provided via naturally driven cross ventilation. The modelled control strategy is based on EN 15251 adaptive comfort model and allows window opening during the day if the indoor operative temperature is greater than the adaptive comfort temperature. We assumed in this case that the building is in free-running mode with no mechanical heating or cooling.

For both simulation scenarios we used wind pressure coefficients from the AIVC dataset for semi-sheltered low-rise rectangular buildings [3.28]. We modelled unintentional infiltration by applying Equivalent

air Leakage Areas (ELAs) evenly over the exterior envelope surface area of the building model.

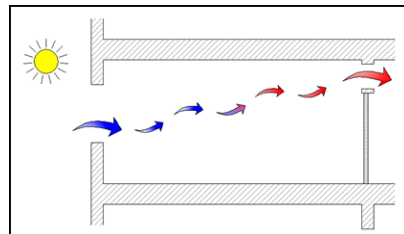
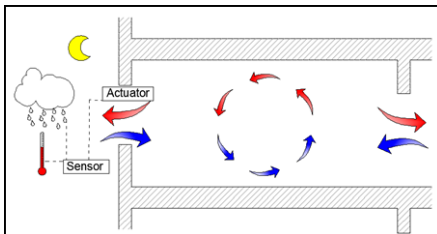
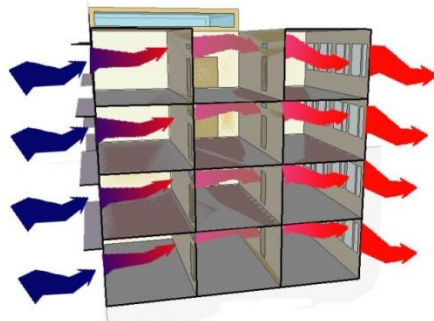
Strategy A

Night stack driven cross ventilation to reduce cooling need



Strategy B

Wind driven cross ventilation during the day to improve thermal comfort



We applied four different ELAs derived from the four classifications of building envelope performance specified in the KlimaHaus build regulations. We calculated ELAs from the maximum ACH at 50 Pascal, as defined in KlimaHaus, using translation equations defined in ASHRAE [4.4].

Window position and dimension were not considered variables. We developed hourly lighting schedules to represent the use of artificial lighting. We generated these schedules by first performing a building simulation run using the daylighting controls option in EnergyPlus. This option uses the anticipated availability of daylight coming through the windows, to moderate electric lighting on needed basis. Performing building simulations using this option is computationally costly, and so this option was only used to generate our electric light usage schedules.

Simulations performed for our parametric analysis used EnergyPlus's FullExterior shading mode which assumes no daylighting modeled; resulting in significantly quicker simulation run times. We used 15 minute simulation run time steps based on analysis by Zhai J. et al. [2.4] that demonstrated 15 minute time steps were sufficient to the coupling of airflow and thermal models.

4.3.Parameter selection and variable range assessment

Our sensitivity analysis took into account only uncertain building properties due to lack of information during early-design-stage. Input parameters that were primarily simulation environments parameters (i.e. convection coefficients, zone air heat balance algorithm) were not varied in our analysis, as these type of parameters would typically remain constant throughout the design process.

We assigned value ranges for the envelope thermal insulation, air tightness (ELA) and density based on a combination of building regulations (D.Lgs.192/05), energy performance requirements (KlimaHaus energy certification) and technical feasibility. For instance, the upper bound U-value was the U-value required by the local building regulation and the lower bound was set by taking into account the technical and economic feasibility of the envelope construction.

Table 4-1. Input parameter variables.

	DESCRIPTION	MIN	MAX
F1	Exterior wall insulation thickness [m]	0.10	0.25
F2	Exterior roof insulation thickness [m]	0.16	0.28
F3	Exterior window U-value [W/m ² K]	0.5	1.7
F4	Exterior window Solar Heat Gain Coefficient (SHGC)	0.3	0.9
F5	Exterior wall density [kg/m ²]	230	430
F6	Slab density [kg/m ²]	150	415
F7	Overhang depth [m]	0.3	1.5

	DESCRIPTION	MIN	MAX
F8	Inside reveal depth [m]	0	0.24
F9	People fraction radiant	0.3	0.6
F10	Lights fraction radiant	0.18	0.72
F11	Effective Leakage Area	0.5	2
F12	Window opening factor	0.4	1
F13	Window discharge coefficient	0.3	0.9
F14	Vent discharge coefficient	0.3	0.9
F15	Number of people per Zone	7	16
F16	Lighting Watts per Zone Floor Area [W/m ²]	5	20
F17	Electric equipment Watts per Zone Floor Area [W/m ²]	5	20
F18	Wind velocity profile: Exponent α , Boundary layer thickness δ [m]	$\alpha=0.10$ $\delta=210$	$\alpha=0.33$ $\delta=460$

We varied electrical equipment gains and lighting gains between the most efficient equipment available on the market (LED lighting and new electrical equipment) and a reference one based on the EU technical background report on indoor lighting [4.5]. We varied the number of people in the zone assuming two different office layouts, open space (7.14 m²/p) and single office (12.5 m²/p) (SIA 2024-2006). This resulted in average daily total internal gains of between 12 W/m² and 40 W/m². We varied the people fraction radiant [2.8] and the lights fraction radiant, taking into account different luminaire configurations [4.6].

We varied the shading overhangs, inside reveal depth and solar heat gain coefficients as per Table 4-1. Variation in these three parameters impacted the internal solar heat gains. In addition, we also varied the window and vent opening factors and their discharge coefficients [3.21]. Variation in these parameters was based on typical window performance, representative of a range of different window types,

operation and wind direction. We considered different wind velocity profiles based on the rationale that the location or orientation of the building might be subject to change during early-design-stage, which we considered likely to impact cooling loads. Table 4-1 lists all the considered variables and their ranges.

Because the principle objective of Strategy A is to provide space cooling, we used the cooling loads as our metric to assess the performance. In Strategy B no cooling system was modelled, therefore our metric of performance was the number of comfortable occupied hours. We calculated the comfort hours based on the three categories of adaptive comfort described in the European Standard EN15251-2007.

4.4.Climate dependency

Prior work by Zhai J. et al. [2.4] indicated that simulated building performance is significantly impacted by the use of locally measured weather, as compared to weather station data. Zhai recommends the use of local weather data when available, particularly for buildings with high solar gains. We performed parametric analysis using three different weather files: Bolzano, Palermo and San Francisco [4.7].

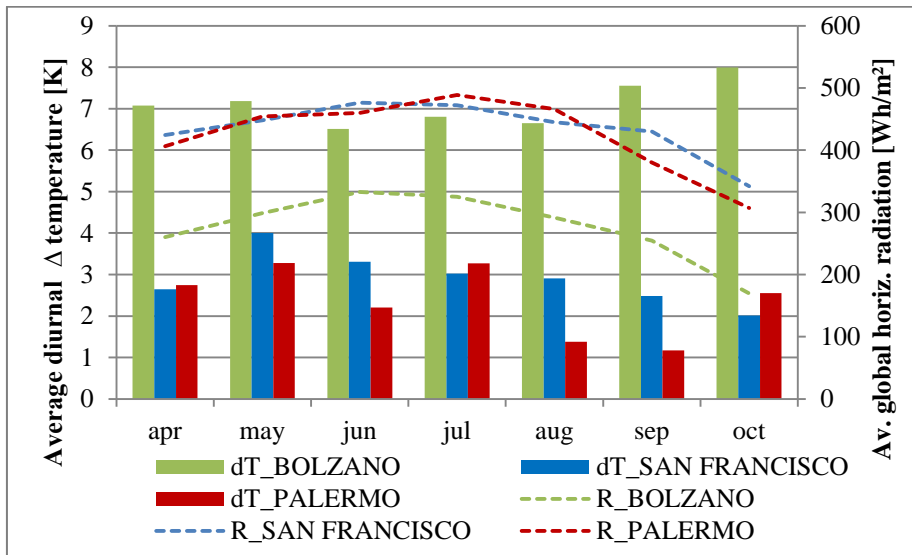


Figure 4-2. Diurnal temperature swing and solar radiation of the three selected locations. EnergyPlus weather data [4.7].

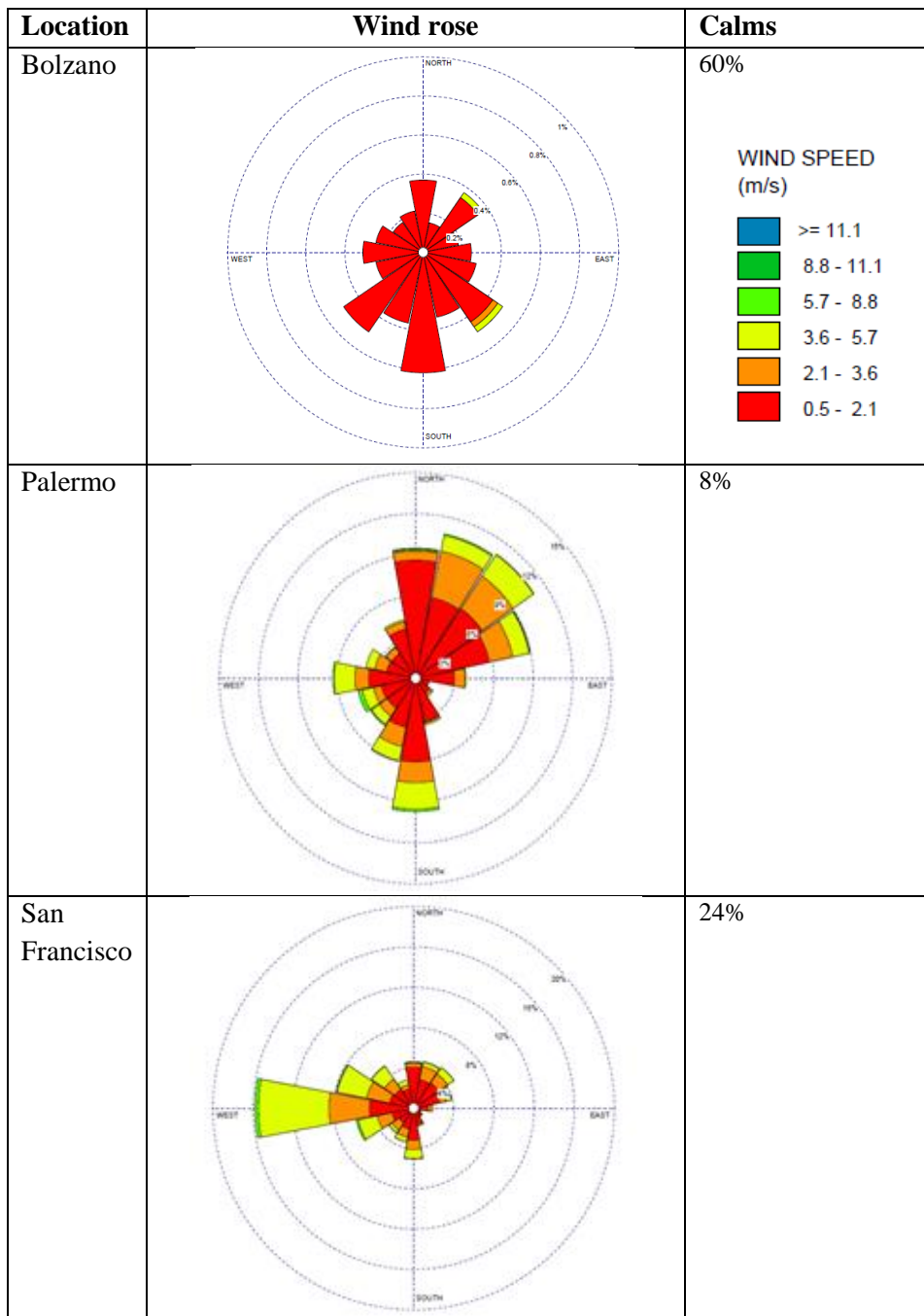


Figure 4-3. Wind rose representing wind speed, direction and frequency in the analyzed climates from April to October during the whole day. EnergyPlus weather data [4.7]. Source: WRPLOT view

Figure 4-2 compares average day-night temperature differences and solar radiation in the three locations, whereas Figure 4-3 compares the wind characteristics in the three locations. Bolzano represents a typical continental climate with large diurnal swing and low wind speed. Palermo represents a typical Mediterranean climate with hot summers and low wind breezes. San Francisco has mild summers and higher wind speeds.

4.5. The Elementary Effect method

We performed a sensitivity analysis using the Elementary Effects (EE) method described in Saltelli et al. [4.8]. This method determines which input variables have negligible, linear or nonlinear effect on the objective with a relatively small number of samples (combinations of input values).

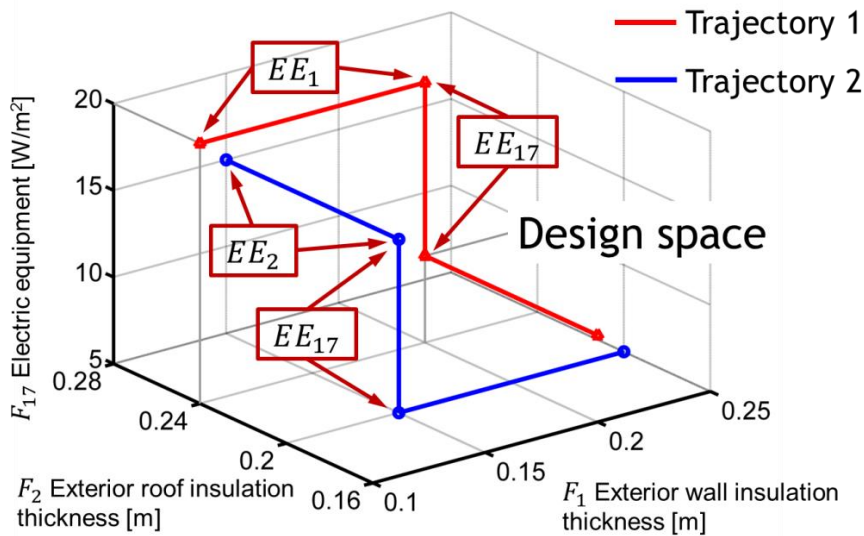


Figure 4-4. Trajectory examples in a 3-dimensional design space. Image courtesy of Filippi Oberegger U.

Rather than testing all possible combinations of the input parameters, the EE method selects representative combinations of input parameters to test. Groups of combinations of input parameters are called “trajectories”. Figure 4-4 represents an example of trajectories in a 3-

dimensional design space. Typically the number of combinations in each trajectory is equal to the number of test parameters plus 1. Each combination of parameter values is a point in the n -dimensional design space. Each point in the design space corresponds to exactly one building design and thus one simulation.

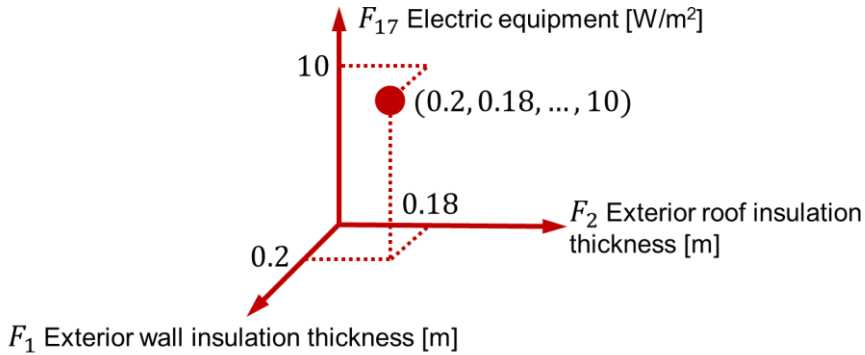


Figure 4-5. Combination of parameter values sample in a 3-dimensional design space. Image courtesy of Filippi Oberegger U.

Figure 4-5 represents an example of a 3-dimensional design space. Within a trajectory, each combination of test parameters differs from the previous by changing only one parameter each time. For a detailed explanation of the parameter selection process see Saltelli et al. [4.8].

The EE method subdivides the variable ranges of each input parameter into equal intervals of equal size. The boundaries of these intervals are called levels. For our parametric analysis, we used four levels (three intervals), based on work by Saltelli that showed that four levels have equal probability of being selected (see Figure 4-6). When applying the EE method, the discrete probability distribution for each factor can be user defined. We have selected uniform distributions for all input parameters, because we consider each of the values to be equally likely in an early-design-stage.

When two combinations of sequential input parameters within a trajectory are simulated, only one variable will differ between them; the difference in the output between these two runs is used to calculate a metric called the elementary effect (EE). The elementary effect (EE) is defined for the i^{th} parameter, on the k^{th} input analysed as:

$$EE_i = \frac{[y(x_1, \dots, x_{i-1}, x_i + \Delta, x_{i+1}, \dots, x_k) - y(\bar{x})]}{\Delta} \quad \text{Equation 4-1}$$

where X_i , $i = 1, \dots, k$ represents the input parameters and Y the output results for the selected parameters combination. p is the number of levels and Δ is equal to $[p/2 (p-1)]$.

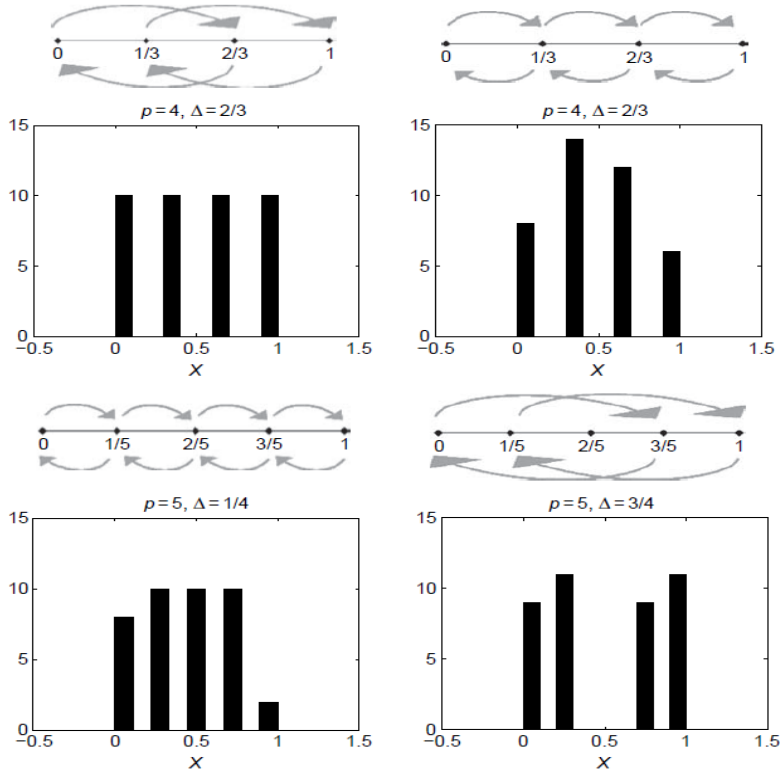


Figure 4-6. Empirical distributions of $r = 20$ trajectories. Source: Saltelli et al. [4.8].

The elementary effect of a factor depends also on the values of the other factors. The sensitivity measures proposed by Saltelli et al. [4.8] are the mean (Equation 4-2), the standard deviation (Equation 4-3) and the mean of the absolute values of the elementary effects (Equation 4-4).

$$\mu_i = \frac{1}{r_i} \sum_{t=1}^{r_i} EE_{i,t} \quad \text{Equation 4-2}$$

$$\sigma_i = \sqrt{\frac{1}{r_i - 1} \sum_{t=1}^{r_1} (EE_{i,t} - \mu_i)^2}$$

Equation 4-3

$$\mu_i^* = \frac{1}{r_i} \sum_{t=1}^{r_1} |EE_{i,t}|$$

Equation 4-4

μ^* quantifies the influence of the factor on the objective. Parameter ranking is based on these values.

High values of σ demonstrate that the factor interacts with other variables and has a nonlinear effect on the objective. Low values of μ , associated with high μ^* values, indicates that there is no direct correlation between this input value and the output value. Whether this factor has a negative or positive impact on the output depends on value of the other significant factors. If μ is equal to μ^* , an increase of the factor corresponds to an increase in the output. If μ is equal to μ^* in magnitude but they have opposite signs, an increase of the factor corresponds to a decrease in the output.

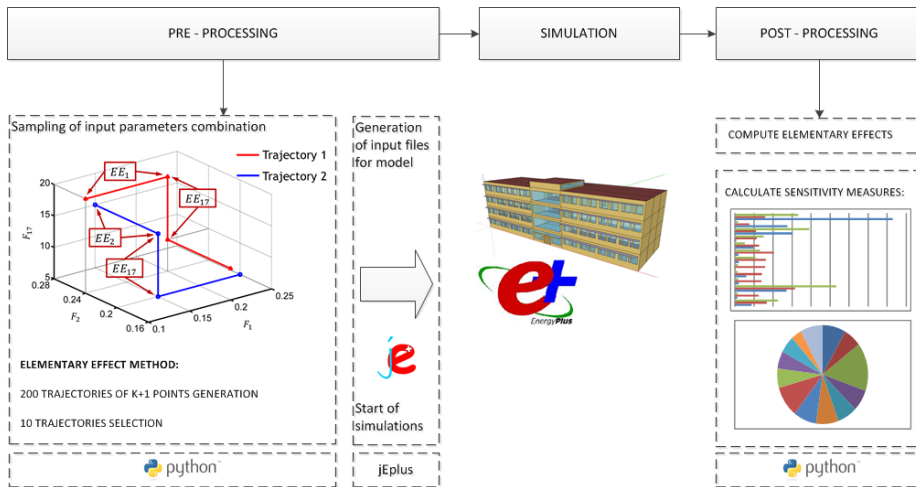


Figure 4-7. Sensitivity analysis methodology overview.

We wrote parameter selection code in Python that generates 200 trajectories consisting of 19 points (the number of input factors plus one), draws 10 trajectories from the 200 available 500 times and selects

the 10 that are farthest among each other. This procedure guarantees a good exploration of the whole design space. Then, the algorithm computes 10 EEs for each input parameters. Finally, the sensitivity statistics are calculated. We run simulations with the selected parameter combinations by means of jEPlus [4.9], an EnergyPlus shell for parametric studies.

The first EE analysis involved 1440 simulations and showed that the solar and internal gains are the most influential parameters.

Therefore, we performed a second elementary effects analysis (840 simulations) fixing internal and solar gains to the lowest reasonable amount to better determine the influence of the other parameters. Table 4-2 lists the values that have been fixed for this second round of parametric analysis.

Table 4-2. Input parameter values that have been fixed for the second analysis.

	DESCRIPTION	VALUE
F4	Exterior Window Solar Heat Gain Coefficient	0.6
F7	Overhang depth [m]	0.5
F15	Number of people per Zone	10
F16	Lighting Watts per Zone Floor Area [W/m ²]	5
F17	Electric equipment Watts per Zone Floor Area [W/m ²]	5

4.6. Results and discussion

Our building model assumptions should be considered in detail, before applying these study results to real building natural ventilation design.

The convection model used in the analysis is not optimal for use with passive cooling strategies because convection coefficients are indirectly predefined by the adaptive convection algorithm [3.12]. As in an early-design-stage no other tools are available, our use of the adaptive convection algorithm can be considered valid.

Our analysis was performed on a rectangular building with a single orientation, and so we were able to make use of published wind

pressure coefficients. The results of the analysis can be considered generalizable to other rectangular buildings, but could be inappropriate for alternative building geometries or orientations.

Bulk airflow model does not consider the internal space layout. Internal walls and furniture may affect the natural ventilation performance. Designers should consider the impact this may have on limiting cross ventilation during the early-design-stages.

The graphs in Figure 4-8 to Figure 4-11 compare the statistical indicators computed by the first EE analysis. The influence percentages are based on the μ^* results. The graphs show similar tendencies in all the considered climate conditions and ventilation strategies. The parameters affecting solar and internal gains (F4, F15-F17) have a dominant influence on natural ventilation performance. In Figure 4-9 and Figure 4-11, the high σ values for parameters F15-F17 for the San Francisco weather suggests that the impact the internal loads have on comfort is strongly influenced by the selected values of the other (non-load) parameters. The positive μ means that an increase of internal gains improves comfort conditions for our Strategy B scenario because of the lower outdoor temperatures in San Francisco. On the contrary, in Palermo comfort can be improved by decreasing both internal and solar gains.

From Figure 4-10 we see that the window discharge coefficient (F13) for Palermo has a notably higher relative impact on the number of comfort hours, compared to the other two climates. We theorize that this is because the forces that drive natural ventilation (wind speed, indoor/outdoor temperature difference) are smaller in Palermo with moderate weather and low average wind speeds.

The graphs in Figure 4-12 to Figure 4-15 compare the statistic indicators computed by the second round EE analysis, where parameters affecting internal and solar gains are fixed. Results show more evident climate dependencies.

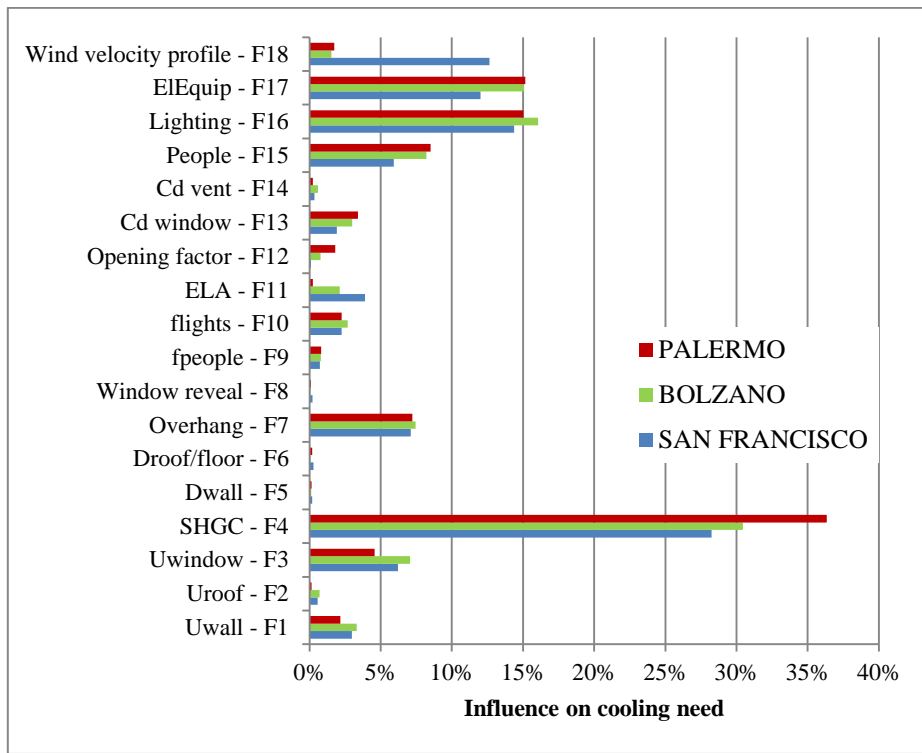


Figure 4-8. I Elementary Effect analysis results: influence on cooling need for Strategy A.

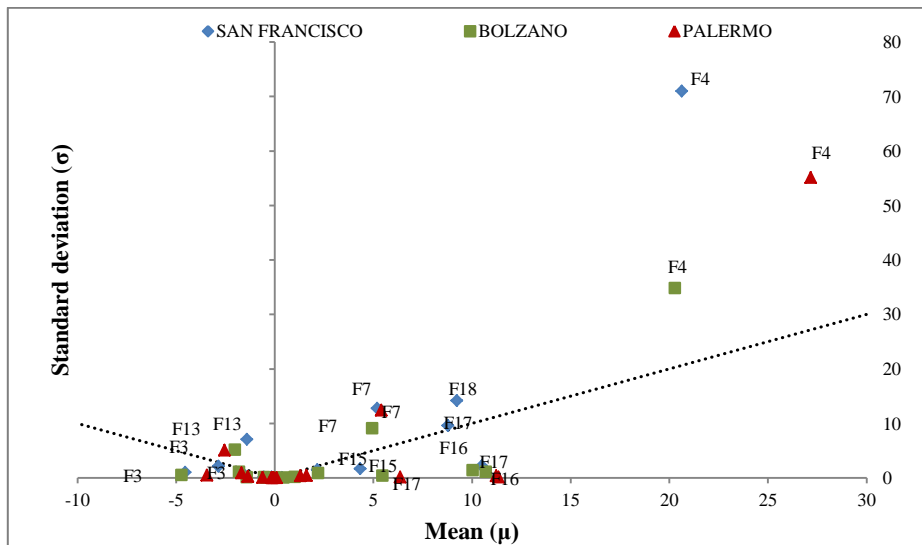


Figure 4-9. I Elementary Effect analysis results: mean and standard deviation of cooling need for Strategy A.

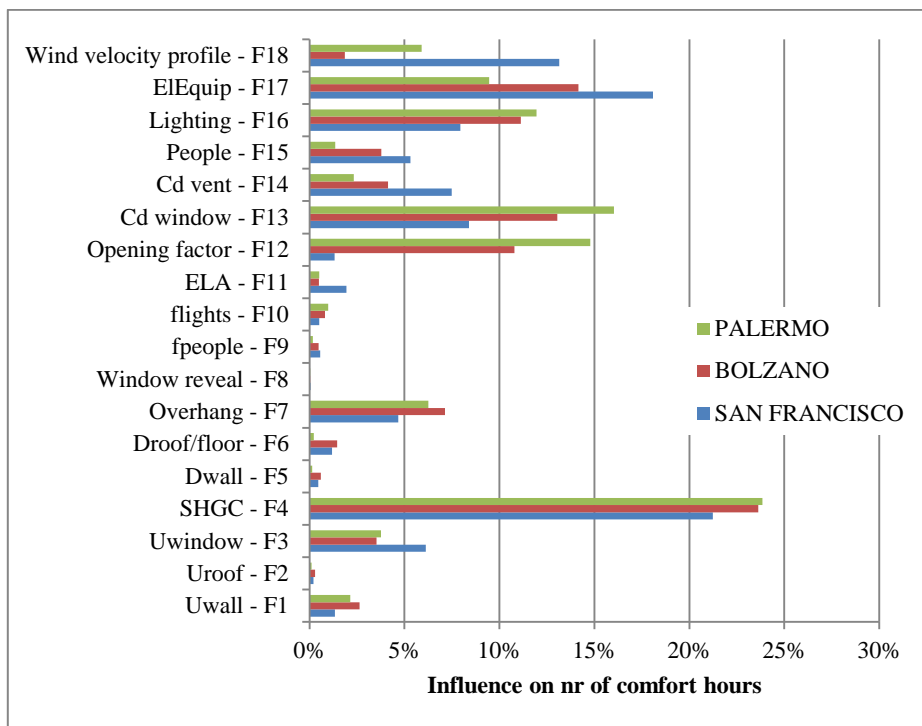


Figure 4-10. I Elementary Effect analysis results: influence on number of comfort hours for Strategy B.

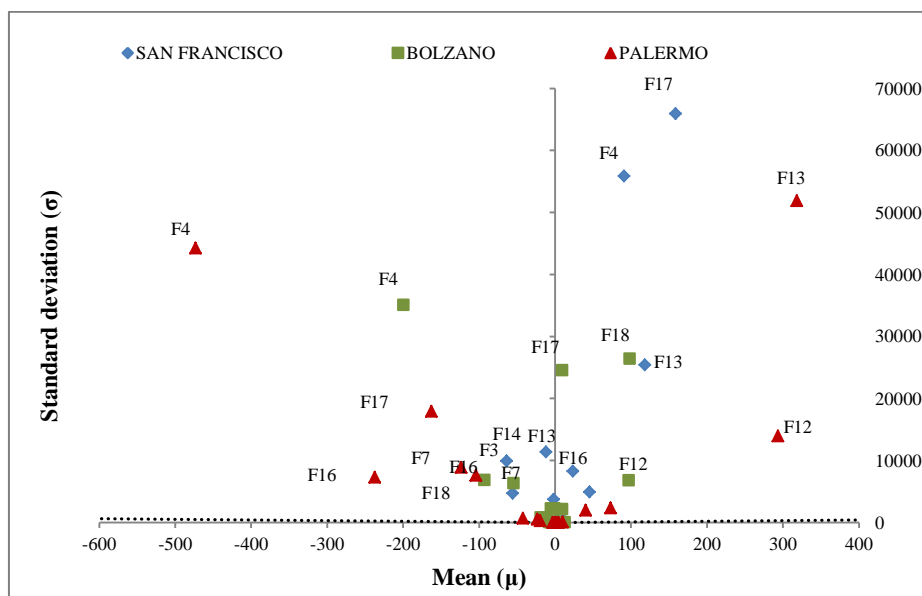


Figure 4-11. I Elementary Effect analysis results: mean and standard deviation of comfort hours number for Strategy B.

Wind velocity profile has the major influence on natural ventilation performance in San Francisco weather. This is because both wind speed and frequencies are higher in San Francisco rather than in Bolzano or Palermo. In windy locations wind velocity profiles parameters have to be carefully estimated depending also on building surrounding area.

Comparing Figure 4-12 to Figure 4-14, it is evident that in Palermo climate window discharge coefficient (F13) and opening factors (F12) have more effect on cross ventilation performance than on passive night cooling. In the Bolzano climate, night cooling performance is more dependent on envelope characteristics (F1 – F8) and on fraction radiant of internal gains (F9 - F10). An increase of the exterior wall density (F5) translates to an increase of the thermal mass of the building, which in turn improves night cooling performance because of Bolzano's large diurnal temperature swings. The effect of exterior roof density (F6) is not evident in the data, because it affects only zone temperatures in the upper floors of the building.

From Figure 4-13 and Figure 4-15 we see that the Effective Leakage Area (F11) has more influence on night cooling performances in Bolzano and San Francisco than in Palermo. Both in Bolzano and San Francisco μ is equal to μ^* for F11, but they have opposite sign. This means that increasing the Effective Leakage Area will decrease the cooling needs in these two cities. In the Palermo climate, low values of μ are associated with high μ^* values. This means that there is not a direct correlation between ELA and the cooling need. Cooling need can either increase or decrease with ELA, depending on the values of our other input parameters.

The positive mean value of F3, F12 and F13 for Palermo in Figure 4-15 show how window U-value, opening factor and discharge coefficient has a greater effect on cross ventilation performance than on night cooling performance in that climate.

Figure 4-13 show that in all the analysed climates, an increase of wall insulation thickness (F1) would cause an increase of cooling need for Strategy A.

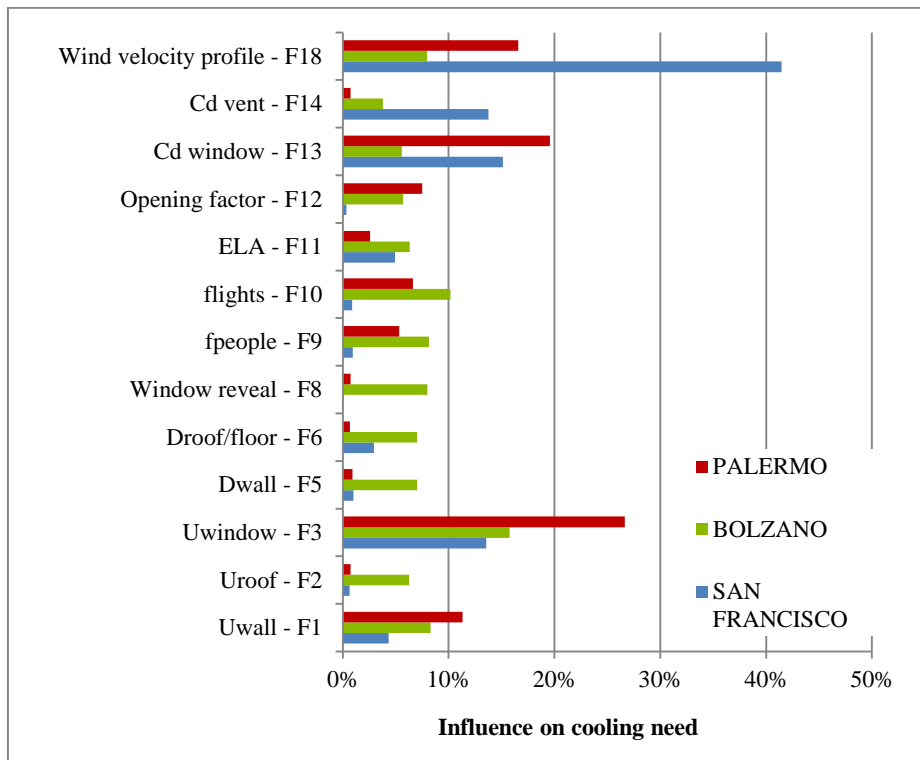


Figure 4-12. II Elementary Effect analysis results: influence on cooling need for Strategy A.

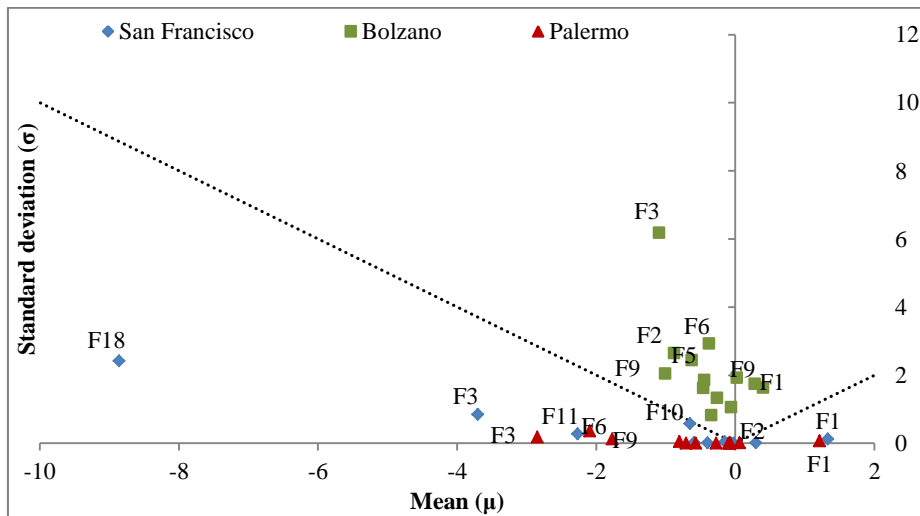


Figure 4-13. II Elementary Effect analysis results: mean and standard deviation of cooling need for Strategy A.

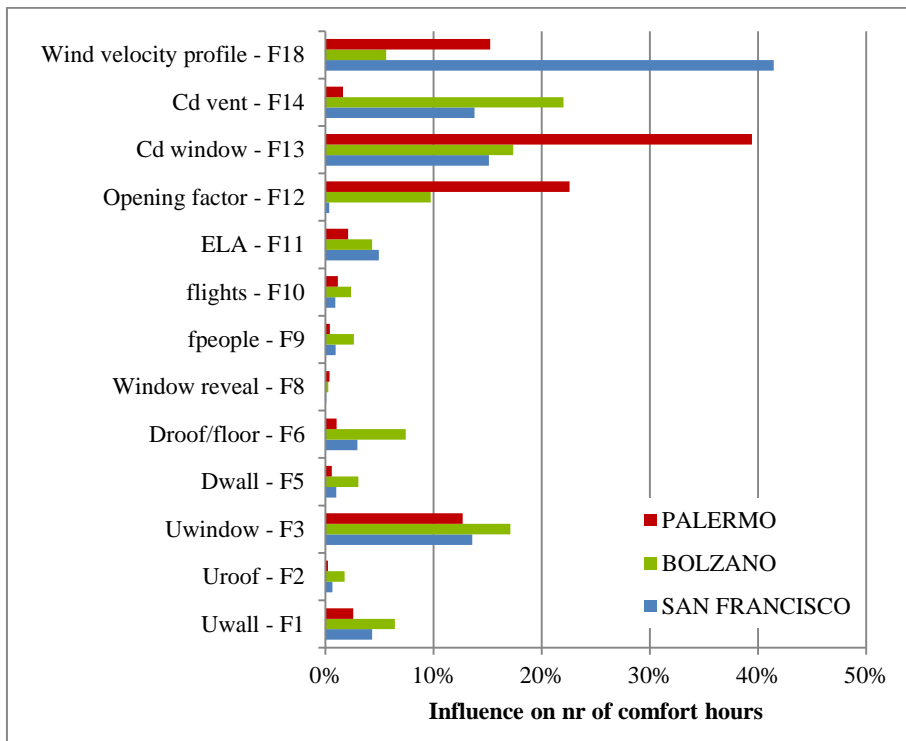


Figure 4-14. II Elementary Effect analysis results: influence on number of comfort hours for Strategy B.

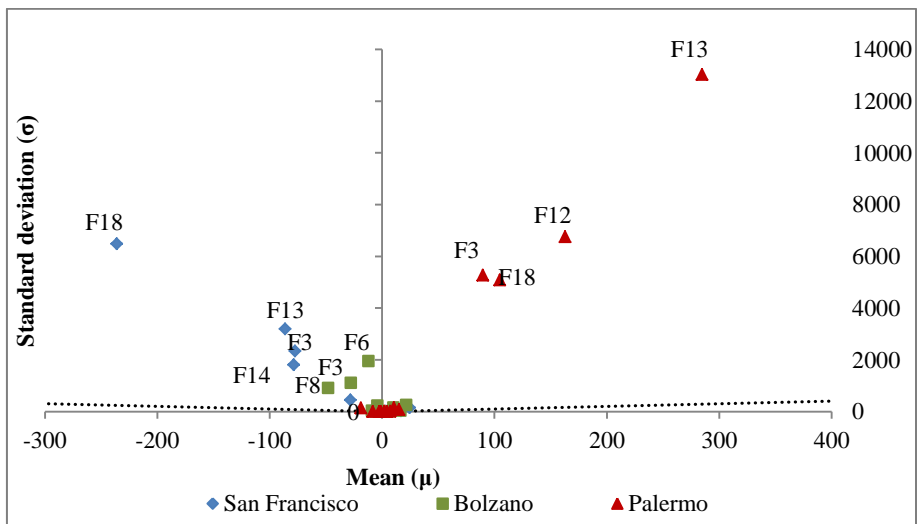


Figure 4-15. II Elementary Effect analysis results: mean and standard deviation of comfort hours number for Strategy B.

Figure 4-13 and Figure 4-15 show that, in the San Francisco case, increasing window and vent discharge coefficient (F13 – F14) will decrease thermal comfort performances but reduce cooling need. We propose that is likely because of the lower outdoor temperatures and the high wind speed in the city.

When windows are open during the day, the indoor temperature cools down quickly below the comfort temperature level. In the Bolzano climate, these parameters have less impact on cooling need and again whether they increase or decrease cooling need depends on the value of the other parameters. Figure 4-13 highlights the higher parameter interaction (higher standard deviations) in the Bolzano weather case compared to the other two climate types.

Wind velocity profile influence seems directly correlated to how windy the location is. The fact that these results were highly dependent on the weather data used highlights the importance of a reliable weather file even in early-design-stages.

The results underline the most important parameters and their effect on night cooling performances and natural ventilation strategies in three different climate types. A ranking of the design parameters influencing the sensitivity to night cooling and thermal comfort performances is reported in Table 4-3 and Table 4-4. The higher is the ranking value the more influent is the parameter.

The sensitivity analysis showed a dominant influence of parameters affecting solar and internal gains on natural ventilation performance in all the considered climates. An accurate assessment of those parameters could reduce significantly the results uncertainty.

Simulation results showed that airflow network parameters had the most significant impact on thermal comfort; these include the window opening factors and discharge coefficients. Airflow parameters influence ventilation flow rates, which directly impact comfort by lowering indoor air temperatures. In case of high wind speeds, window opening factors and discharge coefficients are less significant than wind pressure coefficients.

In climates with large diurnal temperature swings, envelope characteristics have greater impact on both thermal comfort and cooling needs.

The graphs provide quantitative measures of the parameters effect on natural ventilation performances and can be used to support natural ventilation design using building simulation. Generalizing these results to other buildings should be limited to non-residential buildings with regular geometry in similar climate types and wind conditions.

Table 4-3. Ranking parameters of the first EE analysis.

Design parameters		Rank comfort			Rank cooling		
		San Francisco	Bolzano	Palermo	San Francisco	Bolzano	Palermo
F1	Exterior wall U factor	8	9	9	10	12	10
F2	Exterior roof U factor	2	2	2	6	5	3
F3	Exterior window U factor	12	10	11	13	13	13
F4	Exterior Window SHGC	18	18	18	18	18	18
F5	Exterior wall density	3	5	3	2	3	2
F6	Slab density	6	7	5	4	2	4
F7	Overhang depth	10	13	13	14	14	14
F8	Inside reveal depth	1	1	1	3	1	1
F9	People fraction radiant	5	3	4	7	7	7
F10	Lights fraction radiant	4	6	7	9	10	11
F11	Effective Leakage Area	9	4	6	11	9	5
F12	Window opening factor	7	14	16	1	6	9
F13	Window discharge coefficient	15	16	17	8	11	12
F14	Vent discharge coefficient	13	12	10	5	4	6
F15	Number of people	11	11	8	12	15	15
F16	Lighting Watts	14	15	15	17	17	16
F17	Electric equipment	17	17	14	15	16	17
F18	Wind velocity profile	16	8	12	16	8	8

Table 4-4. Ranking parameters of the second EE analysis.

Parameters		Rank comfort			Rank cooling		
		San Francisco	Bolzano	Palermo	San Francisco	Bolzano	Palermo
F1	Exterior wall U factor	8	8	9	10	11	10
F2	Exterior roof U factor	3	2	1	6	4	4
F3	Exterior window U factor	10	11	10	12	13	13
F5	Exterior wall density	6	5	4	2	6	5
F6	Slab density	7	9	5	4	7	1
F8	Inside reveal depth	1	1	2	3	9	3
F9	People fraction radiant	5	4	3	7	10	7
F10	Lights fraction radiant	4	3	6	8	12	8
F11	Effective Leakage Area	9	6	8	11	5	6
F12	Window opening factor	2	10	12	1	3	9
F13	Window discharge coefficient	12	12	13	9	2	12
F14	Vent discharge coefficient	11	13	7	5	1	2
F18	Wind velocity profile	13	7	11	13	8	11

Bibliography

- [4.1] Dominguez-Munoz F., Cejudo-Lopez J.M., Carrillo-Andres A. Uncertainty in peak cooling load calculations. *Energy & Buildings* 2010, vol. 44, pp. 1010-1018.
- [4.2] Hopfe C. Uncertainty and sensitivity analysis in building performance simulation for decision support and design optimization. TU Eindhoven: PhD thesis, 2009.
- [4.3] De Wit S. Uncertainty in predictions of thermal comfort in buildings. Technical University of Delft: PhD Thesis, 2001.
- [4.4] ASHRAE Handbook Fundamentals. 2001, Vol. SI edition, cap. 26.
- [4.5] Green Public Procurement - Indoor lighting. European Commission, DG EnvironmentC1, BU 9. Brussels, 2011.
- [4.6] Illuminating Engineering Society of North America, *Lighting Handbook: Reference & Application*. New York: 8th edition, 1993.
- [4.7] EnergyPlus Energy Simulation Software: Weather Data. [Online] U.S. Department of Energy, 2011. http://apps1.eere.energy.gov/buildings/energyplus/weatherdata_about.cfm?C

FID=5007126&CFTOKEN=a43f11bcc0665041-ACC2CE53-5056-BC19-15947478BCC4B5AC.

- [4.8] Saltelli A., Ratto M., Andres T., Campolongo F., Cariboni J., Gatelli D., Saisana M., Tarantola S. Global sensitivity analysis. The primer. John Wiley & Sons, Ltd, 2008.
- [4.9] Dr Yi Zhang. jEPlus – An EnergyPlus batch shell for parametric studies. [Online] 2011. [Cited: 7 4, 2012.] [http://www.iesd.dmu.ac.uk/~yzhang/jeplus/docs_html/Users%20Manual%20ver1.1.html.](http://www.iesd.dmu.ac.uk/~yzhang/jeplus/docs_html/Users%20Manual%20ver1.1.html)

5. Analysis of predicted and measured performance

Before taking on natural ventilation related risks, building stakeholders require assurances that natural ventilation can meaningfully contribute to comfortable indoor air temperatures and acceptable indoor air quality [5.1]. Ideally, analysis during the early stages of building design can provide this assurance and inform key design decisions that affect natural ventilation performance. By integrating building energy models with multi-zone airflow models, EnergyPlus tool can be used to support early design decisions. As shown in chapter 4, the performance of natural ventilation systems is very sensitive to a number of design parameters that are typically undefined during a building's early-design-stage. Performing a detailed parametric analysis of all of these undefined parameters during the early-design-stage would require significant effort. And, even with such an analysis, the ventilation performance prediction distributions that would result are potentially too variable to be informative. Designers need clearer guidance regarding sources of uncertainty in natural ventilation performance predictions and ways to improve the reliability of these predictions.

Previous studies have compared EnergyPlus's simulated natural ventilation performance with measured data from naturally ventilated buildings [2.4], 0. Zhai et al. [2.4] compared simulated and monitored data for three naturally ventilated office buildings but did not collect coincident weather data or directly measure ventilation rates. Coakley et al. 0 used simulation models that were calibrated to align electrical energy consumption and zone temperatures, with natural ventilation modelled using scheduled ventilation flows in EnergyPlus. We have not identified any prior studies that explore the sources of uncertainty in natural ventilation performance predictions made during the early stage of building design. In addition, no prior studies compare early-

design-stage natural ventilation performance predictions with measured data including on-site weather and measured air change rates.

Within the CEC Natural Ventilation project¹⁵, the Lawrence Berkeley National Laboratory performed a field study of natural ventilation performance using a small office building located in Alameda (California), collecting data on window use, indoor temperature and humidity, measured air change rates, and outdoor weather.

In collaboration with the simulation research group at the Lawrence Berkeley National Laboratory, early-design-stage predictions of natural ventilation performance from EnergyPlus models with different detail level were compared to field measurements of ventilation performance.

Uncertainty analysis assessed the impact of uncertainties in design parameter values on ventilation performance predictions. Sensitivity analysis identified key model input parameters that affect the reliability of these predictions. Based on field study observations, we developed improved EnergyPlus models that reduce the uncertainty in predicted ventilation performance.

This chapter presents the methodology used and the results of this study.

5.1.Methods

First, we performed a field study of natural ventilation performance at a small office building in Alameda, California. We collected data on indoor temperature and humidity as well as measured air change rates. Lawrence Berkeley National Laboratory (LBNL) partners at the University of California (UC), Berkeley Center for the Built Environment (CBE) measured outdoor temperature and humidity, wind speed and direction, and window use during their coinciding study of occupant thermal comfort at the same location.

¹⁵ Natural ventilation for energy savings in California commercial buildings. The aim of the project is to study the potential for natural ventilation retrofits in California's commercial building stock. The project involves UC San Diego, Lawrence Berkeley National Lab, UC Berkeley Center for the Built Environment, ARUP San Francisco, and CPP Wind.

http://ssi.ucsd.edu/index.php?option=com_content&view=article&id=460&Itemid=2

Next, for our case study, we predicted a range of expected natural ventilation performance using a range of values in which design parameters are likely to fall based on the level of design detail that is typical of a building's early design stage. Our case study building's design, location, and climate were based on those of the existing field study building. Our uncertainty analysis determined the probability distribution of likely model outcomes given typical variations in model input parameters. The model outcome that we used to quantify ventilation performance was the number of hours during which the natural ventilation system met or exceeded the equivalent American Society of Heating, Refrigerating and Air Conditioning Engineers (ASHRAE) mechanical ventilation standard. We performed a sensitivity analysis to quantify the effect of uncertainty in the design parameters on the predictions of ventilation performance. This analysis identified a subset of key design parameters that drive uncertainty in early-design-stage ventilation performance predictions.

Next, we used the measured field study data to reduce uncertainty in the key model parameters that the sensitivity analysis identified. These parameters were wind-pressure coefficients, weather data frequency, indoor temperatures, and window opening factors (which identify the operable part of windows and doors). We incrementally replaced the design parameters with values derived from our on-site measurements and related additional analysis. These field-study-based design values were used to incrementally improve EnergyPlus models based on our case study model. Finally, we compared the ranges of predicted ventilation performance from our early-design-stage study to predictions from our improved models and to the results from our field study.

5.1.1. Field study methods

The field study office building occupies the second floor of a two story building (Figure 5-1) constructed in 2004 in Alameda, California. The office space is split into two, 130 m² open plan areas, connected by two large openings. The front room volume is 528 m³. The back room has a false ceiling, so its effective volume is only 351 m³. The office does not

have mechanical ventilation or a cooling system. Fifteen sash windows located on all four sides of the office provide natural ventilation for fresh air and cooling. The windows have internal shades and insect screens manually controlled by the users.

Twelve ceiling fans with fully variable control are available for occupants to use to improve thermal comfort in summer. Additional heating is provided by single-user electrical resistance heaters. The monitoring for our study involved only the building's second story; the ground floor was not monitored.



Figure 5-1. North –east side of the field study office.

5.1.1.1. Window use measurements

To measure window position, LBNL's partners from UC Berkeley CBE installed two digital cameras (Canon PowerShot A570) each with a wide-angle lens converter (Opteka HD² 0.20X Professional Super AF fisheye lens, real angle of view = 174 deg.). The cameras were installed on ceiling joints facing the two open-plan offices; the camera locations are marked in Figure 5-2. The cameras' firmware was modified so that each camera could be controlled automatically using scripting [5.4]. This feature was used to automate the acquisition of JPEG images at five-minute intervals. We chose a five-minute interval between photos

on the assumption that it was extremely unlikely that windows would be open for less than five minutes. A composite of the JPEGs from each day was made into a movie that we visually examined to determine window positions. It was possible to estimate the state of the windows for the majority of the observation periods although excessive glare from low solar altitude compromised our ability to determine window positions during certain periods.

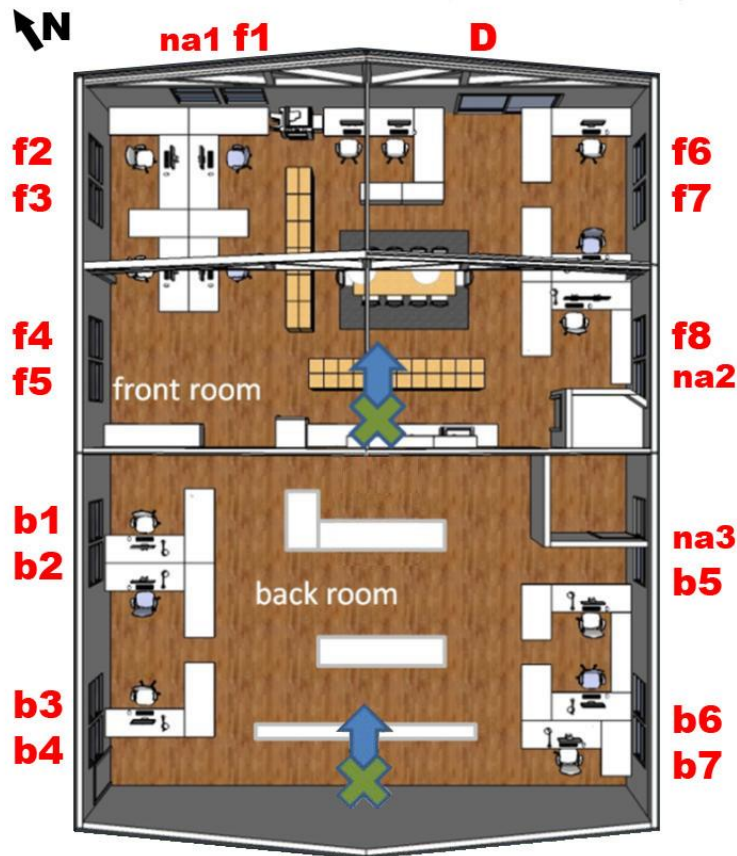


Figure 5-2. Office layout and camera locations. Source: Dutton et al. [5.3]

5.1.1.2. Air change rate measurements

LBNL used a perfluorocarbon tracer method to assess time-averaged ventilation rates. We installed nine vials that passively emitted perfluorocarbon tracer at a constant, known rate throughout the study building. During the data collection period, an automated bag sampling

system collected up to 16 separate cumulative air samples. We collected three sample bags each day. One sample collection bag was filled by the automated system during the four hours from 9am to 1pm, a second was filled from 1pm to 5pm, and a final bag was used to monitor the predominantly unoccupied period from 5pm to 5am the next day. We then used a gas chromatograph with electron capture detector to determine the concentration of perfluorocarbon tracer in each sample bag. We selected the number of vials based on mass balance calculations with the aim of maintaining expected perfluorocarbon tracer concentrations between 0.5 - 2 ppb for the expected range of ventilation rates (1.46 to 3.66 m³/h - m²). We selected target concentrations to insure that measurements were within the quantifiable range of the gas chromatograph. Finally, we used a mass balance calculation to determine the time-averaged air exchange rate in the room for the period during which the sample was collected. This calculation was based on the concentration of perfluorocarbon tracer in each sample bag and the rate at which the perfluorocarbon tracer was emitted from the vials.

5.1.2. Environmental data measurement

We recorded indoor temperature and humidity throughout the monitoring period using HOBO monitors. LBNL's CBE partners installed a weather station on the building's exterior to measure wind speed, wind direction, and outdoor temperature and humidity.

5.1.3. Early-design modelling method

Based on the Alameda field study building geometry, we prepared an early-design-stage case study to analyze potential ventilation rates in a small office building. Using EnergyPlus, we modeled the Alameda office as if it had not yet been constructed. During early-design-stage modeling, the EnergyPlus input values that correspond to key design parameters, such as effective opening area, are often not defined. However, the existing literature offers estimates of the ranges of values into which these parameters are likely to fall. The sources of this information include building standards [5.7], design guides [2.8][5.8],

input databases [3.20] [3.28] [3.30] [3.31], tool manuals [3.1][3.17], and research papers [3.24] [5.9] [5.10] [4.1].

We modelled daylighting controls that would moderate the use of electric lights based on anticipated daylight availability. When the indoor working plane illuminance was estimated to be less than 350 lux during occupied hours, the lights were switched on.

Occupancy data and lighting and equipment schedule are based on Table N2-5 of the 2008 non-residential Alternative Calculation Method Manual [5.5] for California Title 24 – 2008 compliance calculations [5.6].

We used EnergyPlus's airflow network to model ventilation and infiltration airflow rates throughout the building's zones. This network consists of two internal nodes (one for each room), three external nodes at the height of the windows, and one external node at roof height. The office's front and back rooms were connected by two large openings. We modeled unintentional infiltration by applying equivalent air leakage areas (ELAs) at 4 Pa evenly over the exterior envelope surface area of the building model.

We assumed that the physical window area was operable up to a maximum of 50% and a minimum of 10%. We used the EnergyPlus ASHRAE55Adaptive comfort window control strategy, which is based on the ASHRAE 55 thermal comfort standard (see par.3.3.8.1). This window control strategy opened all of the zone's windows and doors during the scheduled occupied hours (h 08:00 - 18:00) if the indoor operative temperature was greater than the adaptive comfort temperature. EnergyPlus's adaptive-comfort-based control mode does not support sub-hourly weather data; therefore, the simulations were run using weather data averaged to one-hour intervals. We modeled the effect of shading from surrounding buildings but ignored shading from internal blinds because its effect on thermal behavior is not relevant to the purpose of this study, and the airflow network model cannot predict the effect of internal blinds on airflows.

For our simulations we used a file based on the weather data collected on site and obtained missing data from local meteorological stations. Measured weather data were collected at the field study site for a total

of 13 months, but coincident measured data for weather, indoor temperatures, opening factors, and airflow rates were only partially available from 23/09/2011 to 04/11/2011. Measured airflow rate data were also missing from 29/10/2011 to 30/10/2011, and opening factors for the front room windows were not available from 26/10/2011 to 28/10/2011 and on 4/11/2011.

Measured atmospheric pressure as well as wind-speed and velocity data from local meteorological station AAMC1 – 941475 – Alameda (CA) were used to fill in the periods of missing local weather data. We replaced missing outdoor dry-bulb temperature, dew-point temperature, and relative humidity data with data from a second weather station located in Alameda [5.17]. We used the National Solar Radiation Database at Oakland airport [5.18] to fill in missing hourly solar radiation data. The early-design-stage model and the first and second incrementally improved model all used an hourly averaged version of the weather file.

Figure 5-3 and Table 5-1 reports weather station data and location and the wind speed profile coefficient used for the data conversion.

The early-design-stage model was run with an hourly averaged weather file, based on the same weather data.

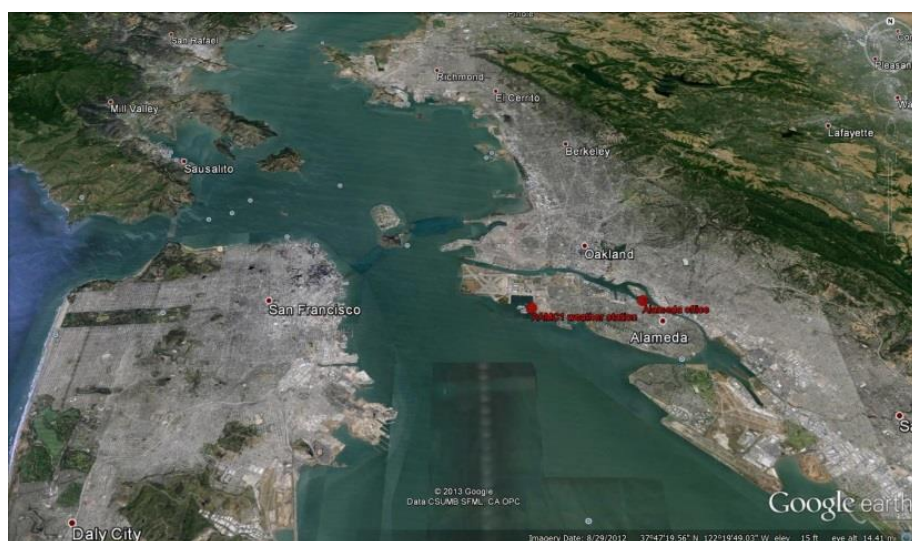




Figure 5-3. Alameda office and AAMC1 weather station location. Source: Google Earth

Table 5-1. Weather station data and wind speed profile coefficients used to convert them into WMO standard conditions.

Weather station	Location	Data frequency	Terrain	Z [m]	δ [m]	α
On site		5min	suburbs	15	370	0.22
Station AAMC1 – 941475 – Alameda (CA) owned by NOAA’s National Ocean Service		6min	ocean	9.1	210	0.10

5.1.4. Uncertainty analysis method

Uncertainty analysis allowed us to estimate the probability distribution of possible outcomes from our model, given input parameters’ probability distributions.

We performed an uncertainty analysis to assess the probability distribution of the number of occupied hours when natural ventilation could meet the mechanical ventilation rate requirements prescribed in ASHRAE 62.1. This standard does not prescribe minimum ventilation rates for naturally ventilated spaces but specifies a required minimum ratio of window open area to floor area and mandates the maximum room depth that can be considered to be naturally ventilated. Quantifying the likely percentage of occupied hours during which

equivalent mechanical ventilation rates are met can help assure designers that a natural ventilation strategy is likely to be effective.

For this analysis, we first assigned probability distributions to several of the input data. We then propagated these uncertainties through our case study model using a Latin Hypercube Sampling method to select random values that represented the model parameter distribution functions. Running multiple simulations with combinations of these input parameters produced estimates of the final uncertainties in the model output.

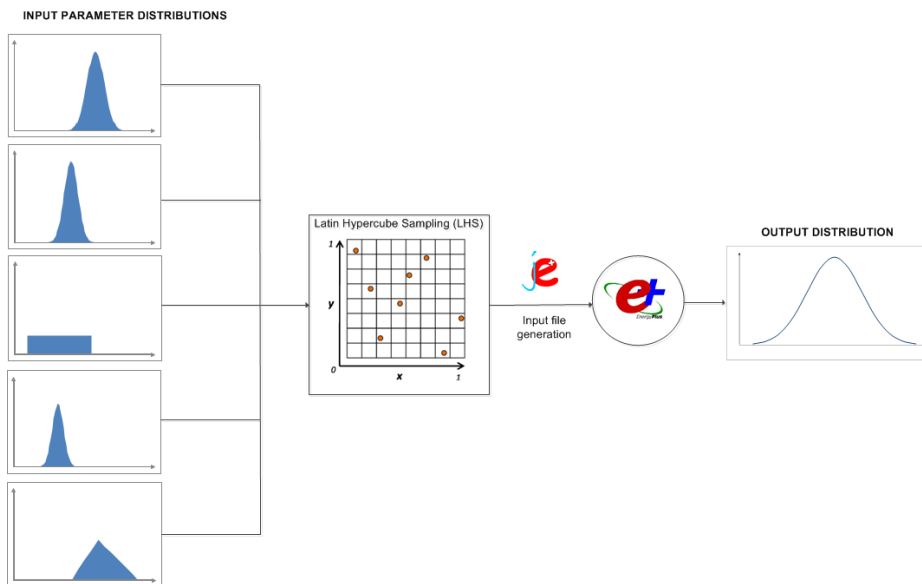


Figure 5-4. Uncertainty analysis methodology overview.

5.1.4.1. Parameter distribution generation method

We limited our analysis to model inputs that are considered “design” parameters; we did not include parameters that are specific to the simulation model, such as convection coefficients or airflow network convergence criteria.

We modelled four alternative building environments represented by wind speed profiles ranging from country/suburbs ($\alpha = 0.14$, $\delta = 270$ m), to urban areas ($\alpha = 0.33$, $\delta = 460$ m), where α is the wind speed profile exponent and δ is the boundary layer thickness. These models were based on values taken from published literature [3.17].

For the building envelope thermal transmittance (U) and window solar heat gain coefficient (SHGC), we assigned normal distributions. We defined the high end of the range of acceptable SHGC inputs based on the California Title 24-2001 minimum SHGC requirements [5.7]. We used this value to set the upper bound of the normal distribution given by the mean (μ) value of this distribution plus three standard deviations (σ), expressed as $[\mu+3\sigma]$. We defined the lower bounds, $[\mu-3\sigma]$, of the thermal transmittance and SHGC values based on the values recommended by the Advanced Energy Design Guideline for small to medium office buildings [5.8].

Table 5-2 reports the minimum requirements for envelope elements' thermal transmittance.

Table 5-2. Minimum requirements California Title 24 – 2001 (zone 3C)

Construction	U factor [W/m ² K]	R [hr ft ² F/Btu]
Exterior walls	0.522	11
Exterior roof	0.324	19
Exterior floor	0.432	11
Exterior window, glazed door	4.599	

According to California Title 24-2001 window Solar Heat Gain Coefficient (SHGC) shall be not greater than 0.55 for windows on non-north facades.

We represented the window opening factors as uniform distributions between 0.1 and 0.5, with opening controls based on the adaptive comfort control model. The opening factors were not required to be identical for each of the eight window pairs but were allowed to vary independently of each other within the range 0.1 to 0.5. We modeled the ELA as a triangular distribution whose average, lower, and upper bounds were taken from the NIST database [3.20].

We used a discharge coefficient of 0.65 with a standard deviation of 0.05, based on an average of previous wind-tunnel measurements of discharge coefficients for sharp-edged openings [3.24] [5.9] [5.10]

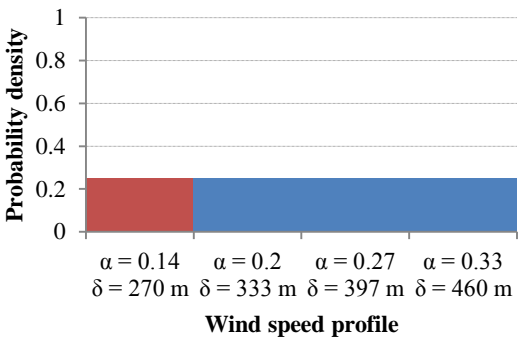
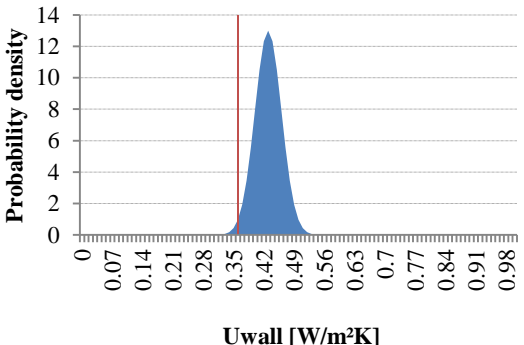
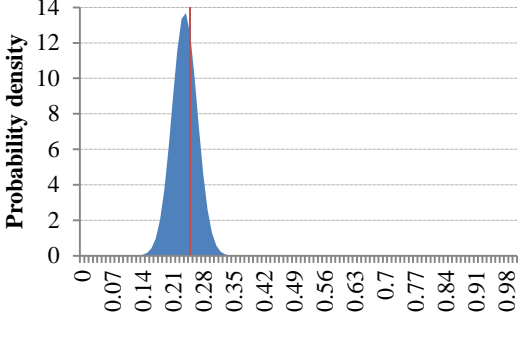
For the wind pressure coefficients we used multiple existing databases, and tools, including:

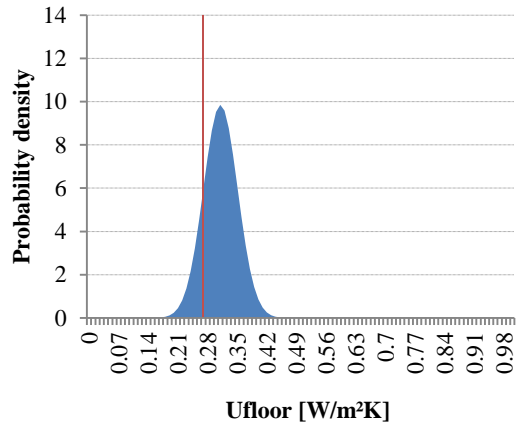
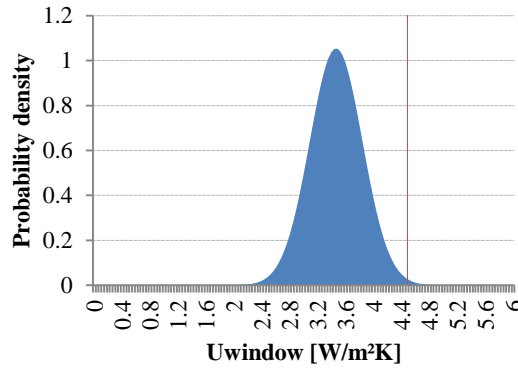
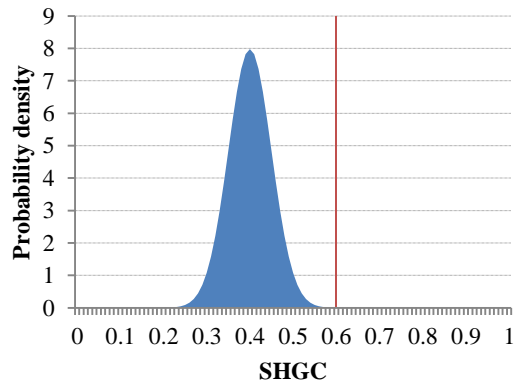
- The AIVC dataset for semi-sheltered low-rise rectangular buildings [3.28], based on wind tunnel tests;
- The TPU data set for gable-roofed low-rise rectangular buildings with 8.6 m height, 16 m breadth and 24 m deep [3.30] based on wind tunnel measurements with a suburban terrain [5.11];
- The ASHRAE handbook local pressure coefficients [2.8] for low-rise buildings sited in urban terrains based on existing wind tunnel data;
- Cp Generator [3.31], a simulation program based on systematic wind tunnel tests and on published measured data.

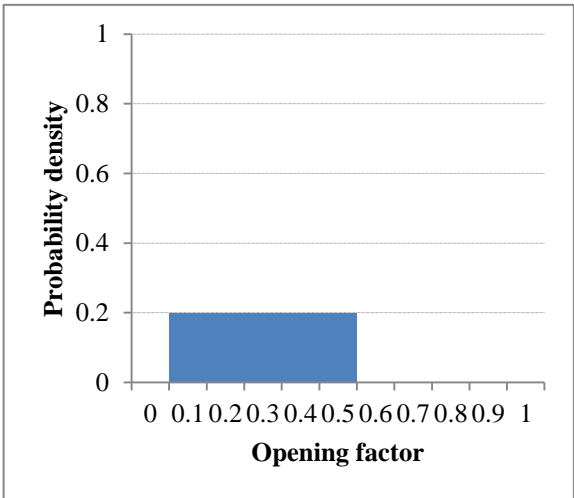
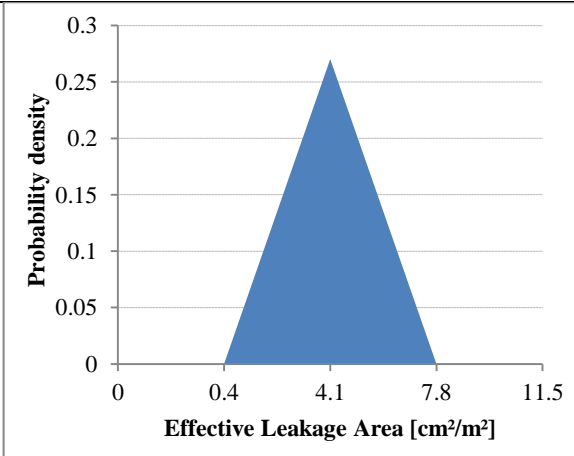
For lighting and electric equipment power densities we used the triangular distributions proposed by Dominguez et al. [4.1]. The lighting power density distribution's upper bound is the value recommended by California Title 24 2001 (128). We based the lighting and electric equipment power density distribution's lower bound on the ASHRAE Advanced Energy Design Guide for small to medium office buildings [5.7].

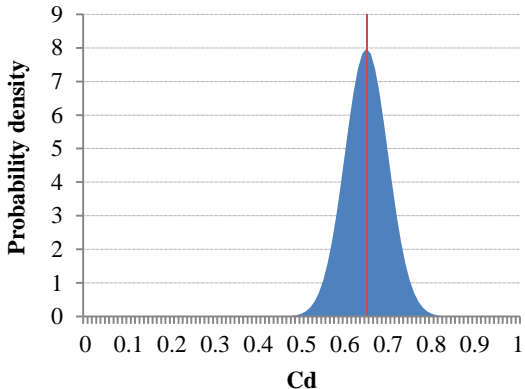
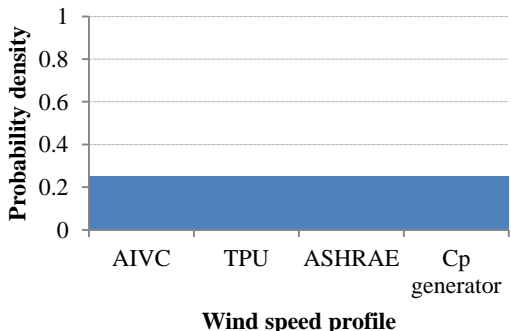
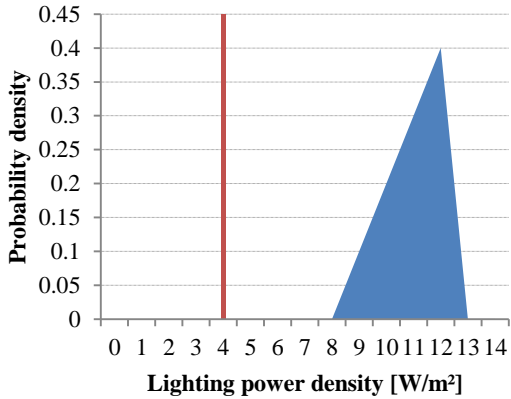
Table 5-3 lists the parameters we analysed and the probability distribution function we used for each.

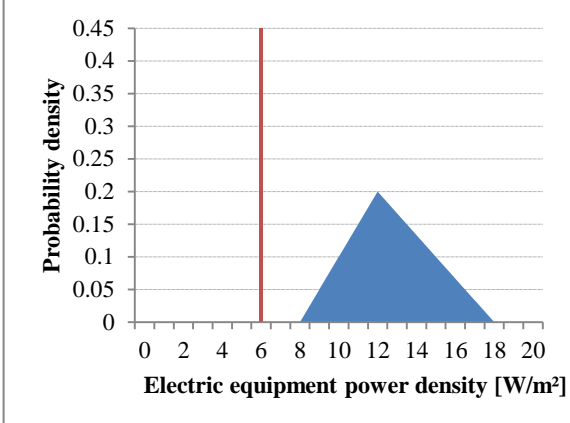
Table 5-3. Early-design-stage uncertainties and better estimated values according to field measurements and onsite inspection.

Factor nr	Description	Distribution function for uncertainty analysis
F1	Wind speed profile (exponent - boundary layer thickness [m])	 <p>Wind speed profile</p>
F2	Uwall [W/m²K]	 <p>Uwall [W/m²K]</p>
F3	Uroof [W/m²K]	 <p>Uroof [W/m²K]</p>

Factor nr	Description	Distribution function for uncertainty analysis
F4	Ufloor [W/m²K]	
F5	Uwindow [W/m²K]	
F6	Solar Heat Gain Coefficient	

Factor nr	Description	Distribution function for uncertainty analysis
F7.1	f1 / na1 window opening factor*	 <p>A histogram showing the probability density of the opening factor. The x-axis is labeled 'Opening factor' and ranges from 0 to 1 with increments of 0.1. The y-axis is labeled 'Probability density' and ranges from 0 to 1 with increments of 0.2. A single blue bar is present between 0.1 and 0.5, with a height of 0.2.</p>
F7.2	f2 / f3 window opening factor*	
F7.3	f4 / f5 window opening factor*	
F7.4	f6 / f7 window opening factor*	
F7.5	f8 / na2 window opening factor*	
F7.6	b1 / b2 window opening factor*	
F7.7	b3 / b4 window opening factor*	
F7.8	b5 window opening factor*	
F7.9	b6 / b7 window opening factor*	
F8	Effective Leakage Area [cm ² /m ²]	 <p>A triangle distribution showing the probability density of the effective leakage area. The x-axis is labeled 'Effective Leakage Area [cm²/m²]' and has values 0, 0.4, 4.1, 7.8, and 11.5. The y-axis is labeled 'Probability density' and ranges from 0 to 0.3 with increments of 0.05. The distribution is a blue triangle with its base from 0.4 to 7.8 and its peak at 4.1 with a density of approximately 0.27.</p>

Factor nr	Description	Distribution function for uncertainty analysis
F9	Discharge coefficient	
F10	Wind Pressure Coefficient array**	
F11	Lighting power [W/m²]	

Factor nr	Description	Distribution function for uncertainty analysis
F12	Electric equipment power [W/m ²]	

* Opening factors values for the better estimated model are scheduled according to the recorded values. See paragraph **Error! Reference source not found.** for comparison between design and real opening factors.

**Wind pressure coefficient for the better estimated model have been estimated through wind tunnel tests. See paragraph 5.1.5.5 for comparison between literature and wind tunnel based wind pressure coefficients.

5.1.4.2. Sampling method

Once we defined the input distribution functions, we need to generate a matrix of sample inputs drawn from these distributions. We generated 3000 randomized input parameter combinations using the Latin Hypercube Sampling (LHS) method [4.8].

With the exception of the wind speed profile exponent, boundary layer thickness, and wind pressure coefficients, the input parameters listed in Table 5-3 are all independent; this allowed each input parameter to be sampled from their marginal distributions.

LHS is commonly used to perform uncertainty analysis because of its accuracy, robustness [5.12], and stratification efficiency [5.13]. We used the JEPlus tool [4.9] to manage the parametric simulations that were run in EnergyPlus.

Macdonald I.A. [5.14] stated that for the same number of simulations LHS method is more robust than stratified and simple sampling method and that Monte Carlo analysis in typical building simulation should use 100 runs and simple sampling, independently from the number of uncertain parameters.

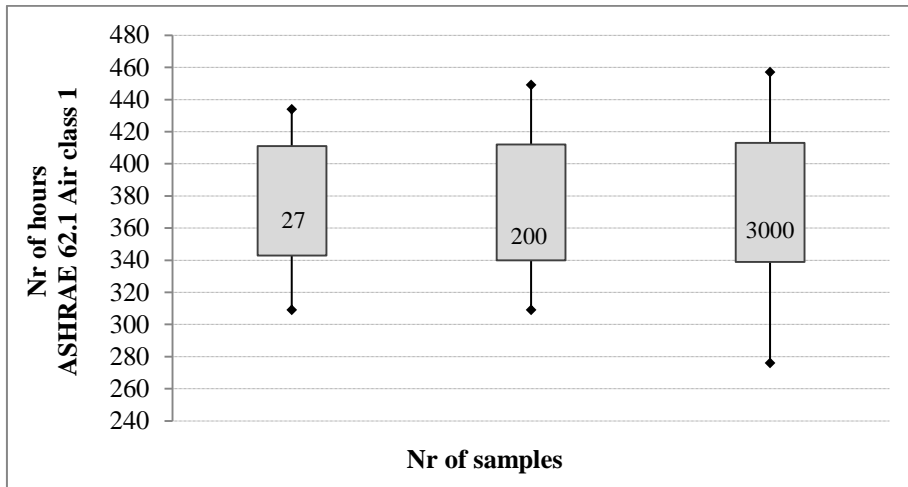


Figure 5-5. Uncertainty analysis results with 27, 200 and 3000 samples.

According to Iman R.L. and Helton J.C. [5.15], the number of sampling depends on the number of uncertain parameters k .

$$LHS = \frac{4k}{3} \quad \text{Equation 5-1}$$

According to Equation 5-1, as we are considering 20 uncertain parameters, 27 runs would be enough to estimate results uncertainty.

We tested this theory by performing 27 runs and comparing the results with the one obtained with 200 runs and 3000 runs. Figure 5-5 compares the results with different number of samples. There is no significant difference between the mean, but standard deviation slightly increases with the number of samples.

Even though mean and standard deviation can be estimated with low number of samples, we run a larger number of simulation to get a higher resolution of the distribution curve.

5.1.4.3. Sensitivity analysis

We performed a sensitivity analysis to determine how the uncertainty in a model's output can be apportioned to different sources of uncertainty in the model's inputs. We used the same simulation settings, runs and output results for both the uncertainty and sensitivity analyses.

For the sensitivity analysis, we employed the Standardized Regression Coefficient method [4.8], which allowed us to explore the map of inputs to outputs generated by the uncertainty analysis without performing additional simulation runs. The method assumes a linear regression between input and output and works best if inputs are pair-wise statistically independent. However, even if the relationship is nonlinear, SRC allows us to quantify the effect of moving each variable away from its mean value by a fixed fraction of its standard deviation, whilst all other variables are kept at their means. Called x_j the input factors and y the output, the method tries to fit a linear multidimensional model between inputs and outputs (Equation 5-2), where regression coefficients are estimated such that the sum of error squares (Equation 5-3) is minimized.

$$\hat{y} = \beta_0 + \sum_{j=1}^k \beta_j x_j \quad \text{Equation 5-2}$$

$$\sum_{i=1}^N (y_i - \hat{y}_i)^2 = \sum_{i=1}^N \left[y_i - \left(\beta_0 + \sum_{j=1}^k \beta_j x_{ij} \right) \right]^2 \quad \text{Equation 5-3}$$

where

i = simulation run

k = number of input parameters

The Standardized Regression Coefficient for the input factor j is defined as in Equation 5-4.

$$SRC_j = \frac{\beta_j \sigma_j}{\sigma_y} \quad \text{Equation 5-4}$$

where σ_y is the variance of the output under consideration calculated as in Equation 5-5.

$$\sigma_y = \left[\sum_{i=1}^N \frac{(y_i - \bar{y})^2}{N - 1} \right]^{1/2} \quad \text{Equation 5-5}$$

and σ_j is the variance of the j input factor calculated as in Equation 5-6.

$$\sigma_j = \left[\sum_{i=1}^N \frac{(x_{ij} - \bar{x}_j)^2}{N - 1} \right]^{1/2} \quad \text{Equation 5-6}$$

where N is the size of the experiment or number of simulation runs.

The higher is the SRC value, the more sensitive the output result is to the input factor. The sign of the SRC indicates whether the output increases (positive SRC) or decreases (negative SRC) as the corresponding input factor increases.

The coefficient of determination R^2 , calculated as in Equation 5-7, indicates the model's fraction of linearity and therefore the fit to the regression. If the fraction is 1.0, the model is linear. If the fraction is instead of the order of 0.9, the model would be 90% linear and the sensitivity analysis might not represent 10% of the model variance [5.16]. The higher the SRC value, the more sensitive the output result is to the input factor. The sign of the SRC value indicates whether the output increases (positive SRC) or decreases (negative SRC) as the corresponding input factor increases.

$$R^2 = \frac{\sum_{i=1}^N (\hat{y}_i - \bar{y})^2}{\sum_{i=1}^N (y_i - \bar{y})^2} \quad \text{Equation 5-7}$$

The SRC is considered a robust and reliable measure of sensitivity even for non-linear models [4.8].

Results of sensitivity and uncertainty analysis are presented and discussed in par. 5.2.

5.1.5. Improving the model

Our case study EnergyPlus model was modified using improved input parameters from the above analysis.

Table 5-3 gives the probability distributions as well as the corrected input values based on the field study, additional analysis and wind tunnel measurements. The model was improved incrementally so that each successive change included the prior changes; this allowed us to quantify the impact of each change on the performance predictions. The five incremental improvements to the model were:

- 1) aligning the model's internal temperatures to measured internal temperatures and sizing openings according to International Mechanical Code (IMC) natural ventilation guidelines (par. 1.2.2);
- 2) improving the window control strategy;
- 3) running the model using a more detailed weather file (five-minute data frequency);
- 4) modeling window use based on observed use;
- 5) improving the accuracy of the wind-pressure coefficients.

5.1.5.1. Indoor temperature alignment

To compare modeled and measured natural ventilation performance, we aligned the internal temperature of the improved case study model with the measured internal temperatures. Under this condition, the differences in ventilation performance are expected to be isolated from potential differences between measured and modeled indoor temperatures, which result in part from discrepancies between actual and modeled envelope performance. To align the internal temperature data, we created a schedule file of hourly, averaged, measured indoor temperatures and used a narrow band around the temperature to control the heating and cooling setpoints of an EnergyPlus ideal loads air object without any limits on system power. This object provides heating and cooling to the space, affecting the room mass balance.

Measured air change rates when the windows were closed were used to define new ELAs. The ELA of the cracks at the ceiling-wall joints, totaling 52 m in length, was set to 1 cm²/m at 4 Pa. The air mass flow coefficient when the window is closed was set to 0.003 kg/s-m. We set the maximum window opening factor according to IMC recommendation at 0.27 for the windows in the front room and 0.48 for the windows in the back room.

5.1.5.2. Improved window control

We changed the window control method from the *ASHRAE55Adaptive* control to the *Temperature* control method. We defined the *Ventilation Control Zone Temperature Setpoint Schedule* using a schedule file with hourly setpoint temperatures based on the adaptive comfort temperature as defined by ASHRAE standard 55. This control allowed modulation of the window opening factors based on the indoor-outdoor temperature difference (lower bound=0 K, upper bound=10 K).

5.1.5.3. Climate file improvement

We used a version of our local weather file, described in par. 5.1.3, with measurements at five-minute intervals.

5.1.5.4. Measurement based window control

We used the measured window use described in par. 5.1.1.1 to create window-use schedules in the EnergyPlus energy management system module. This schedule controlled the window opening factors. We created a schedule file with the hourly averaged, measured opening factors of each window/door. It is not possible to set sub-hourly schedule files. We set the schedule values as output variables for the energy management system sensor with venting opening factors as actuators. Then we set the actuated component (window/door opening factor) equal to the sensor (schedule value).

In the actual field study building, windows are operated individually; several windows were used infrequently or never, and some are not easily accessible because they are located above desks. In the case study model, the occupancy schedule was not aligned with the actual occupancy pattern.

Figure 5-6 to Figure 5-9 give the measured window use, indoor, outdoor and comfort temperatures for the front and back rooms. These plots are combined with the window opening factors predicted by the model.

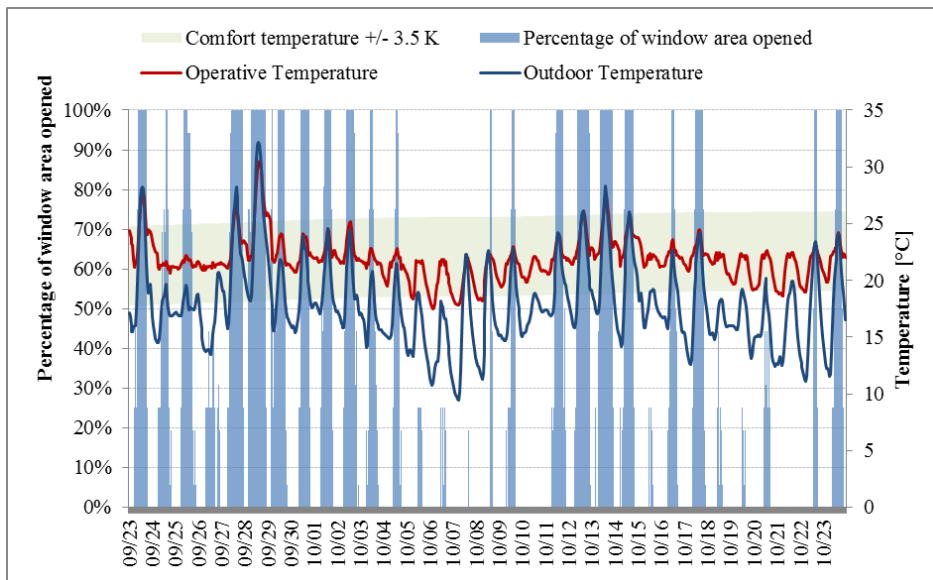


Figure 5-6. Mean early design predicted percentage of window opening in front room, with indoor, outdoor, and comfort temperatures.

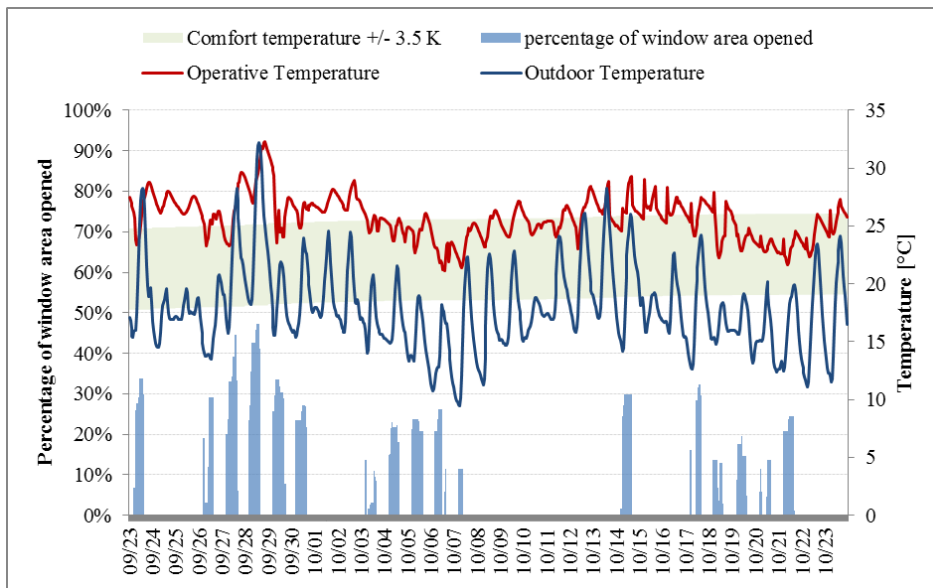


Figure 5-7. Measured percentage of window opening in front room, with indoor, outdoor and comfort temperatures.

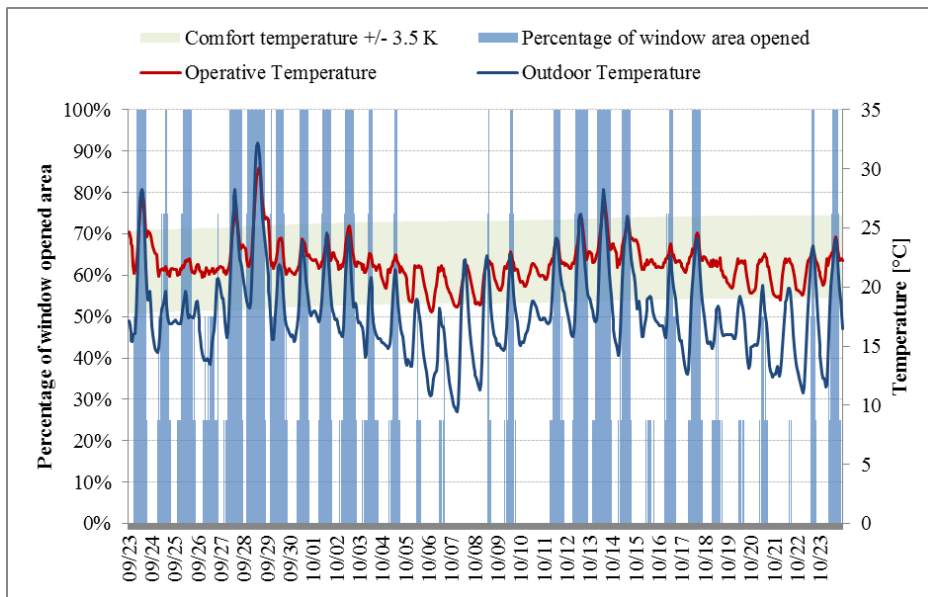


Figure 5-8. Mean early design predicted percentage of window opening in back room, with indoor, outdoor and comfort temperatures.

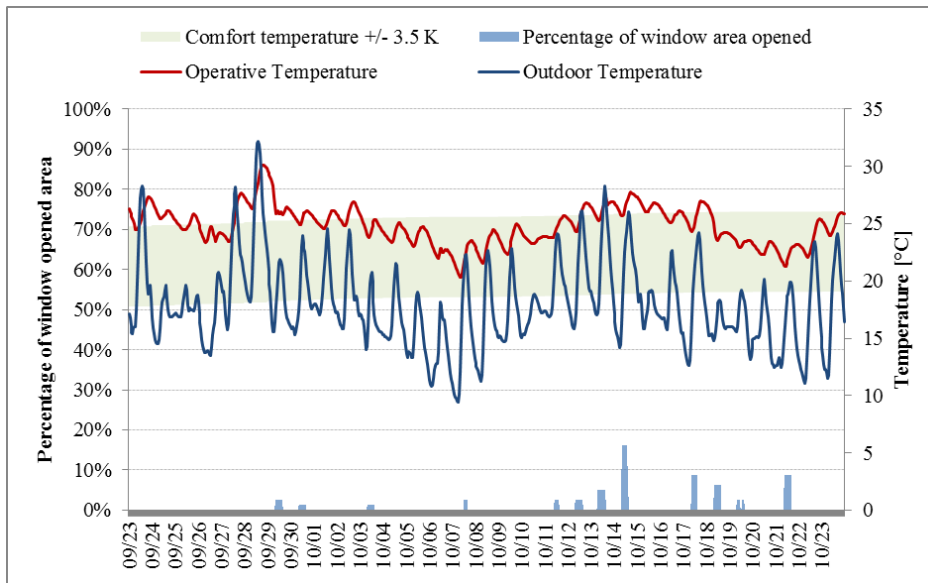


Figure 5-9. Measured percentage of window opening in back room, with indoor, outdoor and comfort temperatures.

Monthly averages of the daily average window-open fraction are presented in Dutton et al. [5.3], which compares measured window use with a stochastic window-use model.

5.1.5.5. Wind pressure coefficients

We based the wind-pressure coefficients used in the improved model on wind-tunnel tests of a mockup of the Alameda building created by CPP engineering. Figure 5-10 shows the wind tunnel model of the office building and the surrounding buildings. Two pressure taps were located on each of the four sides of each window, for a total of eight taps per window as shown in Figure 5-11. CPP tested a range of different natural ventilation configurations including single-sided, cross and corner ventilation (window to door).



Figure 5-10. Alameda building as modeled in the wind tunnel with actual surroundings. Source: CPP engineering

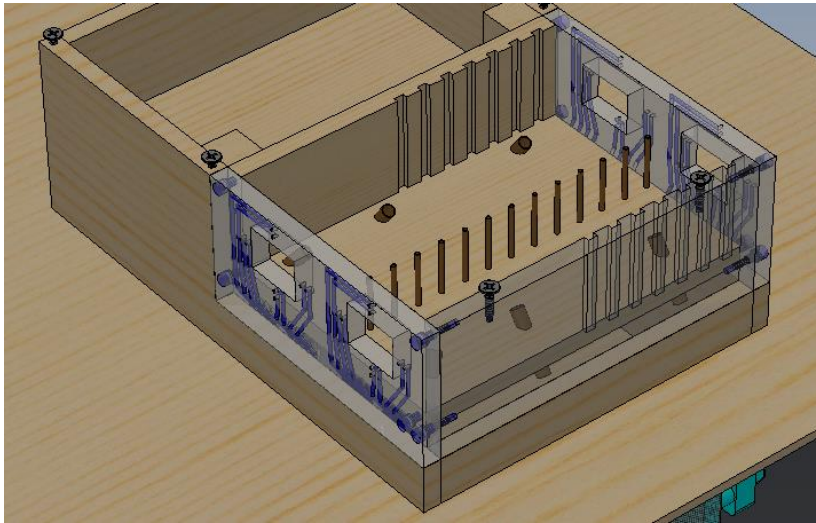


Figure 5-11. Instrumented north-east room from the Alameda building. Pressure taps are visible around the perimeter of each window. Source: CPP Engineering

Table 5-4 reports the different configurations that have been tested. Nearly 800 separate runs were completed for the Alameda building. Tests also included different window opening factors. CPP estimated wind-pressure coefficients for every 15-degree change in wind direction. The overall wind-pressure coefficients were an average of the figures from the taps and the tests.

Table 5-4. Tested natural ventilation configurations and window opening sizes.

Window opening size	1/10	1/4	1/2
Window open form	bottom	left	right
Configuration	cross	single-sided	corner

Figure 5-12 through Figure 5-16 report the measured wind pressure coefficients at each wind tunnel run.

Wind pressure coefficients at windows located close to the building corner have higher uncertainties.

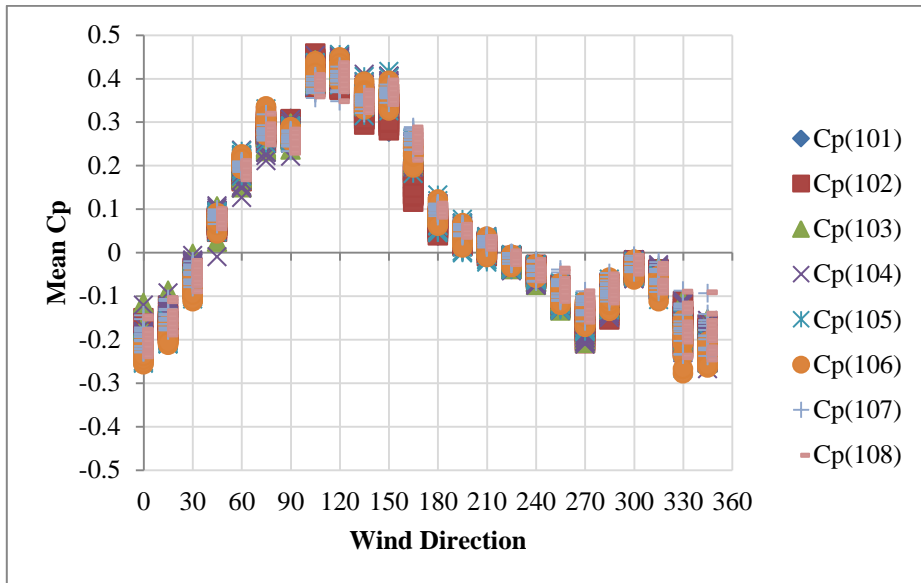


Figure 5-12. Measured wind pressure coefficient at pressure taps (101-108) along the window f8 and na2 perimeter over the simulation runs. Source: CPP Engineering

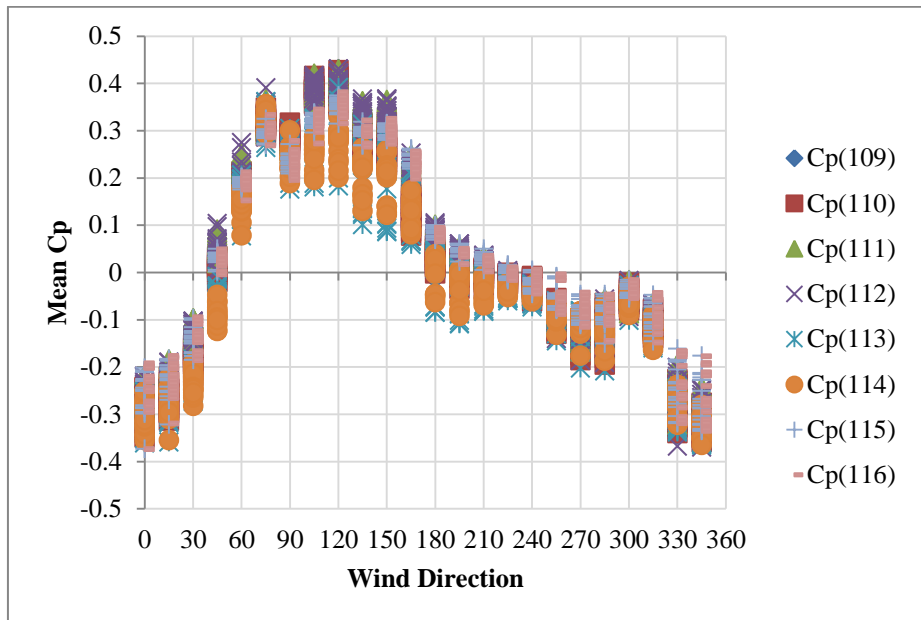


Figure 5-13. Measured wind pressure coefficient at pressure taps (109-116) along the window f6 and f7 perimeter over the simulation runs. Source: CPP Engineering

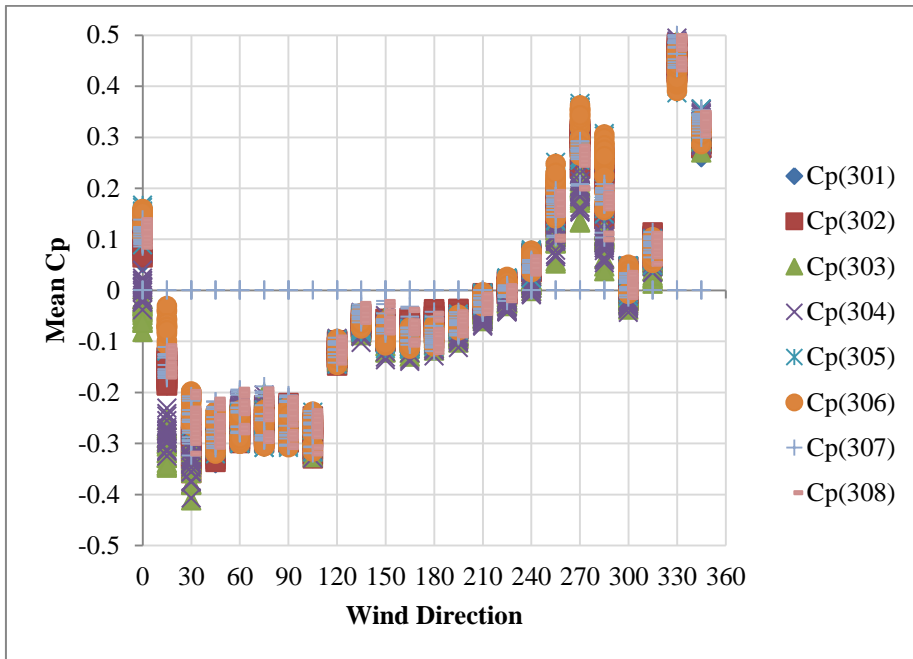


Figure 5-14. Measured wind pressure coefficient at pressure taps (301-308) along the window f2 and f3 perimeter over the simulation runs. Source: CPP Engineering

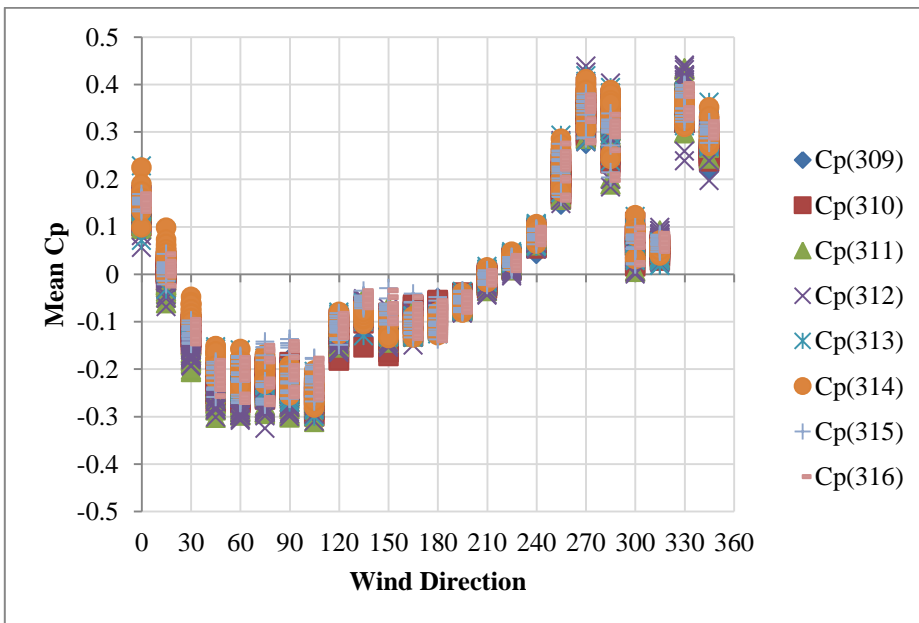


Figure 5-15. Measured wind pressure coefficient at pressure taps (309-316) along the window f4 and f5 perimeter over the simulation runs. Source: CPP Engineering

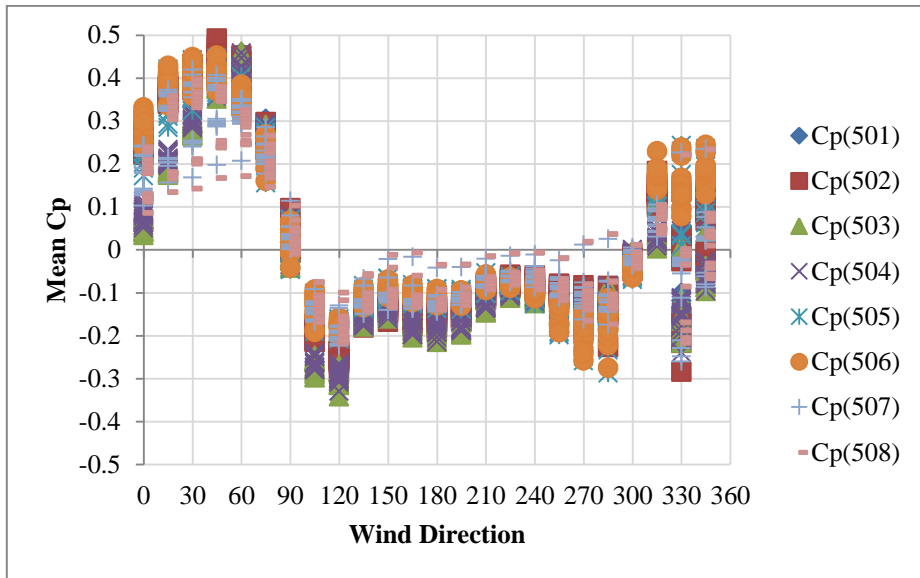


Figure 5-16. Measured wind pressure coefficient at pressure taps (501-508) along the door perimeter over the simulation runs. Source: CPP Engineering

Figure 5-17 through Figure 5-19 compare wind pressure coefficients gathered from literature (and used in the uncertainty analysis) to wind pressure coefficient calculated using Cp generator [3.31] as well as wind pressure coefficients from wind tunnel measurements.

The wind tunnel measured wind pressure coefficients are significantly lower than the ones from literature dataset. This led to an overestimation of wind pressures in the early design stages. Wind pressure coefficients estimated by Cp generator tool are closer to the values from wind tunnel measurements with an average root mean square error (RMSE) of 0.25 versus a RMSE of 0.41 for the literature based values. We assume this is because the Cp generator tool also models nearby buildings.

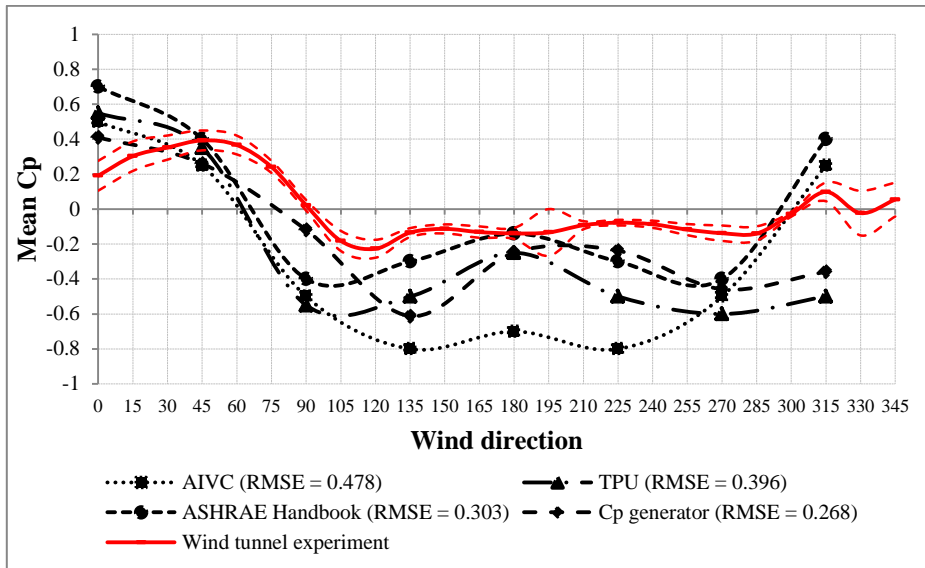


Figure 5-17. Literature data sets and wind tunnel measured mean wind pressure coefficients for the north façade. Root mean square error (RMSE) are estimated by comparing literature data set with the wind tunnel measurements.

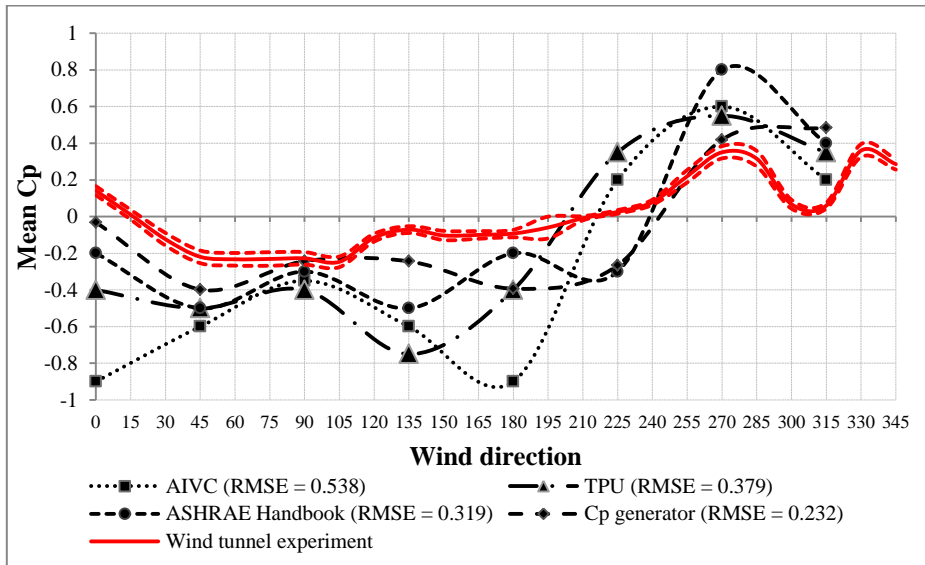


Figure 5-18. Literature data sets and wind tunnel measured mean wind pressure coefficients for the east façade. Root mean square error (RMSE) are estimated by comparing literature dataset with the wind tunnel measurements.

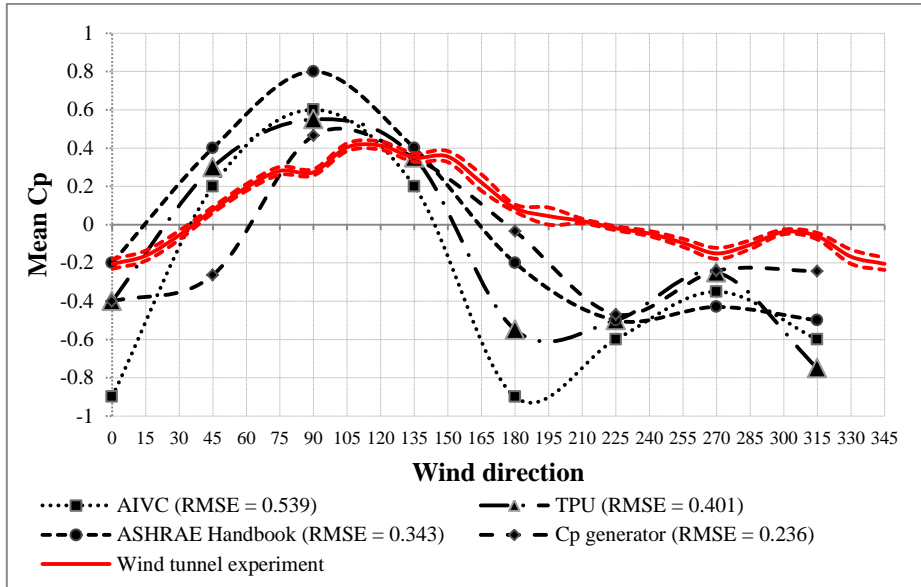


Figure 5-19. Literature data sets and wind tunnel measured mean wind pressure coefficients for the west façade. Root mean square error (RMSE) are estimated by comparing literature dataset with the wind tunnel measurements.

5.2.Results

5.2.1. Field study results

Figure 5-20 and Figure 5-21 show the average, whole building, measured air change rates and corresponding measured wind speed for the front office. Figure 5-22 and Figure 5-23 give the corresponding results for the back office. These plots are combined with the predicted average air change rates from the improved model. Three air change rates are presented for each day: 09:00 represents the average air changes per hour (ACH) from 9am to 1pm; 13:00 represents the average ACH from 1pm to 5pm; and 17:00 represents the average nighttime ACH from 5pm to 9am the next day. The measured air change rates vary significantly over the daytime sample period.

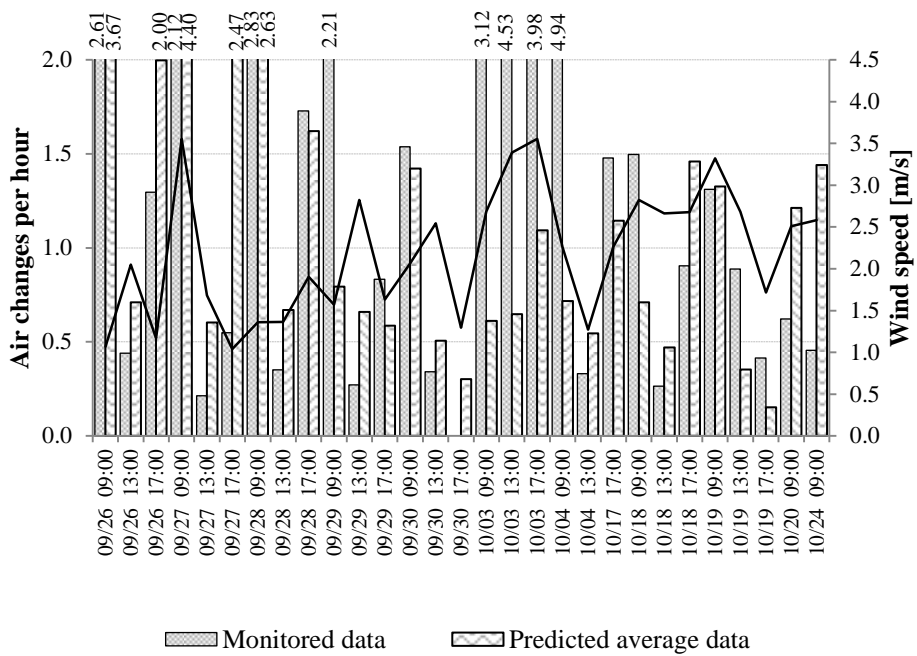


Figure 5-20. Measured and simulated airflow rates by the improved model in the front room.

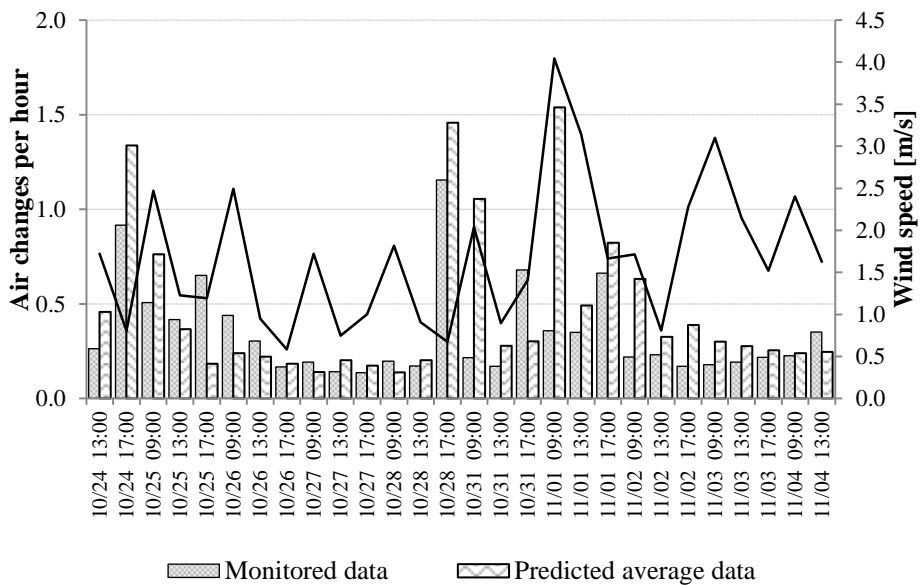


Figure 5-21. Measured and simulated airflow rates by the improved model in the front room.

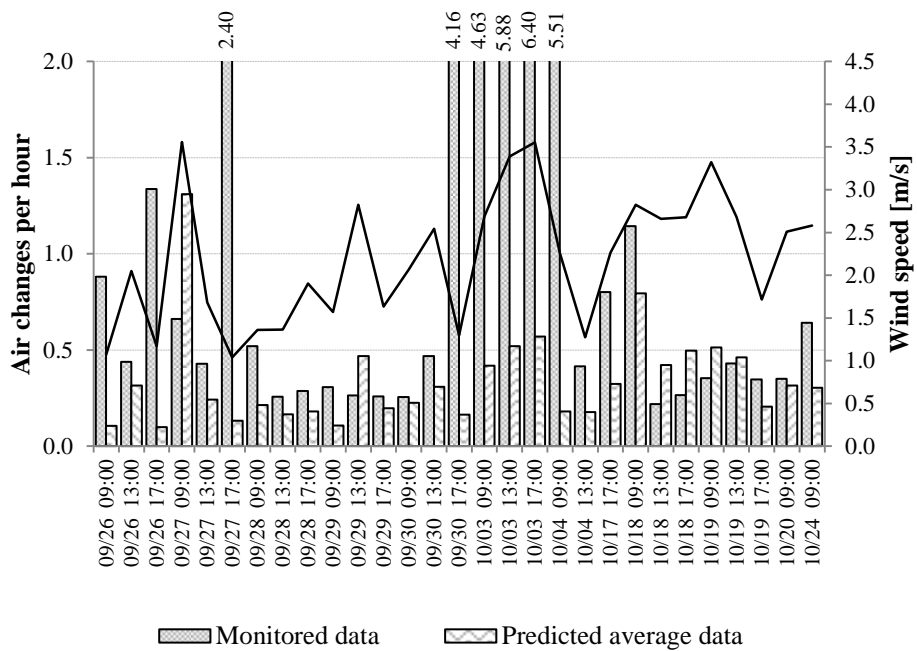


Figure 5-22. Measured and simulated airflow rates by the improved model in the back room.

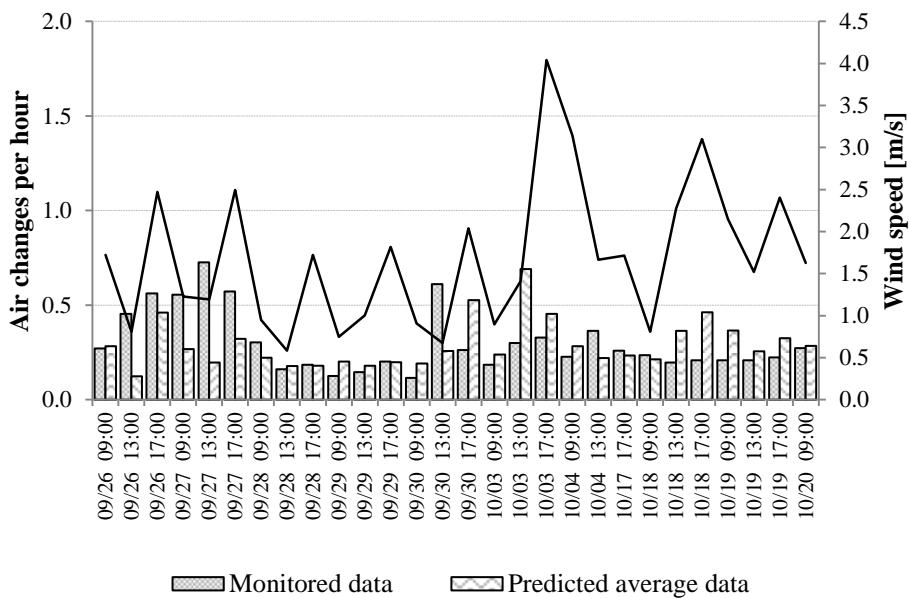


Figure 5-23. Measured and simulated airflow rates by the improved model in the back room.

Average ventilation rates (ventilation rates) were 0.94 ACH from 9am to 1pm, 1.13 ACH from 1pm to 5pm, and 0.57 ACH for the nighttime period. On average, nighttime ventilation rates were notably lower than daytime rates. During the sample period, average measured ventilation rates from 9am to 5pm were 0.91 ACH for the front office and 0.84 for the back office.

5.2.2. Uncertainty analysis results

The uncertainty analysis assessed the likely number of occupied hours during which natural ventilation would be sufficient to provide minimum air change rates specified in ASHRAE standard 62.1. According to Equation 5-8 from ASHRAE standard 62.1, required minimum air change rates for an equivalent mechanically ventilated office would be 0.42 ACH for the front room and 0.56 ACH for the back room.

$$V_{bz} = R_p P_z + R_a A_z \quad \text{Equation 5-8}$$

where

A_z = net occupiable floor area of the zone [m^2]

P_z = the largest number of people expected to occupy the zone during typical usage

R_p = outdoor floor rate required per person [l/s/pers]

R_a = outdoor floor rate required per unit area [l/s/m^2]

The outdoor floor rate required per person and per unit area are determined from Table 6-1 in the standard, where the suggested values for office spaces are $R_p = 2.5 \text{ l/s/pers}$ and $R_a = 1/\text{s/m}^2$.

Front and back rooms have the same area, but the front room can be occupied by 9 people, whereas the back room by 6 people only.

Figure 5-24 shows a frequency distribution of the percentage of hours when the building is expected to be occupied (8am to 6pm) when the measured air change rate is above the minimum required by ASHRAE 62.1. For the majority of modelled scenarios (90%), ASHRAE 62.1 requirements are met during 66% and 86% of the hours.

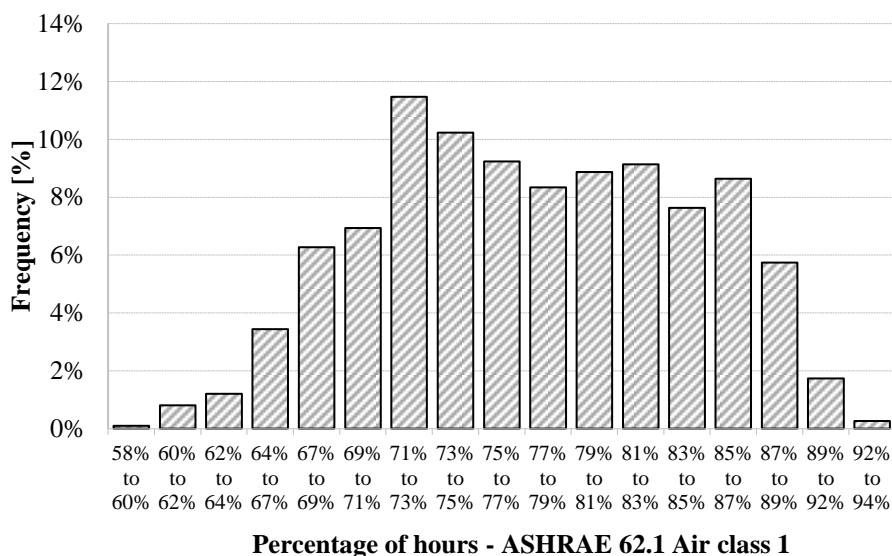


Figure 5-24. Frequency distribution of percentage of occupied hours when ACH met ASHRAE standard.

5.2.3. Sensitivity analysis results

Sensitivity analysis results were used to identify the input parameters that have the most significant impact on the uncertainty in predicted air change rates. Figure 5-25 gives the SRCs calculated for every input factor in the uncertainty analysis. Input parameters (or factors) are labeled F1 to F12; Table 5-3 describes each. The coefficient of determination, R^2 , is 1.05 for the front room and 1.06 for the back room data, indicating a good fit to the regression [4.8]. The magnitude of the SRC indicates the relative importance of each input parameter in the prediction of air change rates.

The analysis found that the wind-speed-profile parameter (F1) had the most significant impact on air change rate. The majority of the sensitivity analysis runs in which the ASHRAE ventilation standard was met during less than 71% of the occupied hours had a low wind-speed profile (city). Most of the results in which more than 90% of hours met the ASHRAE standard had a high wind-speed profile (country).

The three next-most-significant parameters, SHGC (F6), lighting (F11), and electrical equipment power density (F12), are all related to internal gains. We concluded that this was because the window control algorithm based the window opening factors on the internal temperature, which is, in turn, influenced by these internal loads. The same logic applies to envelope-performance-based parameters such as the wall (F2), floor (F4), and roof (F3) conductivity, which indirectly impact indoor temperatures. Wind-pressure coefficients (F10) had a more significant impact on airflows in the back room than in the front room. The team theorized that this was because the back room has fewer ventilation openings than the front room.

Window opening factors (F71-F79) appear to have minimal influence. The proposed explanation is that each window-open factor only affected a single window. Discharge coefficients (F9) appear to have more influence than window opening factors; this was assumed to be because the same discharge coefficient value is applied to all windows at the same time.

Because the model's adaptive control algorithm is driven by indoor temperatures, predicted occupant behavior was also indirectly influenced by building design parameters that affected indoor temperatures. A sensitivity analysis that excluded the parameters affecting thermal comfort found that window opening factors are the main drivers of natural ventilation. This leads us to conclude that the choice of window control model applied during design plays a significant role in ventilation performance prediction. We hypothesized that the ELA (F8) had significantly more influence on the infiltration rates in the front room than in the back room because the front room has longer ceiling-wall joints and a larger number of windows.

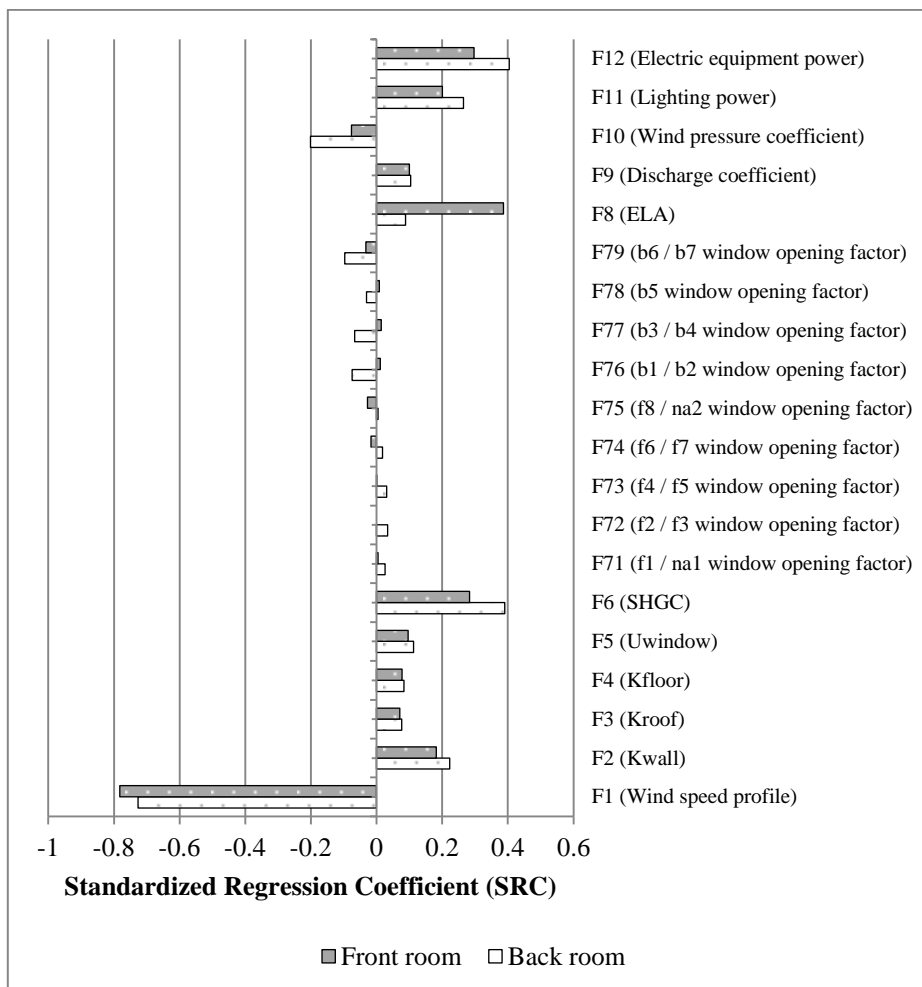


Figure 5-25. Standard Regression Coefficient of each input parameter considered.

5.3.Discussion and analysis

Error! Reference source not found. compares the case study uncertainty analysis results, the improved models' results, and the measured data. Table 5-5 describes each incremental model improvement and estimates the predicted average air change rate during occupied hours.

The total occupied hours between 23/09/2011 and 04/11/2011 were assumed to be 473, with airflow measurements available for 207 of those hours. For this analysis, we assumed that the air change rates

measured at four-hour intervals were constant during all four hours of the interval. We calculated percentages of occupied hours during which ASHRAE 62.1 requirements were met, as predicted by the improved models, only for the time during which airflow measurements are available.

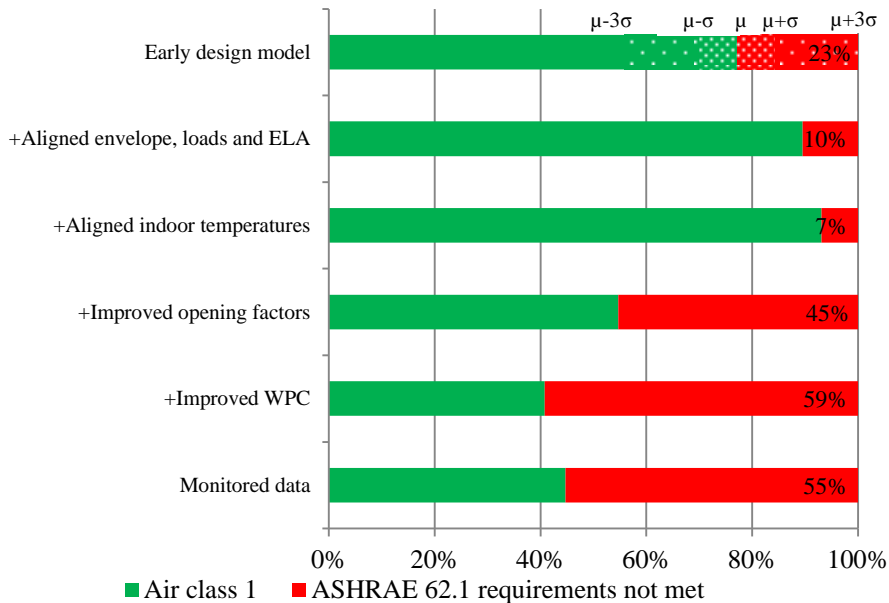


Figure 5-26. Percentage of occupied hours when ASHRAE 62.1 requirements are met predicted by early design model, better estimated models and measured.

Table 5-5. Model descriptions and average predicted air change rate.

Model	Description	Average ACR
EDM	Early design model	-
1) +IT	+ Measured indoor temperatures scheduled as setpoint	12.15
2) +TOF	+ Improved adaptive comfort control	7.48
3) +WF	+ Improved weather file with five-minute data frequency	5.70
4) +OF	+ Observed opening factors	1.00
5) +WPC	+ Improved wind-pressure coefficients based on wind-tunnel measurements, referred to in the text as the improved model	0.74
M	Monitored data	0.94

The green area of the graph in **Error! Reference source not found.** gives the percentage of occupied hours during which ASHRAE ventilation requirements were met. For the early-design-stage model, the results represent the range of predicted outcomes. The mean value of the most likely outcome is represented by the green area, and standard deviations from the mean are indicated by a patterned overlay. By setting measured indoor temperatures as scheduled setpoints, we overrode the influence of internal loads and envelope thermal characteristics on indoor temperature. The adaptive comfort window opening control mode significantly overestimates the air change rate, in part because this mode does not allow modulation of window opening area according to indoor-outdoor temperature difference. The model air change rate predictions improved when we used the EnergyPlus temperature-based ventilation control mode with the zone air temperature setpoint as the comfort temperature. In this case EnergyPlus allows modulation of window opening area to reduce the large temperature swings that can result if the windows are open too far when they are venting, especially when there is a large inside-outside temperature difference.

When simulated window-use behavior was replaced by a schedule based on measured window use, the model's predictions improved significantly: the predicted number of ASHRAE-compliant hours shifted from 93% to 55%. Replacing wind-pressure coefficients based on the literature with those estimated using wind-tunnel measurements further reduced the variance between measured and predicted number of ASHRAE-compliant hours.

Combined measured airflow rates for the back and front offices complied with ASHRAE 62.1 during 45% of the time, compared to the early-design-stage case study mean estimate of 77% compliance. The improved model's predictions came much closer to the measured results in this case, predicting 41% of compliant hours. However, when air change rates for the back and front offices were compared separately, the improved model marginally under-predicted average ventilation rates in the front office and significantly under-predicted the back-office ventilation rates. Average ventilation rates during occupied

periods were predicted using the improved model, which resulted in 0.74 ACH for the front room and 0.29 ACH for the back room, compared to a measured 0.91 ACH for the front room and 0.83 ACH for the back room. The average early-design-stage model predictions were 4.89 ACH for the front room and 7.25 ACH for the back room.

The difference in average measured ventilation rates between the front and back rooms indicates that significant inter-zonal mass transfers are occurring, in contrast to the results predicted by the model. The average mass transfer predicted by the improved model was $0.0055 \text{ m}^3/\text{s}$ from front to back rooms and $0.0044 \text{ m}^3/\text{s}$ from back to front. No measurements were collected of the actual inter-zonal mass transfer between the front and back offices to verify our conclusion. In all of the models presented, the airflow network model appears to under-represent inter-zonal mass flow between zones.

These results highlight a known limitation of the airflow network model, which is that it does not model the wind-driven mass flows between zones.

Figure 5-6 to Figure 5-9 compare measured and early-design modeled window use and show a significant disparity between modeled and measured occupant behavior. In the actual measured building, windows were operated individually, and several windows were inaccessible to occupants and thus never used. In contrast, the adaptive-comfort model is based solely on occupants' assumed thermal comfort with no consideration of occupants' requirements for fresh air or of the previous state of the windows, both of which have been found to influence window use [5.19] [5.20].

The graphs in Figure 5-20 through Figure 5-23Figure 5-23 compare the measured air change rate to the air change rate predicted by the improved model. The improved model deviated most significantly from the measured data during warmer periods (September, early October), when the windows are more likely to be opened, and during periods when wind speeds are high. These deviations did not affect the number of ASHRAE 62.1-compliant hours because both measured and predicted ACH exceeded ASHRAE 62.1 requirements.

The improved model significantly underestimated air change rates in the back room. For most of the time, only one window was open in the back room, so the underestimation might result from the airflow network model not taking into account wind pressures in case of single-sided ventilation.

During colder-period nights, the calculated coefficient of variation of the RMSE between measured and predicted air change rate is around 5%, indicating that the infiltration model is accurate.

However, on 03/10/2011 and 04/10/2011, the measured air change rates were more than four times higher than predicted. Analysis revealed that during other periods when conditions were similar to those during this period, the measured air change rates were significantly lower. This suggested that the results for the period in question could be a result of measurement error. Analyzing the recorded images in detail, we noticed situations in which windows or doors were open, but roller blinds or insect screens were closed, which can reduce the discharge coefficient, especially if conditions are windy.

The opening factor schedule of the improved model used hourly frequencies because EnergyPlus does not support schedules with more frequent time steps. Because of the variability of wind conditions, hourly averaged opening factors may cause deviation from the measured values.

Anecdotal observations in the field study building indicated that occupant schedules were rarely consistent, with the number of occupants at any given time of day varying significantly from day to day. During early-design-stage modeling, we recommend that, when possible, designers avoid using idealized occupancy models that do not represent the potential variation in real-world occupancy. When no changes in building use are foreseen, designers should interview the prospective building occupants to establish reliable occupancy patterns, activities, and typical behavior. If this is infeasible, occupancy models should include multiple scenarios that realistically represent a range of possible occupancy patterns.

Occupants were observed to typically operate only the windows nearest their work stations and to not operate windows optimally, either from the perspective of energy performance or thermal comfort.

Several model implementation issues contributed to the observed over-prediction of Ventilation rates in the early-design-stage model. First, EnergyPlus's adaptive-comfort-based window control is active only when occupants are present, but once a single occupant is present, all of the windows in the occupied zone have the potential to be opened. The potential of a window to be opened should be proportional or keyed to the number of occupants present. Second, EnergyPlus assumes that all occupants within a zone experience the same thermal conditions, which are based on the zone operative temperature. Therefore, unless otherwise specified, all windows in a zone will be open when the adaptive control algorithm predicts hot discomfort, regardless of the number of occupants.

Ideally, window-use behavior should be considered at the level of individual occupants rather than at the zone level. However, the amount of effort required to implement individualized window control is significant, so we do not anticipate that designers will adopt this approach. As a viable alternative, we recommend that designers use EnergyPlus's temperature-based control with the temperature setpoints based on an annual schedule of adaptive comfort temperatures, per our model with improved adaptive control (TOF). This approach introduces a degree of moderation in window use, based on the difference between indoor and outdoor temperatures.

A second alternative approach that is not explored in this study would be to model this behavioral diversity using stochastic window-use models. However, Dutton et al. [5.3] found that a stochastic model derived from one study might not be broadly applicable or able to accurately predict occupant behavior.

Automated windows would increase the reliability of performance predictions, but manually controlled windows reduce costs and enhance workspace quality from a psychological point of view. Signaling systems that apprise building occupants when to open and close windows represent a good compromise between the two solutions.

Even though low levels of participation have been observed, Ackerly et al. [41] make recommendations to maximize the potential of this solution.

Occupant behavior can also be indirectly influenced by a building's interior design. In the Alameda field study office, some windows were always closed because they are not easily accessible to occupants. The impact of a space's interior layout on window operation complicates the relationship between occupants and windows. We recommend that designers reduce the likelihood that windows specified on plans will become obsolete because of poor interior design. To achieve this goal, we recommend an integrated design process in which interior designers collaborate with the building design team, with a stated goal of ensuring that all windows are accessible to occupants. A collaborative process reduces adverse impacts of the building design on natural ventilation performance and allows designers to consider information about building occupant patterns and typical behavior in formulating the building's design.

In the Alameda office, roller blinds were often closed while windows remained open during periods of glare or high indoor temperature. This increased the uncertainty surrounding airflow predictions. To avoid this type of situation, some new buildings (e.g., Green Office Meudon in France, Nicosia town hall in Cyprus, Net Zero Energy Retrofit 2020 Testbed at the Cork Institute of Technology in Ireland) have been designed so that air and light paths are dissociated. For example, one part of the building façade is glazed to naturally illuminate the space, with sun blinds installed to control glare, while the operable part of the façade is opaque and designed to maximize natural ventilation performance.

We expect that many key input parameters will be unknown during early-design stage modeling and remain unknown until later on in the design process or even until the building is occupied. For this reason, we recommend the use, when possible, of passive cooling methods, including exterior shading and increased thermal mass, to reduce buildings' sensitivity to internal loads, including occupancy. Reducing buildings' sensitivity to variations in thermal mass is expected to

reduce the likelihood of thermal discomfort resulting from variations in internal loads.

5.4. Conclusions

Natural ventilation rates predicted using the EnergyPlus airflow network were sensitive to a number of key model parameters. These parameters include, in order of significance, the occupant behavior model, wind-speed profile, internal heat gains (electrical and lighting), SGHC and envelope conductivity, and wind-pressure coefficients. Internal gains and envelope conductivity affected modeled occupant comfort and thus indirectly influenced predicted ventilation rates resulting from increased window use.

The adaptive-comfort-based window-use behavior model in EnergyPlus showed poor agreement with observed window use.

Compared to the adaptive-comfort-based window control, model-predicted ventilation rates were more accurate with EnergyPlus's temperature-based window control model (using temperature setpoints based on an annual schedule of adaptive comfort temperatures, per our TOF model).

Observed occupancy diverged significantly from the idealized occupancy schedules found in ASHRAE guidelines, and occupants typically only operated the windows closest to them.

EnergyPlus's adaptive-comfort-based window control is active only when occupants are present, but once a single occupant is present, all of the windows in the occupied zone have the potential to be opened.

Using five-minute, site-specific, measured weather data improved the accuracy of model predictions compared to predictions generated using hourly weather data.

Using wind-pressure coefficients based on wind-tunnel testing or from C_p generator improved model predictions of the number of ASHRAE-compliant hours, compared to using standardized coefficients from literature.

The interior layout of the office space affected the number of the windows that occupants used regularly, with several of the windows remaining unused.

With sufficient input data, employing EnergyPlus in combination with an airflow network can provide informative predictions of natural ventilation performance. Using calibrated models, we were able to predict, to within an acceptable margin, the observed average ventilation rates and the number of compliant hours.

Bibliography

- [5.1] De Gids W. F. Barriers to natural ventilation design of office buildings. National report: The Netherlands., UK, Building Research Establishment (BRE), 1998, a NatVent European Report, 1998.
- [5.2] Coakley D., Raftery P., Molloy P. Calibration of whole building energy simulation models: detailed case study of a naturally ventilated building using hourly measured data. Building simulation and optimization. Loughborough (UK), 2012.
- [5.3] Dutton S., Zhang H., Zhai Y., Arens E. Application of a stochastic window use model in Energyplus. SimBuild. Madison, Wisconsin, 2012.
- [5.4] Konis K.S. Effective Daylighting: Evaluating Daylighting Performance in the San Francisco Federal Building from the Perspective of Building Occupants. University of California, Berkeley: PhD Thesis, 2011.
- [5.5] Nonresidential Alternative Calculation Method (ACM). California Energy Commission. CEC-400-2008-003-CMF, 2008.
- [5.6] Building energy efficiency standard for residential and nonresidential buildings. California Energy Commission. CEC-400-2008-001-CMF, 2008.
- [5.7] Building energy efficiency standards for residential and non residential buildings. California Energy Commission. CEC 400-01-024, 2001.
- [5.8] ASHRAE, The American Institute of Architects, Illuminating Engineering Society of North America, U.S. Green Building Council, U.S. Department of Energy. Advanced Energy Design Guide for small to medium office buildings. Achieving 50% energy savings toward a Net Zero Energy building. . Atlanta : American Society of Heating, Refrigerating and Air-Conditioning Engineers, Inc., 2011.
- [5.9] Chia-Ren Chu, Yu-Wen Wang. The loss factors of building openings for wind-driven ventilation. Building and Environment 2010, vol. 45, pp. 2273-2279.
- [5.10] Ohba M., Irie K., Kurabuchi T. Study on airflow characteristics inside and outside a cross ventilation model, and ventilation flow rates using wind

- tunnel experiments. *Journal of Wind Engineering and Industrial Aerodynamics* 89, pp. 1513-1524, 2001.
- [5.11] Architectural Institute of Japan (AIJ). Recommendations for Loads on Buildings, 2004.
 - [5.12] Hopfe C., Hensen J.L.M. Uncertainty analysis in building performance simulation for design support. *Energy and Buildings* 2010, vol. 43, pp. 2798-2805.
 - [5.13] Tian W. A review of sensitivity analysis methods in building energy analysis. *Renewable and Sustainable Energy Reviews* 2013, vol. 20, pp. 411-419.
 - [5.14] Macdonald I. A. Comparison of sampling techniques on the performance of Monte Carlo based sensitivity analysis. *Building Simulation*. Glasgow, 2009.
 - [5.15] Iman R.L., Helton J.C. A comparison of uncertainty and sensitivity analysis techniques for computer models. NUREG/CR-3904. Sandia National Laboratories, 1985.
 - [5.16] Saltelli A. *Sensitivity Analysis in Practice: a guide to assessing scientific models*. Wiley & Sons, 2007.
 - [5.17] [Online] <http://www.hamconinc.com/weather/>.
 - [5.18] 724930 - Oakland Metropolitan Arpt. National Solar Radiation Database: 1991-2005 update TMY3. [Online] http://rredc.nrel.gov/solar/old_data/nsrdb/1991-2005/tmy3/by_state_and_city.html#C.
 - [5.19] Dutton S., Shao L. Window opening behaviour in a naturally ventilated school. *SimBuild - 4th National Conference of IBPSA - USA*. New York City, 2010.
 - [5.20] Haldi F., Robinson D. Interactions with window openings by office occupants. *Building and Environment* 2009, vol. 44, pp. 2378-2395.

6. Design procedure

Starting from the topics discussed in the preceding chapters, a natural ventilation design method is here proposed. It aims at providing an engineering based method for natural ventilation design of non-residential buildings.

The method is meant to be applied through an IDP and many design iterations have to be considered.

Figure 6-1 shows an overview of the whole natural ventilation procedure within the main steps of the building design. Before starting the design, a climate suitability evaluation must be performed taking into account macro and micro climate conditions and the main constraints given by the building functions and the client requirements. Based on climate analysis, the most suitable ventilation strategy can be assigned. Within the schematic design stage, the general configuration of the airflow paths is assessed and the inlet and outlet locations are roughly defined. During the design development airflow components are sized and the target achievement verified.

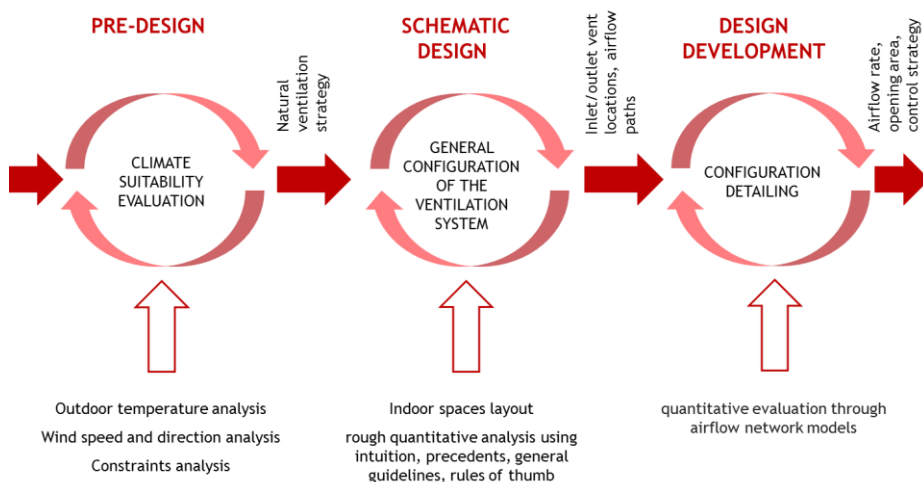


Figure 6-1. Overview of the proposed natural ventilation design method.

It is important to consider the natural ventilation as part of the building design and therefore natural ventilation has to be compatible with the whole building system as well as actually and cost-effectively implemented through available technologies. This can involve compromises that can be easily addressed during early-design-stage phases, but would require more complicated solutions and additional costs during later design stages.

6.1.Pre-design phase

In the pre-design phase, climate suitability needs to be addressed and constraints analysed in order to assure the natural ventilation feasibility. In case of existing buildings to be refurbished, the feasibility check list reported in Table 6-1 can be used.

Table 6-1. Natural ventilation feasibility Check List. Source: MacConanhey E. [6.1]

Data review	Question to be asked (if answer is yes, move to next question)
Building envelope	Is the building envelope performance optimized to minimize solar gain into the building? Target a maximum total solar load of 40 W/m ² of sun patch floor area in a cooling condition.
Internal heat loads	Is the total internal heat load minimized to less than 20 W/m ² for naturally conditioned space or, within the cooling capacity of auxiliary systems?
Monthly mean maximum and mean minimum outdoor temperature	In looking at the climate data's monthly mean maximum and mean minimum temperature, are there at least six months where the monthly maximum temperature is less than 27°C but mean minimum is higher than 0°C?
Frequency of occurrence psychrometric chart	In further looking at climate data, does the frequency of occurrence psychrometric chart for occupied hours have more than 30% of the time between 15°C to 27°C and less than 70% relative humidity?
Ambient environment, possible locations of openings	Is the surrounding environment suitable for direct intake of air from outside? (i.e., there are no security concerns, the ambient environment is sufficiently quiet, air quality meets Standard 62.1 standards, openings are not near street level, near highways, or industrial plants, or at elevation of a neighbour's discharge.)

Window locations and sizes, accessibility	Can the equivalent of 4% to 5% of the floor area as window opening area be found with direct access to the window by everyone within 6 m?
Wind rose, feasible flow Paths: inlet to outlet under all wind conditions	Can one rely on wind-driven effects for cooling? Is there a direct low-pressure airflow path from a low level opening to a high-level opening with-in the space, and will it be preserved once furniture/TI work is complete?
High afternoon temperatures	Does the climate have regular outside air temperatures over 27°C? If yes, review whether exposed thermal mass is possible.
Diurnal range on hot days	Does the climate have a diurnal range that has night-time temperatures below 18°C for at least 8 hours a night on the worst-case days? If yes, move to multi-zone modelling of thermal mass and consider night purge.
Dew-point temperatures throughout year	Throughout the year, do you have consistent outside air dew points throughout the year of less than 17°C? If yes, move to multi zone modelling and consider a radiant cooling system.

6.1.1. Climate suitability analysis

The first step to design natural ventilation is to analyse the climate potential, in other words the natural forces that drives natural ventilation (outdoor temperature and wind velocities and direction).

Available weather data file are commonly derived by data gained from weather stations at standard conditions, typically located in airports. However such files do not represent in a detailed manner the microclimatic conditions of the building surroundings and phenomena such as heat island effect and street canyons are neglected.

Within the URBVENT project, wind speed in canyons was studied among a range of different wind speed and directions [6.2]. They concluded that inside the urban canyon the potential of natural ventilation for both single sided and cross ventilation configurations is seriously reduced. In the analysed case study, a naturally ventilated apartment located at the third floor of a multi-story building located in a street canyon in the downtown of Athens, airflow rate for single side and cross ventilation configurations is reduced by 82 and 68%,

respectively, compared to an undisturbed location. This is mainly due to the important wind speed reduction. In particular, it was found that for undisturbed wind speed below 5 m/s, the air flow inside the canyon is driven by thermal phenomena. Comparison of the ambient temperature inside the canyon against temperatures measured in a reference suburban station show that the temperature in the canyon was almost 2 °C higher than the reference one.

Urban heat island phenomena in the central European area are being investigated within the EU project “Development and application of mitigation and adaptation strategies and measures for counteracting the global Urban Heat Island phenomenon”. The Urban Heat Island intensity, which denotes the temperature difference between urban and rural temperature, can range from 1 up to 7 K during the night [6.3].

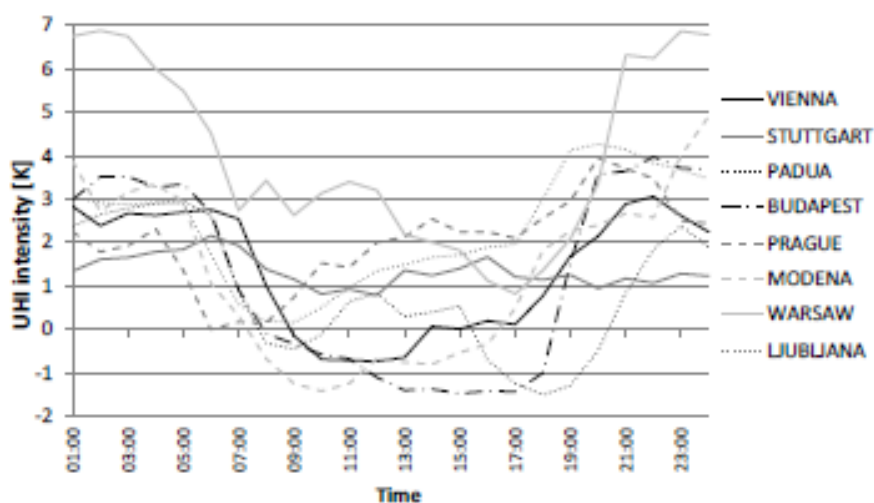


Figure 6-2. Mean hourly UHI intensity for a reference day in different European cities. Source: Kiesel K. et al. [6.3]

Roulet C.A. et al. [6.4] studied natural ventilation at mesoscale (the scale of the building-environment interaction in urban context) using GIS data to perform a multicriteria evaluation of meteorological data and morphological indicators. The GIS collected data include among others weather data, layout and height of the building, length and width

of the street. The resulting map identifies the most convenient zone in the city for natural ventilation implementation in buildings.

Once weather conditions are defined, criteria for natural ventilation potential assessing can be defined similarly to degree-hours. Cumulative sum of temperature differences (degree-hours) are a representative indication of the energy saved for cooling by natural ventilation. However, degree-hours approaches have to rely on data for numerous years (5-20) in order to be statistically significant.

One of the most interesting method to estimate night cooling potential, is the one proposed by Artmann N. et al. [6.5]. The Climatic Cooling Potential (CCP) is defined through an approach based on a building temperature variable within a temperature band given by summer time thermal comfort. The building temperature is assumed to oscillate harmonically according to a predefined function to simulate the dynamic effect of heat storage in the structure materials.

$$T_{b,h} = 24.5 + \cos\left(2\pi \frac{(h - h_i)}{24}\right) \quad \text{Equation 6-1}$$

where

$T_{b,h}$ = building temperature at a certain hour h [$^{\circ}\text{C}$]

h_i = initial time of night ventilation

Applying this definition the highest temperature occurs at the beginning of night time ventilation and the temperature range is $T_b = 24^{\circ}\text{C} \pm 2.5^{\circ}\text{C}$.

It is a rough analysis to estimate the potential of passive night cooling. Besides external hourly air temperature, only few input data about the building are needed.

The mean CCP over a time interval of N night is defined as a summation of products between building/external air temperature-difference and time interval (Equation 6-2).

$$CCP = \frac{1}{N} \sum_{n=1}^N \sum_{h=h_s}^{h_f} m_{n,h} (T_{b,n,h} - T_{e,n,h}) \quad \text{Equation 6-2}$$

$$\begin{cases} m = 1 & \text{if } 14^{\circ}\text{C} \leq T_e \leq 26^{\circ}\text{C} \\ m = 0 & \text{other} \end{cases}$$

where

CCP = climatic cooling potential [Kh]

T_b = building air temperature [K]

T_e = external air temperature [K]

N = number of nights

h = time of the day

h_i = scheduled initial time of night-time ventilation

h_f = scheduled final time of night-time ventilation

The heat flux \dot{q} which could be potentially rejected per CCP - Degree Hour can be calculated as in Equation 6-3.

$$\frac{\dot{q}}{CCP} = \frac{\rho c_p H ACH}{3600 t_{occ}} \quad \text{Equation 6-3}$$

where

\dot{q} = heat flux which could be potentially rejected [W/m^2]

CCP = climatic cooling potential [Kh]

t_{occ} = time of building occupancy

H = floor height [m]

For instance, considering that the expected total internal heat gains in an office building will be around 40 W/m^2 , an airflow of 9 ACH overnight could potentially offset the internal heat gains in the Bolzano climate.

This method allows the building designer to quickly evaluate the potential effectiveness of night cooling strategies, given knowledge of the likely internal heat gains in the building and the estimation about the airflow rates. It has to be considered only as a preliminary analysis on the assumption that thermal capacity of the building mass is sufficiently high and therefore does not limit the heat storage process.

Other authors suggest to use the balance point temperature instead of the building temperature defined by Equation 6-1. The balance point temperature is defined as the outdoor air temperature at which the total heat gains equals the total loss (Equation 6-4).

$$T_b = T_{hsp} - \frac{q_i}{\dot{m}c_p + \sum UA} \quad \text{Equation 6-4}$$

where

- T_{hsp} = heating setpoint temperature [K]
- q_i = internal heat gains [W/m²K]
- \dot{m} = mass flow rate of ventilation air [kg/s]
- c_p = air specific heat capacity [J/kgK]
- U = average envelope thermal transmittance [W/m²K]
- A = exposed surface area [m²]

Ghiaus C. [6.6] uses the free running temperature instead of the balance point temperature. The free-running temperature has an equivalent definition: it represents the indoor temperature of the building in thermal balance with the outdoor environment when neither heating nor cooling is used.

However, the CCP refers to a simple calculation which assumes that the thermal capacity of the building mass is sufficiently high and therefore does not limit the heat storage process.

The Natural Ventilation Potential (NVP) is in existing literature defined as the possibility to ensure an acceptable indoor air quality through natural ventilation, where the acceptable indoor air quality is defined by standards and/or national regulations.

Germano et al. [6.7] assessed the NVP using probability distribution of temperature and wind velocities and directions. In the same way the proposed methodology is to assess natural ventilation potential for cooling need reduction. It is here assumed that wind and stack have no opposite effect.

Yang L. et al. [6.8] proposed a method to estimate natural ventilation potential by assessing pressure differences due to stack and wind forces and compare them with the required pressure difference for acceptable indoor air quality and thermal comfort. The method assumes that the

building is north-south oriented, both south and north facades have the same opening area and indoor temperature is constant. The NVP index is here calculated in terms of pressure difference Pascal hours (PDHP). It is defined as the sum of the positive differences between hourly effective pressure difference (ΔP_{eff}) and required pressure difference (ΔP_R) (Equation 6-5).

$$PDHP = 1 \text{ hour} \times \sum_{\text{hours}} |\Delta P_{eff} - \Delta P_R| \quad \text{Equation 6-5}$$

Researchers at NIST [6.9] developed a method based on a single-zone model of natural ventilation heat transfer in commercial buildings to characterize:

- the natural direct ventilation rates needed to offset given internal heat gains rates to achieve thermal comfort during overheated period;
- the potential internal heat gain that may be offset by night-time cooling for those days when direct ventilation is insufficient.

The internal temperature is assumed to be constant. The conductive heat losses during warm periods are expected to be small relative to internal gains for commercial buildings.

In the night-time cooling case the building is considered very massive so that all the daytime heat gains are expected to be stored in the building structure. In this way, the maximum heat transfer rate at which energy may be removed from thermal mass can be calculated. Based on this method, NIST developed a web based tool useful to estimate the required ventilation rates when direct ventilation is effective and the internal gains that can be offset on the subsequent day for a nominal unit night-time air change rate when night cooling is effective [6.10].

Climate consultant [6.11] is a graphic based computer program developed by the University of California (Los Angeles) that helps designers analysing climate conditions. It organizes and represents information obtained from annual hourly EnergyPlus weather data file (.epw). In this case internal gains and building use are not taken into account. However, the psychrometric chart shown in Figure 6-3 is one

of the feature of the program which helps defining climate suitable design strategies. Each dot on the chart represents the temperature and humidity of each of the 8760 hours per year. Different design strategies are represented by specific zones on the chart. The percentage of hours that fall into each of the 16 different design strategy zones gives a relative idea of the most effective passive heating or passive cooling strategies. Climate Consultant analyses the distribution of this psychrometric data in each design strategy zone in order to create a unique list of Design Guidelines for a particular location.

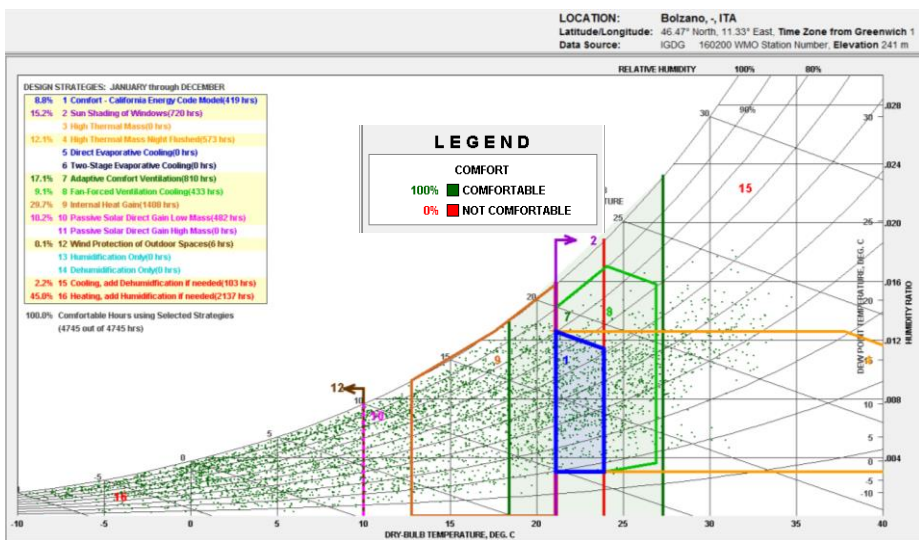


Figure 6-3. Design strategies for the Bolzano climate. Source: Climate consultant 5.4

The best wind speed and frequency characteristic visualization graph is the wind rose. A wind rose depicts the frequency of occurrence of winds in each of the specified wind direction sectors and wind speed classes for a given location and time period.

WRPLOT View [6.12] provides wind rose plots and frequency analysis for several meteorological data formats over defined schedules and data period.

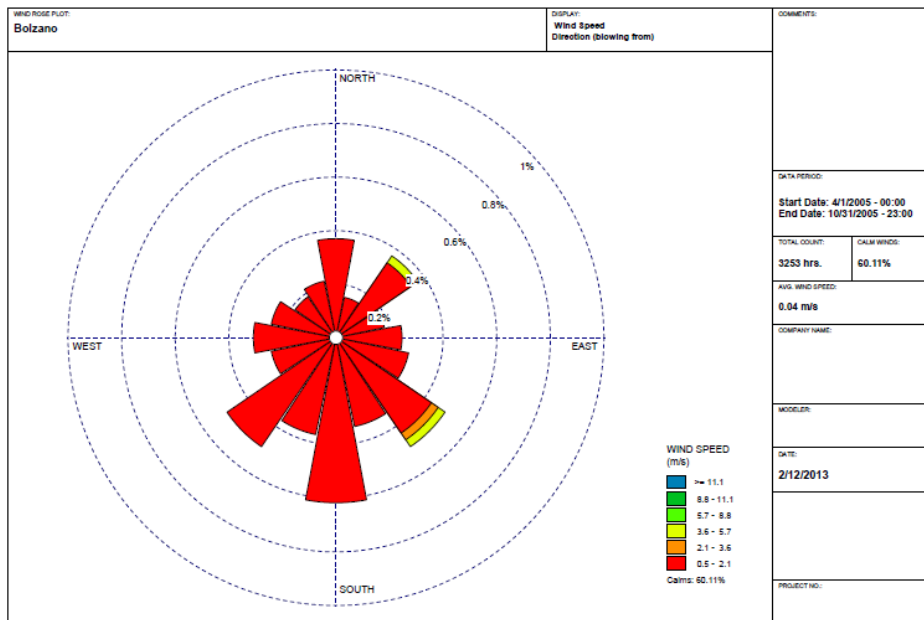


Figure 6-4. Wind speed, direction and frequency analysis for Bolzano from 1st April until 31st October. Source: WRPLOT

6.1.2. Constraints analysis

Designers are faced with many and sometimes conflicting requirements by designing natural ventilation, related to:

- urban regulation constraints (historical, landscape..)
- noise and pollution
- indoor comfort need
- responsibility on actual building indoor air quality
- particular building use
- aesthetic appearance
- building standard and regulations (acoustic, fire, zoning..)
- safety
- user control
- costs

Besides the outdoor temperature and wind conditions, natural ventilation design is also influenced by pollution and noise level of the outdoor environment. Noise is a constraint only when the building is occupied.

The responsibility on actual building indoor environmental quality is easily managed moving the problem to HVAC plants rather than to try to exploit apparently almost un-predictable natural sources availability. Natural ventilation can compromise the safety of the building while leaving windows open, but user control availability is required to achieve better comfort conditions.

Those constraints are related to the design complexity and can be easily identified through an integrated design process. Since such a wide range of parameters have to be considered, there is rarely an unique solution.

It is necessary to integrate the natural ventilation in the overall building design, especially in relation to room partitioning, air tightness, building geometry and envelope porosity.

An example of how to deal with design constraints is given by the new Technology Park design. A shared natural ventilation solution from architectural and constructive point of view has been found out through the integrated design process. The agreed solution balances performance needs with constraints given by fire regulations, acoustic comfort and user's needs, and to keep acceptable the architectural impact of the solution.

To maintain the indoor spaces layout flexibility it was not possible to plan ventilation shaft or stack devices and to estimate accurately the pressure drops due to the internal walls and vent size.

Furthermore, the plan of natural ventilation has to strictly comply with fire regulations and plans. The building is therefore divided into fire compartments enclosed with a fire resistive construction that have to be by definition air tight or closable. A natural ventilation configuration that involves more fire compartments should use components with high fire resistance ratings. Due to the high additional costs it was decided to study a natural ventilation configuration for every fire compartment.

Furthermore, acoustic problems due to air connections between offices and plans should not be neglected as the future users need privacy during the working hours.

Another constraint was about the architectural impact of the solutions. The monolithic block feature has to be maintained by reducing as much as possible the movable part in the façade, operable windows included.

6.2.Schematic design

During schematic design phase, the architect typically works with the client and other design team members to explore alternative concepts for addressing the client's needs. Once a preferred design direction is selected, the design phase typically ends with a presentation of the proposed design including plans of each floor level, major elevations, outline specifications and other information needed to clearly describe how the design meets the client's project program and goals. Drawings are presented at the smallest scale that can clearly illustrate the project. Outline specifications give a general description of the work. Within the outline specifications, a description of the energy concept is increasingly required in public design tenders and considered as an evaluation criteria [6.13] [6.14].

This is due to the fact that the architectural solutions planned during this phase have a major influence on the building energy performance. As discussed in par. 1.3, the trend towards low energy buildings forces designers to use passive solutions, in particular natural ventilation. Since the natural ventilation impacts the building shape and the indoor spaces layout, designers have to consider natural ventilation as part of the architectural features of the building. At the schematic design stage some key decisions, decisive for the success of natural ventilation, are taken. Those includes building orientation, building shape, envelope porosity, indoor spaces layout and function location.

At this stage the natural ventilation strategy has to be defined according to the climate suitability analysis, taking into account the constraints identified and depending on the target that natural ventilation has to reach, which typically are to:

- reduce cooling need
- improve thermal comfort
- ensure an acceptable indoor air quality (IAQ)

The targets to be accomplished have to be fixed in terms of key performance indicators, such as cooling need, percentage of comfort hours, airflow rates over a defined period of time etc.

The term “configuration” refers to the flow pattern of the air as it passes through openings in the external and internal surfaces of the building. The natural ventilation configuration is often depicted by arrows in architects schemes. Although this might be simplistic, it is the key issue for design. The task of the design team is to achieve this flow pattern with the required air flow rates, over a wide range of conditions. As also reported in par. 2.1, configuration options are described in literature [1.2] as:

- single-sided ventilation
- wind- driven cross ventilation
- stack driven cross ventilation
- combined wind and stack driven cross ventilation

A building can include one or more of the identified configuration options.

Design concept analysis are required to inform the decision making process about the impact of natural ventilation strategies and configurations on key performance indicators. The energy analysis carried on at this stage are comparative rather than predictive, meaning that they are not likely to predict the real future building performance but they allow to choose the most effective strategy. Building designers are interested to obtain a quick comparison of the performances of different natural ventilation strategies and configurations.

As things stand now, the most used tool in this phase are general design guidelines and handbooks [1.2] [1.3]. Etheridge D. [2.21] proposes the use of graphs and non-dimensional parameters based on empirical correlations.

However, as natural ventilation relies on variable forces and flow patterns have to be assured over a wide range of conditions, airflow network seem a more suitable model to compare natural ventilation configurations in a quick and inexpensive way. An additional advantage of the airflow network model compared to the static methods

is the capability to set controls in terms both of time schedule and external conditions.

The thermal model coupling with EnergyPlus allows to count for the factors interrelation which is relevant if the natural ventilation strategy target is to reduce cooling need, as in this case thermal mass plays an essential role.

After this stage it has to be clear what are the airflow rate needed to reach the defined target.

The result presentation should be clear and attractive, as it is an instrument of communication with the design team.

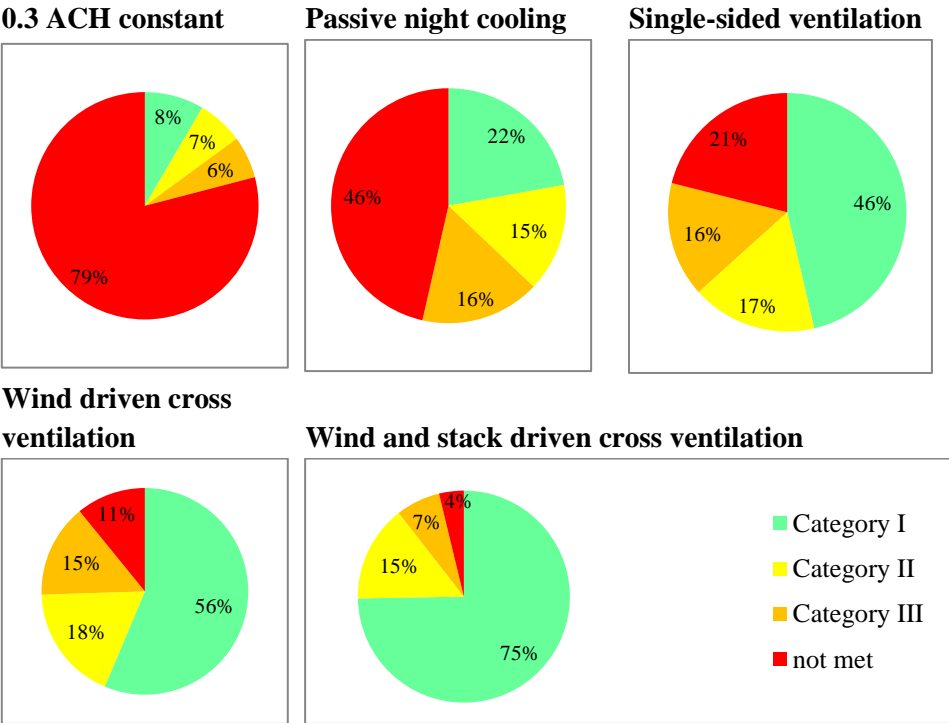


Figure 6-5. Natural ventilation strategies and configuration thermal comfort performance. Categories are defined in EN 15251:2008 – Table 1.

Figure 6-5 shows an example of results presentation that allows the comparison of different natural ventilation configurations. Thermal comfort performances of different natural ventilation configurations and strategies are compared for the reference office building described in chapter 4, in the Bolzano climate. The pie graphs show the

percentage of occupied hours when operative temperature is within the comfort ranges established by the standard EN 15251:2008 and when the requirements are not met.

An useful graph representation is the Givoni chart. Predicted hourly indoor temperatures and relative humidity obtained by a 'free floating' simulation can be plotted on the psychrometric chart. The points which fall into the blue zone identify the hours when heating is needed. The points which fall into the red zone identify the hours when cooling and dehumidifying are needed. The points which fall into the yellow zone identify the hours when cooling and humidifying are needed. When the points fall into the comfort zone (green), thermal comfort can be assured by passive solution only and no HVAC system is needed. Comfort zone can be extended (green dashed line) if air velocity is above 1 m/s.

Airflow network cannot predict indoor air velocity. However, they can output airflow rates through each component of the network. Given the airflow rate, indoor air velocity can be estimated through empirical models (see par. 2.2.1). Air velocity can be also increased by using ceiling fans as shown in some Net ZEB solution sets in par. 1.3. In Figure 6-6 indoor temperature and humidity conditions are reported for the case of natural ventilation with constant air change rate required by the national legislation (0.3 ACH). In Figure 6-7 indoor temperature and humidity conditions are reported for the case of stack and wind driven cross ventilation configuration.

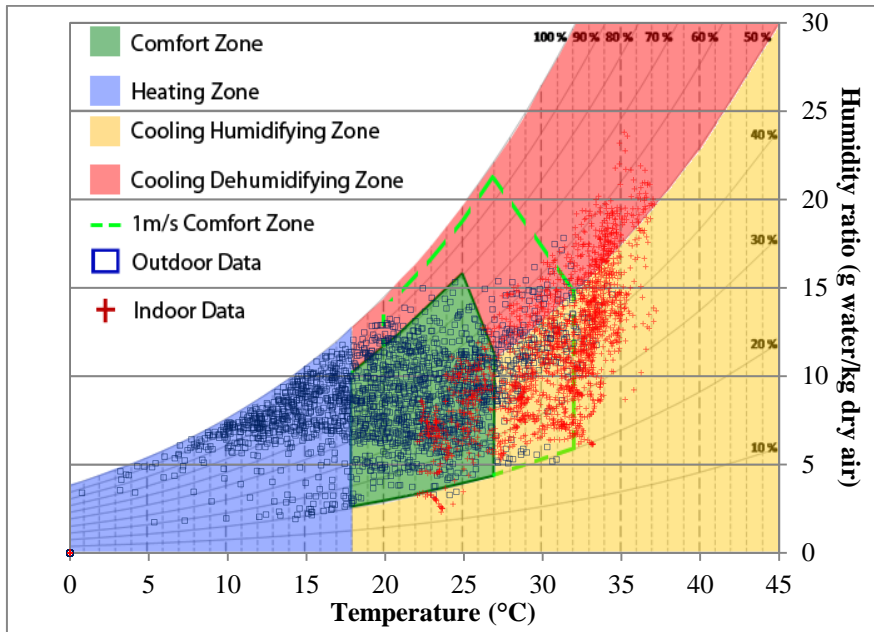


Figure 6-6. Psychrometric scatter plot which indicates temperature and humidity levels through the summer period if a constant air change rate of 0.3 is provided.

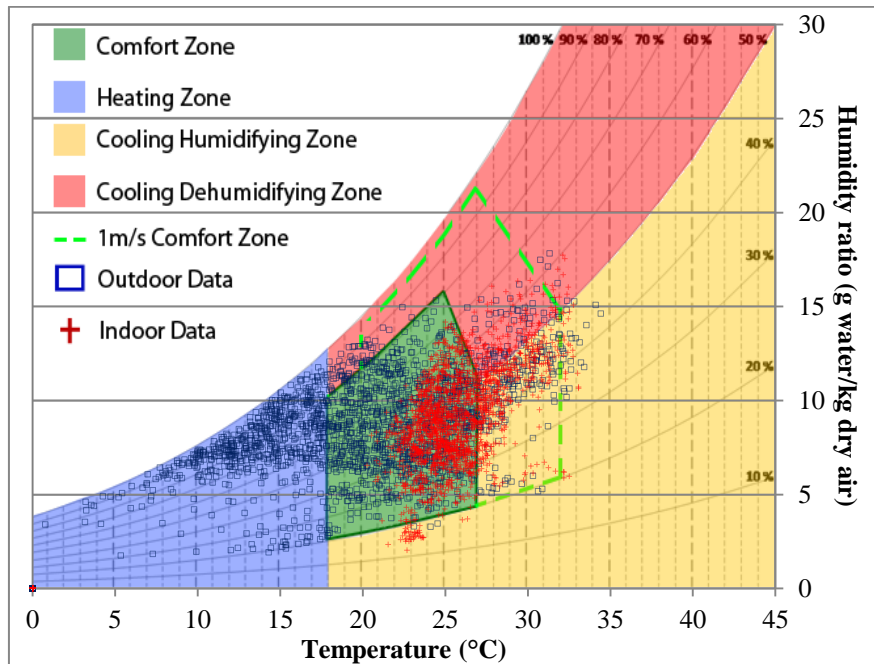


Figure 6-7. Psychrometric scatter plot which indicates temperature and humidity levels through the summer period in case of stack and wind driven cross ventilation.

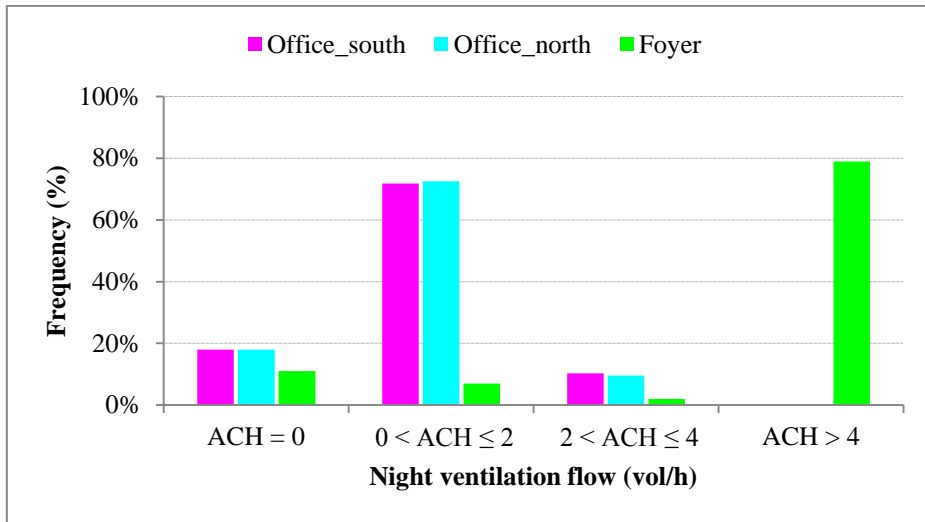


Figure 6-8. ACH frequency in the building zones during night (from June to September) due to the natural ventilation. Source: Belleri et al. [1.27]

Airflow rates resulting from different configurations can be easily compared by frequency as we did in the graph in Figure 6-8 within the IDP of the new Technology Park in Bolzano [1.27]. By this representation, the design team is able to take decisions depending on natural ventilation strategy and the required airflow rates. For instance, in case of passive night cooling high and more frequent airflow rates will be preferred. In case the natural ventilation strategy is to ensure thermal comfort, lower and frequent airflow rates allow avoiding uncomfortable draught.

6.3.Design development

Design development produces details of all the technical aspects of the design, including architectural, HVAC, electrical, structural, plumbing and fire protection system. Design development documents should be detailed enough to allow cost estimation and to prove standard and building regulation accomplishment.

At this stage, the natural ventilation configuration has to be detailed with opening type, size and position (see par. 6.3.1). Key performance indicators can be calculated by using building energy simulation tools coupled with airflow network. Target accomplishment can be verified

assessing results uncertainty range and reliability by means of parametric analysis. Uncertainty and sensitivity analysis have been performed on two case studies and the methodologies applied are presented in chapter 4 and 5.

Two sensitivity analysis methods have been presented. The Elementary Effect method (par. 4.5) allows to underline the most influencing parameters on a given output result. The Standard Regression Coefficient method (par. 5.1.4.3) allows to identify the main sources of uncertainty in the results.

A generalizable outcome of the performed parametric analysis is the high influence of internal and solar heat gains, not only because they affect directly the energy use and the thermal comfort, but also because the control strategy is usually based on indoor temperatures.

Therefore, an accurate assessment of the input parameters affecting solar and internal heat gains, as the solar heat gain coefficient, the lighting and the electric equipment power density, would significantly reduce the results uncertainty. Exchange of information about the building use, the equipment installed and the lighting system between building owner and future users and the design team help to better define this kind of input data.

Except in case of night cooling strategies, envelope thermal characteristics do not need to be accurately defined to have reliable predictions.

Other input parameter specification needs depend more specifically on climate, natural ventilation strategy and target requirements. Therefore, a sensitivity analysis on the specific case has to be carried on.

The uncertainty analysis allows defining the output reliability. Since in the design development phase still some input parameters cannot be well defined yet, presenting the predicted performance to the design team in a deterministic way might mislead the results interpretation.

6.3.1. Detailing of natural ventilation

Different methods and tools are available to determine the opening area needed to get the required airflow rates.

Sizing rules of thumb and non-dimensional graph methods can be found in Allard F. et al. [1.2].

Airflow network models can be used iteratively to search for acceptable component sizes.

A valid alternative is the software tool LoopDA [2.31] which implements the loop equation design method developed by Emmerich S.J. and Dols S.W. [6.15]. The loop equation design method (see par 2.2.2) is applied to a multi zone model to account for internal resistances. Compared to the airflow network model, the equations are reversed. Instead of defining the physical characteristics of the flow components (opening area and position) and calculate airflow through them, the loop equation method requires the user to define the design airflow rates through the components and determines the physical characteristics of the components to provide the required flow rates.

The plot in Figure 6-9 shows the asymptotic relationship between the inlet and outlet opening area of the central stack in the new Technology Park building to meet the design airflow rate. From the resulting relationship the stack inlet area has been selected as 5 m^2 which sets the outlet stack area at 10 m^2 .

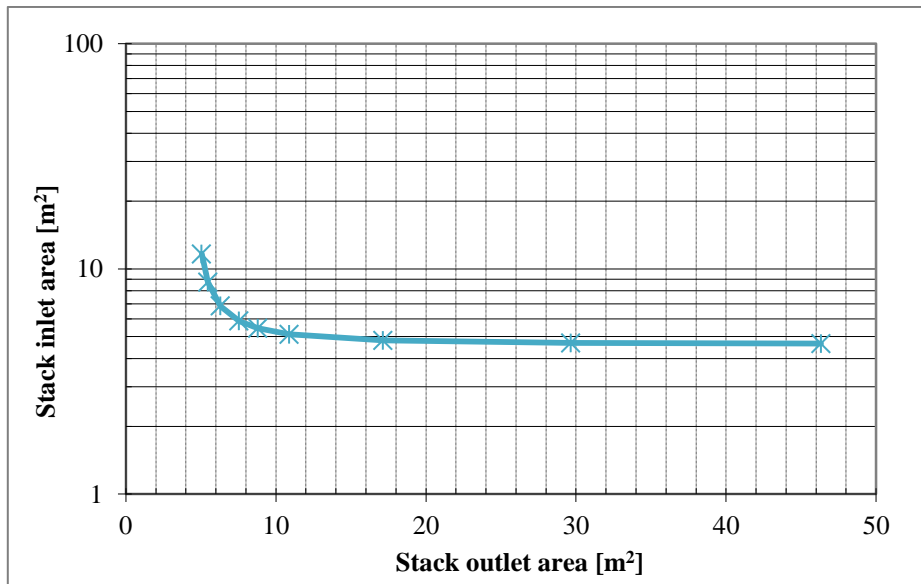


Figure 6-9. Relationship between inlet and outlet opening area of the central stack in the new Technology Park building calculated by LoopDA.

LoopDA can be used to analyse the natural ventilation configuration by performing simulations ranging from steady state to a seasonal or annual analysis using weather data for the location.

If the opening area correspond to the glazed area, other important factors as daylighting and internal solar gains have to be taken into account in the opening area sizing. In this case building energy simulation coupled with airflow model allows to consider airflow, thermal and radiation problem as a whole.

6.3.2. Control strategy definition

Many non-residential buildings are controlled through a Building Management System (BMS), which can integrate natural ventilation controls. Compared to manual control, a control system allows to avoid heat losses, discomfort situations or undesired draught. The presence of automated controls also enhances the performance prediction reliability and reduces discomfort crisis occurrence. One of the main source of uncertainty in building energy simulation is the user behaviour. Therefore, reducing their interaction with the building, increase the performance prediction accuracy. However, occupants are expected to exercise some control on the system. The correct balance between occupant control and BMS is still under discussion.

If opening automation is expected, the control strategy algorithms have to be defined in the design development phase considering users expected behaviour and building occupation patterns.

Control strategies shall also take into account rain protection, fire prevention, indoor acoustical environment and security. Generally rain detector are combined with wind speed velocity and direction sensors. In case of rain, windows located on the upwind façade are closed. Fire prevention is achieved by using smoke sensors and controlling openings connecting different fire compartments. Indoor acoustical environment controls are usually manual. In case of privacy need, users can close windows and vents manually. Demand controls based on CO₂ levels are suitable to zone with variable occupancy, such as conference and meeting rooms.

For the cost estimation, sensor number, characteristics and location have to be evaluated.

The main sensors to control natural ventilation are:

- *Temperature sensors.* The difference between indoor and outdoor temperature determines whether the introduction of outdoor air in the building is efficient. The sensors have to be positioned far from the window where the air is mixed and protected by direct solar radiation;
- *Multigas or CO₂ sensors.* The CO₂ sensors allows evaluating the indoor pollution due to the users presence. Most of the CO₂ sensors are infrared, they have low accuracy and high costs. They have to be calibrated every 6 – 12 months. Multigas sensors detect more pollution sources, but need a more frequent calibration;
- *Wind velocity and direction sensors.* The wind direction can be measured to define which windows to close or open, while wind velocity can be used to determine the opening type and the opening factor or to close the window in case of strong winds;
- *Rain detector.* It is necessary to prevent the entrance of water in the building. They can be combined with the wind direction sensors to control the closing of upwind windows.

Table 6-2 reports sensors accuracies and related standards.

Controls for natural ventilation purposes are often provided by technology producers. Air vents and windows are available that automatically adjust their area in response to the pressure acting across them. Main technology products and related available controls are reported in Annex I.

The EnergyPlus airflow network allow different control strategy implementation, which are described in par. 3.3.8, but not all the above mentioned aspects can be taken into account. Each opening group pertaining to a configuration should refer to a determined configuration strategy which has to be verified and optimized. GenOpt [6.16] allows the integration with EnergyPlus to solve optimization problems by minimizing a defined cost function. Define the cost function as the number of comfort hours or the cooling need, the control algorithm setpoint can be parameterized to search for an optimal control setting.

Table 6-2. Measurement tool characteristics.

Sensor	Measurement range	Accuracy	Standard	Note
Temperature sensor	from 10°C to 40°C	$\pm 0.5^{\circ}\text{C}$	UNI EN ISO 7726	It has to be protected from hot and cold wall radiation effect and from solar direct radiation.
Anemometer	from 0.05 m/s to 1 m/s	$\pm (0.05 + 0.05 \vee) \text{ m/s}$	UNI EN ISO 7726	It measures both wind velocity and direction.
Hygrometer	from 0.5 kPa to 3.0 kPa	$\pm 0.15 \text{ kPa}$	UNI EN ISO 7726	It has to be positioned next to the temperature sensor.
Infrared CO₂ sensors	from 5% to 100%	$\pm 70 \text{ ppm}$	UNI EN 15242	It is expensive and does not detect indoor pollution due to sources different from occupants.

6.4. Construction documents

Construction documents describes in detail the components of a project that need to be fabricated and assembled in order for it to be built. The contributions of all the consultants involved in the project have to merge into a coherent, clear and comprehensive document. The document includes drawings containing construction details presented in large scale and construction specifications, considered as written requirements for materials, equipment and construction systems, as well as standards for products, workmanship and the construction services required to produce the work.

Annex I reports some technology products available on the market and suitable to natural ventilation systems.

Airflow network can be further detailed once the opening typology and product type are defined by determining the discharge coefficients. Those can be reported in the product data sheet or measured at full scale or model scale through laboratory experiments.

At this stage the control strategy has to be defined in detail by mapping the sensors and the actuators needed and implementing the control algorithms defined.

If the wind is the natural ventilation dominant driving force and the building is located in an irregular surrounding area, it is worth to better determine the wind pressure coefficients through a wind tunnel test or an external CFD analysis. Chapter 5 includes a comparison of wind pressure coefficients from existing literature and database with the one estimated with wind tunnel test.

Wind speed profile has been identified as one of the main source of uncertainty.

To verify comfort conditions in particular situations, temperature and velocity fields within the occupied spaces have to be estimated. The calculation of temperature and velocity fields requires the use of CFD. The airflow network model can contribute in this case to the boundary conditions definition and to determine the most critical situation to be analysed.

6.5.Summary and recommended guidelines

The previous considerations can be summarized by Table 6-3 which reports the tools effective to support design decision within the identified design phases.

Climate suitability can be assessed by analysing the natural ventilation main drivers: indoor-outdoor temperature difference and wind pressure. The climate suitability tool developed by NIST [6.10] allows to estimate the natural direct ventilation rates needed to offset given internal heat gains rates to achieve thermal comfort during overheated period and the potential internal heat gain that may be offset by night-time cooling for those days when direct ventilation is insufficient.

Climate Consultant [6.11] helps defining the whole solution set by giving a list of design solutions suitable to the analysed climate.

Wind rose plots and wind velocity frequencies can be processed by WRPlot view [6.12] over defined schedules and data period to address the potential of a wind driven ventilation strategy.

Table 6-3. Tools to support design decisions within the design process.

Design stage	Tool	Outcome
Pre-design	Climate suitability tool [6.10]	<ul style="list-style-type: none"> – natural direct ventilation rates needed to offset given internal heat gains rates to achieve thermal comfort during overheated period; – potential internal heat gain that may be offset by night-time cooling for those days when direct ventilation is insufficient.
	Climate consultant [6.11]	List of design guidelines for the particular location
	WRPlot view [6.12]	wind rose plots and frequency analysis over defined schedules and data period.
Schematic design	LoopDA [2.31]	Opening sizing
	Airflow network Sensitivity analysis	Airflow rate Indoor temperature Most influential parameters
Design development	Airflow network Uncertainty analysis	Natural ventilation performance assessment and uncertainty

The climate analysis should also take into account building surroundings (e.g. street canyons, heat island effects..).

Once the most suitable ventilation strategy to the climate has been selected, it is necessary to integrate the ventilation system itself into the overall design of the building, especially in relation to airtightness, room partitioning and accessibility. Since such a wide range of parameters is involved both from architectural and constructive point of view, a solution has to be found out through an integrated design process. Par. 1.4 shows the building professionals role and the information sharing needs regarding natural ventilation within the integrated design process. Design constraints are due to other important requirements fulfilment such as fire safety, acoustics and building structure.

A rough component sizing can be performed by using LoopDA [2.29] By integrating building energy models with multi-zone airflow models, EnergyPlus tool can be used to support early design decisions. As shown in chapter 4, these models might be sensitive to a number of key

parameters which cannot be addressed at schematic design stage. Therefore, a sensitivity analysis following the methods described in chapter 4 must be performed.

Internal and solar heat gains can be generalized as the most influential parameters, not only because they affect directly the energy use and the thermal comfort, but also because the control strategy is usually based also on indoor temperatures.

Therefore, an accurate assessment of the input parameters affecting solar heat gains and internal loads, like the solar heat gain coefficient, the lighting and the electric equipment power density, would significantly reduce the results uncertainty. Exchange of information about the building use, the equipment installed and the lighting system between building owner and future users and the design team might help to better define this kind of input data. In case that no information is available, different internal loads scenario must be defined to evaluate natural ventilation performance at different internal loads levels.

Other input parameter specification needs depend more specifically on climate, natural ventilation strategy and target requirements. Therefore, a sensitivity analysis on the specific case has to be carried on.

At design development stage, dynamic simulations are required to assure building code and standard accomplishment. Uncertainty analysis should be used to inform decision makers by quantifying the uncertainty of performance predictions. Sensitivity analysis is at this stage used to identify key model input parameters that impact the reliability of these predictions. Chapter 5 presents methods to perform this kind of sensitivity and uncertainty analysis and to improve simulation models that reduce the uncertainty in model predicted ventilation performance, based on field study observations.

From the analysis performed the following modelling guidelines have been gathered:

- use EnergyPlus's temperature based control with the temperature set points based on an annual schedule of adaptive comfort temperatures;

- avoid when possible using idealized occupancy models and consider window use behaviour at the level of individual occupants, also considering interior layout;
- if possible, do on-site inspections, measure local weather conditions, and perform wind tunnel tests;
- calibrate weather files from a local meteorological station with site-specific measurements of wind speeds (wind speed profile);
- prefer the use of a c_p generator [3.31], taking into account surrounding buildings geometry, instead of standardized coefficients from literature;
- use of passive cooling methods (i.e. exterior shading, increased thermal mass) to reduce buildings' sensitivity to internal loads, including occupancy.

Bibliography

- [6.1] MacConahey E. Mixed mode ventilation - Finding the right mix. ASHRAE Journal. September 2008.
- [6.2] Georgakis Ch., Santamouris M. Experimental investigation of air flow and temperature distribution in deep urban canyons for natural ventilation purposes. *Energy and Buildings* 2006, vol. 38, pp. 367-376.
- [6.3] Kiesel K., Vuckovic M., Mahdavi A. Representation of weather conditions in building performance simulation: a case study of microclimatic variance in central europe. *Building Simulation*. Chambery, 2013.
- [6.4] Roulet C-A, Germano M., Allard F., Ghiaus C. Potential for natural ventilation in urban context: an assessment method. *Indoor Air*. Monterey (CA), 2002.
- [6.5] Artmann N., Manz H., Heiselberg P. Climatic potential for passive cooling of buildings by night-time ventilation in Europe. *Applied Energy* 2007, Vol. 84, pp. 187-201.
- [6.6] Ghiaus C. Free-running building temperature and HVAC climatic suitability. *Energy and buildings* 2003, Vol. 35, pp 405-411.
- [6.7] Germano M., Ghiaus C., Roulet C-A. Natural ventilation potential. *Natural ventilation in the urban environment*. London: EARTHSCAN, 2005.
- [6.8] Yang L., Zhang G., Yuguo L., Youming C. Investigating potential of natural ventilation driving forces for ventilation in four major cities in China. *Building and Environment* 2005, Vol. 40, pp. 738-746.

- [6.9] Emmerich S. J., Polidoro B., Axley J. W. Impact of adaptive thermal comfort on climatic suitability of natural ventilation in office buildings. *Energy and Buildings* 2011, Vol. 43, pp. 2101-2107.
- [6.10] NIST. Climate Suitability Tool. Multizone Modelling website. [Online] 09 2010. <http://www.bfrl.nist.gov/IAQanalysis/software/CSTprogram.htm>.
- [6.11] Climate Consultant 5.4. Energy Design Tools. [Online] 03 2013. <http://www.energy-design-tools.aud.ucla.edu/>.
- [6.12] Lakes Environmental. WRPLOT View - Wind rose plots for meteorological data. [Online] 06 2011. <http://www.weblakes.com/products/wrplot/index.html>.
- [6.13] Paoletti G., Belleri A., Lollini R. Nearly Zero Energy requirements in public design tenders - Experiences of two case study. *Sustainable Buildings*. Graz, 2013.
- [6.14] Helsinki central library open architectural competition. [Online] 2012. <http://competition.keskustakirjasto.fi/>.
- [6.15] Emmerich S. J., Dols S. W. Natural ventilation review and plan for design and analysis tools. NISTIR 6781, 2001.
- [6.16] GenOpt - A generic optimization program. Wetter M. Seventh International IBPSA Conference. pp. 601-608. Rio de Janeiro, 2001.

Conclusion

Natural ventilation is widely applied to recently designed buildings as it is an effective passive measure to achieve the Net Zero Energy target. Existing standard and building regulations include only some rules of thumb about room geometry and percentage of window area. Ventilative cooling as strategy is not included yet in standard energy performance regulations.

Within the existing natural ventilation modelling techniques, airflow network models seem the most promising tool to support the natural ventilation design as they can be coupled with the most widely used building energy simulation tools. This work allows overcoming some of the barriers to its usage during early-design-stages, such as model zoning, input data estimation, model reliability and results uncertainty.

Two main quantitative analysis methods have been identified with the aim to identify the most important design parameters and the model robustness depending on design uncertain parameters.

A sensitivity analysis on different natural ventilation strategies performance has been carried out on a reference office building model considering key design parameters that cannot be clearly specified during early-design-stages. The results underline solar gains and internal loads as the most influential parameters in every analysed climate. Other parameters' effect on natural ventilation strategies performance is more climate dependent. Apart internal gains and among the assessed parameters, openings area influenced the most the predicted number of hours where thermal comfort can be assured. Envelope characteristics (thermal transmittance, density and air tightness) were found to have significant influence on cooling needs in climates with large diurnal temperature swing.

In collaboration with the Lawrence Berkeley National Laboratory, the airflow network modelling reliability at early-design-stage has been tested by comparing results from early-design-stage model and better

detailed input data model, as well as with measured data of an existing naturally ventilated building, located in Alameda (California).

Early-design-stage modelling may cause an overestimation of natural ventilation performances mainly due to the window opening control standard object implemented in building dynamic simulation tools, which assume all the windows within the same zone are operated in the same way.

With suitable input data, by using EnergyPlus in combination with an airflow network I was able to provide informative predictions of natural ventilation performance. Using calibrated models, I was able to predict, within an acceptable range of uncertainty, the observed average ventilation rates and the number of compliant hours.

The use of reliable weather data is also important as wind related data account for most of the uncertainties.

Finally, a natural ventilation design guidelines are proposed to explain how existing natural ventilation design tools and methods can be applied within the whole design process.

Natural ventilation allows to effectively contribute to achieve Net Zero Energy target and good indoor environmental quality level, but if handled in the right way just from the concept design phase.

This PhD work provides methods to integrate natural ventilation in the whole building design and to improve natural ventilation predictability with the most widely used building energy simulation tools.

The following aspects have been identified for further development:

- to perform occupant behaviour studies to better define window opening control algorithms and integrate them in building dynamic simulation tools;
- to develop energy efficient controls optimization algorithm, allowing to keep high comfort level as well as indoor healthy;
- to define a procedure for the definition of more detailed wind speed profiles (considering both spatial and timing dimension) based on on-site measured wind speed;
- to define a monitoring procedure to assess natural ventilation performance.

Publication List

2014

Belleri A., Lollini R., Dutton S., *Natural ventilation design: an analysis of predicted and measured performance*, Building and Environment, to be submitted

Belleri A., Virzi F., Noris F., Lollini R., *Cost optimal solution sets for Net Zero Energy residential buildings*, World Sustainable Energy Days, 26-28 February 2014, Wels/Austria.

2013

Belleri A., Dutton S., Filippi Oberegger U., Lollini R.. *A sensitivity analysis of natural ventilation design parameters for non-residential buildings*, Building Simulation 2013, 25-29 August 2013, Chambéry, France

Belleri A., Noris F., Filippi Oberegger U., Lollini R.. *Evaluation tool for Net Zero Energy Buildings: application on office building*, World Sustainable Energy Days, 27 February – 1 March 2013, Wels/Austria.

Paoletti G., Belleri A., Lollini R.. *Integrazione del requisito energetico nZEB all'interno dei bandi pubblici*, Convegno AICARR, 17 October 2013, Bologna.

Paoletti G., Belleri A., Lollini R., Mahlkecht H.. *Nearly zero energy target integration in public design tenders*, Sustainable Buildings conference, 25-28 September 2013, Graz.

Aelenei D., Aelenei L., Musall E., Cubi E., Ayoub J., Belleri A., *Design strategies for non-residential Zero Energy Buildings. Lessons learned from Task 40/Annex 52 "Towards Net Zero Energy Solar buildings"*, CLIMA 2013, 16-19 June 2013, Prag.

2012

Belleri A., Lollini R., *Uncertainties in Airflow Network modelling to support natural ventilation early stage design*, AIVC-Tighvent conference, 10 - 11 October 2012

Lion L., Belleri A., Giovannini L., Zardi D., *Natural ventilation strategy potential analysis in an existing school building*, AIVC-Tighvent conference, 10 - 11 October 2012

Belleri A., Castagna M., *Natural night ventilation as passive design strategy for a net zero energy office building*, 7th International Conference on Improving Energy Efficiency in Commercial Buildings (IEECB), Frankfurt, April 2012

Belleri A., Lollini R., *A scuola di Net ZEBs: monitoraggio del bilancio energetico di un edificio Net Zero*, Azero_03, April 2012

2011

Napolitano A., Lollini R., Belleri A., *Implicazioni progettuali per diverse accezioni di “Nearly Zero Energy Buildings”*, 29° Convegno Nazionale AICARR, SAIE – Bologna, 2011

Annex I

Solutions and technology products